IMPROVING THE OUTCOME OF EXPERIMENTAL ACUTE PANCREATITIS: THE EFFECTS OF KYNURENIC ACID, SZR-72 AND ANALGESIA

Ph.D. Thesis

Eszter Sára Kormányos, M.D.

Supervisors:

Zoltán Rakonczay Jr. M.D., Ph.D., D.Sc.

Lóránd Kiss Ph.D.

Doctoral School of Theoretical Medicine

Department of Pathophysiology

Department of Medicine

University of Szeged

Szeged, Hungary

2022

PUBLICATIONS

Publications closely related to the subject of the thesis

I. Balla Z*, **Kormányos ES***, Kui B, Bálint ER, Fűr G, Orján EM, Iványi B, Vécsei L, Fülöp F, Varga G, Harazin A, Tubak V, Deli MA, Papp C, Gácser A, Madácsy T, Venglovecz V, Maléth J, Hegyi P, Kiss L, Rakonczay Z Jr. Kynurenic acid and its analogue SZR-72 ameliorate the severity of experimental acute necrotizing pancreatitis. Front Immunol. 2021; 12:702764. doi: 10.3389/fimmu.2021.702764. **[IF$_{2021}$: 8.786]**, Q1 *Authors share co-first authorship

II. Bálint ER, Fűr G, Kui B, Balla Z, **Kormányos ES**, Orján EM, Tóth B, Horváth G, Szűcs E, Benyhe S, Ducza E, Pallagi P, Maléth J, Venglovecz V, Hegyi P, Kiss L, Rakonczay Z Jr. Fentanyl but not morphine or buprenorphine improves the severity of necrotizing acute pancreatitis in rats. Int J Mol Sci. 2022; 23(3):1192. doi: 10.3390/ijms23031192. **[IF$_{2021}$: 6.208]**, Q1

Publications related to the subject of the thesis

I. Fűr G, Bálint ER, Orján EM, Balla Z, **Kormányos ES**, Czira B, Szűcs A, Kovács DP, Pallagi P, Maléth J, Venglovecz V, Hegyi P, Kiss L, Rakonczay Z Jr. Mislocalization of CFTR expression in acute pancreatitis and the beneficial effect of VX-661 + VX-770 treatment on disease severity. J Physiol. 2021; 599(22):4955-4971. doi: 10.1113/JP281765. **[IF$_{2021}$: 6.228]**, Q1

II. Kui B, Balla Z, Vasas B, Végh ET, Pallagi P, **Kormányos ES**, Venglovecz V, Iványi B, Takács T, Hegyi P, Rakonczay Z Jr. New insights into the methodology of L-arginine-induced acute pancreatitis. PLoS One. 2015; 10(2):e0117588. doi: 10.1371/journal.pone.0117588. **[IF$_{2015}$: 3.057]**, Q1

Scientometrics

https://m2.mtmt.hu/gui2/?type=authors&mode=browse&sel=10045525&view=pubTable

Number of full publications	4
First author publications	1
Cumulative impact factor	24.279
Number of independent citations	36

TABLE OF CONTENTS

LIST OF ABBREVIATIONS

3-HK – 3-hydroxykynurenine

AP – acute pancreatitis

BQ – buprenorphine

GAPDH – g*l*ycerinaldeh*y*de-3-phosphate-dehydrogenase

GPR35 – G protein-coupled receptor 35

HEPES – 4-(2-hydroxyethyl)-1-piperazineethanesulfonic acid

HPRT – hypoxanthine phosphoribosyltransferase

HSP – heat shock protein

i.p. – intraperitoneal(ly)

i.t. – intrathecal(ly)

IL – interleukin

KYN – kynurenine

KYNA – kynurenic acid

LO – L-ortnithine-hydrochloride

MPO – myeloperoxidase

NMDA – N-methyl-D-aspartate

NMDAR – N-methyl-D-aspartate receptor

pCO_2 – partial pressure of CO_2

RBCV – red blood cell velocity

RCF – relative centrifugal force

ROS – reactive oxygen species

RT-PCR – reverse transcription polymerase chain reaction

SZR-72 – 2-(2-N, N dimethylaminoethylamine-1-carbonyl)-1H-quinolin-4-one hydrochloride

TBS – tris-buffered solution

TNF-α – tumor necrosis factor-alpha

INTRODUCTION

The physiology of the pancreas

The pancreas is a heterocrine gland of the gastrointestinal tract located retroperitoneally in the upper abdomen. The exocrine parenchyma is mostly composed of acinar and ductal epithelial cells (Czakó et al., 2009). Its function is to produce pancreatic juice, which consists of inactive digestive enzymes synthesized by acini and HCO_3^--rich fluid secreted by ductal epithelial cells. The 1.5-2 liters of fluid per day, that is excreted into the duodenum, flushes potentially harmful enzymes out of the ductal system, preventing their premature activation. Its high HCO_3^- content provides the enzymes optimal pH in the intestinal lumen to digest lipids, proteins, and carbohydrates (Hegyi et al., 2015). It is essential that the enzymes trypsin, chymotrypsin, amylase, lipase become active only in time, after reaching the duodenum. Once inside the lumen, enteropeptidase cleaves and activates trypsinogen to trypsin, initiating an activation cascade. Endocrine cells of the pancreas are organized into groups within the organ called the islets of Langerhans. They produce insulin, glucagon, and somatostatin, among others, and their main function is to control blood glucose levels.

Acute pancreatitis

Definition, epidemiology, classification, and etiology

Acute pancreatitis (AP) is a sudden, sterile inflammation of the pancreas. The disease can be limited to the pancreas itself, but can often affect peripancreatic tissues or, in severe cases, even distant organs, leading to life-threatening multiple organ failure. Despite advanced medicine in the 21st century, the mortality rate of AP is still remarkably high (Peery et al., 2022). This is further exacerbated by the fact that this gastrointestinal disease can affect not only the older, comorbid groups but also the healthy, younger generation. The annual incidence of AP is approximately 10-45/100,000 population and this is rising slightly in developed countries up to this day (Roberts et al., 2017).

The clinical picture of AP can vary from abdominal discomfort lasting only a few days to hemodynamic shock and death. Because of its unpredictable outcome and wide spectrum of complications, it was important to create a standardised nomenclature. The revised Atlanta classification categorized AP into 3 groups based on severity: mild, moderately

severe, and severe (Banks et al., 2013). The majority of AP cases (~75%) are mild, 15% are moderate and 10% are severe. Mild AP is limited to the pancreas, causing edematous inflammation with practically zero mortality. In moderately severe cases, local pancreatic complications (peripancreatic fluid accumulation, necrosis) are accompanied by transient distant organ failure (heart, lungs, kidneys) that resolves within 48 hours. However, in severe AP, pancreatic necrosis can even cause damage to the surrounding blood vessels, leading to serious blood loss, and distant organ failure becomes persistent (>48 h). In addition, a colonic bacterial infection of the necrotic pancreas can further worsen the already disappointing outcome. The mortality of severe AP can reach up to 30% (Párniczky et al., 2016).

Etiological factors of AP can be classified into four main categories (Yadav et al., 2013). The first is toxic and metabolic disorders: alcohol consumption, hyperlipidemia, hypercalcemia, drugs, and poisons. The second group is mechanical causes: gallstones, papilla dysfunction, congenital malformations, anatomical abnormalities, trauma. The third category includes genetic causes such as mutations in the trypsinogen gene. The fourth, „other" class includes infections, vascular factors, and unknown causes. The prevalence of the listed factors varies widely. Most commonly, in about 40% of cases, biliary obstruction (gallstones, Vater papilla stenosis) is observed. Ethanol abuse is the cause in 30%, most of which are accompanied by a high-fat diet (Forsmark et al., 2016; Pandol et al., 2007).

Pathogenesis

The exact pathogenesis of AP remains to be unclear. Researchers agree that to interpret the complex pathomechanism of AP, initiating factors must first be identified. Several steps in the early stages of AP have already been described (Barreto et al., 2021): nuclear factor-kappa B (NF-κB) activation caused by toxic intracellular Ca^{2+} overload (Rakonczay et al., 2008), mitochondrial dysfunction and damage (Biczó et al., 2011; Maléth et al., 2011), impaired autophagy (Biczo et al., 2018), reactive oxygen species (ROS) release (Criddle, 2016), inhibition of digestive enzyme secretion and drop in intracellular adenosine triphosphate (ATP) levels (Mukherjee et al., 2016), premature trypsinogen activation (Dawra et al., 2011), decreased ductal HCO_3^- and fluid secretion (Pallagi et al., 2014), pancreatic ductal cystic fibrosis transmembrane conductance regulator dysfunction (Hegyi et al., 2015), and reduced gastrointestinal blood flow (Sadowski et al., 2015). Some of these events lead to the release of tumor necrosis factor-α (TNF-α), cytokines [e.g. interleukin-1β (IL-1 β)], and chemokines, which participate in leukocyte recruitment. Neutrophils are the

first immune cells reaching the pancreatic parenchyma. These cells further activate trypsinogen in acinar cells (Gukovskaya et al., 2002), release inflammatory cytokines and chemokines, secrete myeloperoxidase (MPO) and ROS [e.g. hydrogen peroxide (H_2O_2)], all of which contribute to the exacerbation of AP in a vicious circle (Sendler et al., 2018).

Several protective factors and mechanisms are responsible for keeping digestive enzymes inactive within the pancreas, or washing out those that are already activated: α1-antitrypsin, α2-macroglobulin, serine protease inhibitor Kazal type 1 (SPINK1), autolysis of prematurely activated trypsin, and so on (Barreto et al., 2021; Mayerle et al., 2019). However, as soon as the rate of enzyme activation exceeds the capacity of the defense mechanisms, the process shifts towards self-digestion. In addition, trypsin also plays a pathophysiological role in activating the complement system, fibrinolysis, and coagulation, helping the disease to spread beyond the pancreas. The vascular endothelium is also affected leading to impaired microcirculation and increased permeability. This allows the release of free radicals, proinflammatory cytokines, and proteolytic enzymes causing thrombosis, tissue bleeding, and ultimately necrosis (Cruz-Santamaría et al., 2012). In patients with AP, cytokines and enzymes that are initially present only in the pancreas may enter the circulation and play a critical role in inducing systemic inflammatory response syndrome (Weber et al., 2001). Eventually, this allows pancreatic inflammation to cross the boundaries of its original organ and cause acute respiratory distress syndrome, kidney failure, metabolic disorders, shock, and multiple organ failure. Finally, if that was not enough, damage to the intestinal mucosal barrier creates an opportunity for superinfection of the necrotized pancreas (Schepers et al., 2019).

But how can it be predicted that a patient's pancreatitis will not remain mild but will become severe? Can we intervene somewhere in this chain of events to save a patient's life? The answer lies in the detailed understanding of the cellular events that take place during AP and the development of an effective cure.

Treatment and pain management

Unfortunately, there is still no specific cure for AP, the therapeutic arsenal has not expanded much in recent decades, and predominantly conservative treatment is still used today. Fluid and electrolyte replacement should be started within the first 24 hours (Tenner et al., 2013). If the AP is not mild, it is recommended to relieve the pancreas with a nasojejunal tube. In this way, the barrier integrity of the intestinal mucosa can be maintained,

thus preventing bacterial translocation (Petrov et al., 2008). The need for further treatments depends on the complications of the disease.

The most common symptom that affects almost all patients is abdominal pain of varying intensity. Non-steroidal anti-inflammatory drugs and opioids can be used intravenously to relieve pain (Cai et al., 2021). However, to achieve a continuous effect it is advisable to apply a pump instead of a bolus, and patient-controlled administration is even better. Morphine and its derivatives are often avoided as they can cause sphincter of Oddi spasm (Thompson, 2001). Thoracic epidural anesthesia may be considered in patients with pain that is difficult to tolerate. The advantage of this method is not only to effectively alleviate pain, but also to improve the perfusion of the gastrointestinal tract (Wang et al., 2022). Despite all this knowledge, there is still no widely accepted recommendation for analgesia, and its effect on AP progression is unclear.

Based on literature data and our experimental results, we decided to investigate the effect of analgesia on experimental AP more closely. In our work, we tested different analgesics (Bálint et al., 2022), including buprenorphine (BQ), hoping to gain a better insight into pancreatitis from the perspective of pain relief.

Kynurenic acid

Tryptophan is an essential amino acid that can only be obtained through diet. A small amount of L-tryptophan will be the precursor of two important neurotransmitters, serotonin and melatonin, or enter protein synthesis during metabolism. However, a greater proportion (95%) of L-tryptophan is metabolized via the kynurenine pathway (Figure 1). As the first step in this downward catabolic branch, L-tryptophan is converted to N-formyl-L-kynurenine by indoleamine-dioxygenase or tryptophan-dioxygenase. The expression of these two enzymes is enhanced by inflammation and stress [IL-1β, interferon-γ (IFN-γ), TNF-α, cortisol] (Zhou et al., 2021). Formamidase then metabolise N-formyl-L-kynurenine into L-kynurenine. From here, (1) kynurenine aminotransferases convert L-kynurenine to kynurenic acid (KYNA), or (2) L-kynurenine is broken down to 3-hydroxy-L-kynurenine (3-HK) and then in several steps to quinolinic acid, or picolinic acid. The final end product of the kynurenine-pathway is nicotinamide adenine dinucleotide (NAD^+) (Roth et al., 2021).

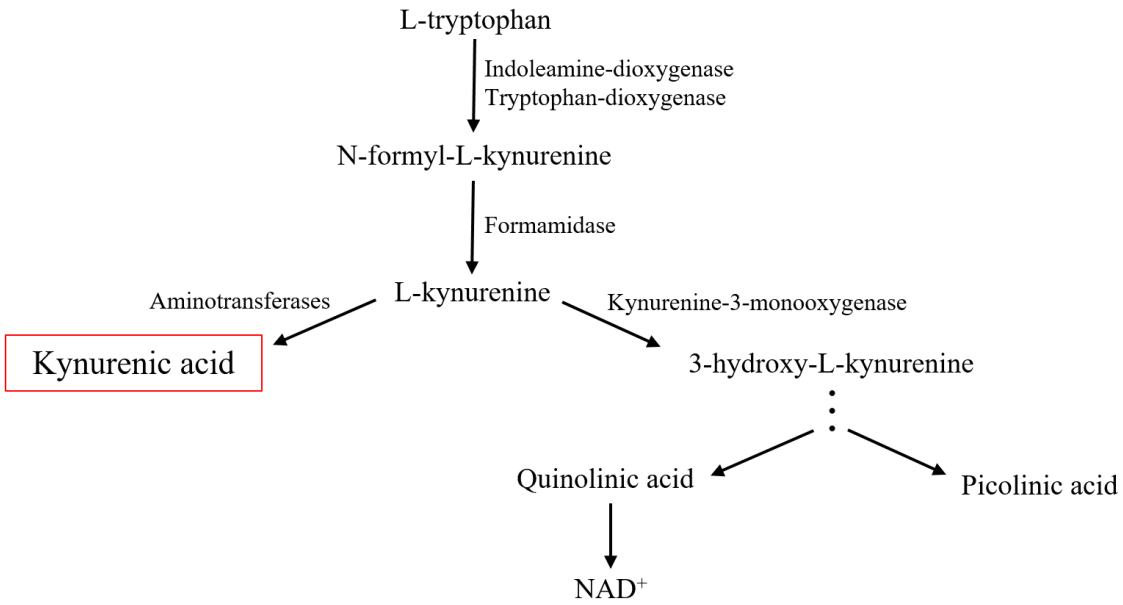

Figure 1. Kynurenine pathway. Flowchart shows only the parts relevant to this study.

KYNA acts as an antagonist at three ionotropic glutamate receptors: N-methyl-D-aspartate (NMDA), α-amino-3-hydroxy-5-methyl-4-isoxazole propionic acid (AMPA), and kainate (Tanaka et al., 2020). Several studies have already described that glutamate receptors are present in the cells of the islets of Langerhans (Marquard et al., 2015). However, the distribution of these receptors in the exocrine pancreas is unknown. Although KYNA is commonly referred to in connection with the central nervous system, it is also abundant in the gastrointestinal tract, including pancreatic juice (Paluszkiewicz et al., 2009). Furthermore, KYNA is a ligand for the G protein-coupled receptor 35 (GPR35) (Wang et al., 2006). Since its discovery in 1998 (O'Dowd et al., 1998), GPR35 has been found to be predominantly expressed in the digestive system and immune cells (Fallarini et al., 2010; Mackenzie et al., 2011). Although the detailed biochemistry and physiological role of GPR35 are not yet fully understood, it appears to play an important role in immunological processes and in the maintenance of intestinal homeostasis (Kaya et al., 2021). KYNA was also considered to be an antagonist of the α7 nicotinic acetylcholine receptor, but this finding has recently become controversial (Stone, 2020).

The role of KYNA in pathological conditions

Researchers show growing interest in the immunomodulatory properties of tryptophan-kynurenine pathway metabolites, which are important participants in cellular processes, especially in neuronal cells. They also have numerous effects on both innate and

adaptive immune responses (Mándi et al., 2012). KYNA, as an antagonist of the NMDA receptor (NMDAR), has neuroprotective effects (Vécsei et al., 2013). It reduces ischemia/reperfusion-induced retinal ganglion cell death as well (Nahomi et al., 2020). KYNA is also closely associated with intestinal inflammation. Patients with irritable bowel syndrome showed elevated mucosal and decreased plasma KYNA levels (Keszthelyi et al., 2013). It is important to note that NMDAR antagonists are a separate class of analgesics used in clinical care.

Recently, several studies have investigated SZR-72, the synthetic derivative of KYNA (Figure 2). We already know that the blood-brain barrier is impermeable to KYNA but SZR-72 can directly cross it (Fukui et al., 1991; Lukács et al., 2017). SZR-72 effectively modulates mitochondrial respiration, while KYNA could restore microcirculation in sepsis (Juhász et al., 2020).

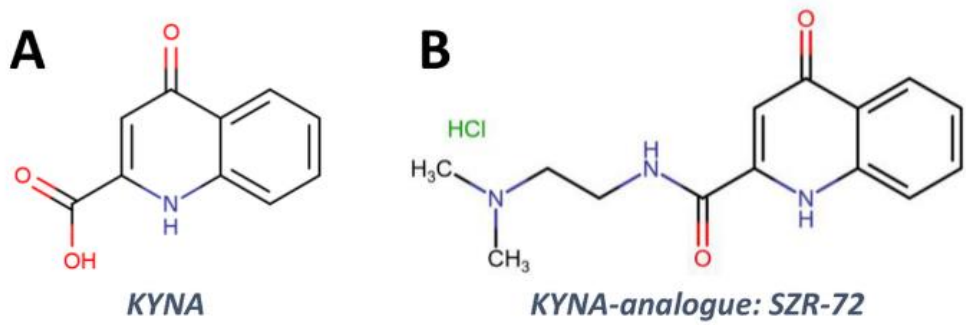

Figure 2. The structure of kynurenic acid (KYNA) and its analogue SZR-72 (2-(2-N,N-dimethylaminoethylamine-1-carbonyl)-1H-quinolin-4-one hydrochloride).

Both KYNA and SZR-72 suppress pro-inflammatory factors released by mononuclear cells and neutrophils e.g. TNF-α, high mobility group box protein 1, and human neutrophil peptide 1–3, and SZR-72 seemed to be more effective (Tiszlavicz et al., 2011). Both KYNA and SZR-72 have been reported to improve intestinal hypermotility and reduce inflammatory parameters in rat colitis through antagonism of NMDAR (Érces et al., 2012; Varga et al., 2010).

Metabolites and disturbances of the tryptophan-KYN pathway have also been shown to influence the severity of AP. Overall, 3-HK generates free radicals and causes cytotoxicity, while KYNA inhibits inflammation, prevents lipid peroxidation and ROS generation (Wang et al., 2015). 3-HK concentration is increased during AP in human samples and its plasma levels correlate with the progression of systemic inflammation and the severity of AP (Skouras et al., 2016). The inhibitors of kynurenine-3-monooxygenase reduce the production of 3-HK. Administration of such an inhibitor prevented multiple organ

failure in experimental AP in rodents (Mole et al., 2016). In contrast to 3-HK, the effect of endogenous KYNA or its synthetic derivative, SZR-72 on AP is unknown.

The GPR35 receptor should also be mentioned, as KYNA is its most potent endogenous ligand and its role has been described in several processes. It is strongly associated with type 2 diabetes, ulcerative colitis, and cardiovascular diseases (Divorty et al., 2015). Furthermore, KYNA stimulates the energy utilization of adipocytes by activating GPR35 and thus inducing lipid metabolism and anti-inflammatory gene expression (Agudelo et al., 2018). Moreover, KYNA has an antinociceptive effect via GPR35 (Cosi et al., 2011). As we can see, although we know more and more about the molecules and receptors of the KYN pathway, their role in AP remains to be discovered.

AIMS

Since there is still no specific cure for AP, the aim of this study was to find a possible starting point for future therapy, and at the same time, get closer to understanding the development and progression of AP.

1. According to the literature, KYNA and its derivative, SZR-72, have demonstrated anti-inflammatory properties in several diseases. It was therefore considered worthwhile to investigate their effect on the outcome of AP.

   Our specific aims were to investigate:

   - the effects of KYNA/SZR-72 on experimental AP and pancreatic acinar cells *in vitro*
   - whether KYNA and SZR-72 act through NMDAR

2. Pain management is essential in patients with pancreatitis. However, we do not know exactly how pain relief affects the outcome of the disease.

   Our specific aim was to investigate the effect of the partial opioid agonist buprenorphine on experimental AP.

MATERIALS AND METHODS

Materials

All chemicals were purchased from Sigma-Aldrich (Budapest, Hungary) unless indicated otherwise. SZR-72 [2-(2-N, N dimethylaminoethyl-amine-1carbonyl)-1H-quinolin-4-one hydrochloride] was synthesized by the Institute of Pharmaceutical Chemistry (University of Szeged, Hungary). The solutions used for *in vivo* measurements were freshly prepared before each experiment. L-ornithine-HCl (LO, 300 mg/ml), kynurenic acid (KYNA, 50 mg/ml), and SZR-72 (50 mg/ml) were dissolved in physiological saline (PS) and the pH of the solutions was adjusted to 7.35-7.4 (KYNA and SZR-72 precipitate above pH 7.4).

Animals

For the KYNA/SZR-72 experiments, male Sprague-Dawley rats weighing 200-250 g were used, and the analgesia (BQ) was tested on female Wistar rats of the same weight. The animals were kept at a constant room temperature of 23 °C with a 12-hour light-dark cycle and were allowed free access to water and standard laboratory chow for rodents (Biofarm, Zagyvaszántó, Hungary). Our experiments were executed according to the European Union Directive 2010/63/EU and the Hungarian Government Decree 40/2013 (II.14.). Experiments were approved by both local (University of Szeged) and national ethics committees (X/3353/2017.) for investigations involving animals.

In vivo experiments: induction of AP; treatment with KYNA, SZR-72, and BQ; tissue harvesting

Necrotizing AP was induced by a single intraperitoneal (i.p.) injection of 3 g/kg LO in the morning. KYNA or SZR-72 was administered 1 h before the induction of AP as a single i.p. injection (75, 150, 300 mg/kg). Control animals were treated with PS instead of LO, KYNA, and/or SZR-72.

BQ was administered via two routes: i.p. and intrathecally (i.t.) (Figure 3). For i.t. administration, animals were anesthetized with ketamine hydrochloride and xylazine (72 and 8 mg/kg i.p., respectively). An i.t. catheter (PE-10 tubing Intramedic, Clay Adams; Becton Dickinson; Parsippany, NJ, USA; I.D. 0.28 mm; O.D. 0.61 mm) was inserted via the cisterna

magna into the subarachnoid space 8.5 cm deep caudally (Yaksh et al., 1976). Thus, the catheter tip was placed between vertebrae Th12 and L2, at the height of the spinal segments that innervate the hind legs (Dobos et al., 2003). To prevent infections, rats received subcutaneous injections of gentamicin (10 mg/kg) right after the surgery and were housed individually. Rats that showed postoperative neurological deficits or whose hind legs were not paralyzed after administration of 100 μg lidocaine were excluded (about 10%). BQ and LO were applied after 4 days of recovery. Due to its prolonged analgesic effect, the recommended dose interval for BQ is 8 to 12 h (Foley et al., 2019). I.t. injections of 3 and 6 μg/kg BQ were given 1 h before LO and were repeated at 7 and 12 h after AP induction. 10 μL of BQ was infused through the catheter for 120 s, followed by a 10 μL flush of PS. I.p. injections of 0.1, 0.5, and 1 mg/kg BQ were given 1 h before and 12 h after the LO administration. These BQ doses are based on literature data (Guarnieri et al., 2012; Tejwani et al., 2002).

Animals were sacrificed 24 h after the LO injection (at the peak of pancreatic inflammation) by deep anesthesia with 45 mg/kg i.p. pentobarbital (Bimeda MTC, Cambridge, Canada). Blood was collected via cardiac puncture, then the pancreas was rapidly removed. Pancreatic tissue was cleaned from fat and lymph nodes on ice, then cut into pieces. One large piece was immediately frozen in liquid nitrogen and stored at –80 °C until biochemical assays were performed. Another piece of the pancreas was fixed in an 8% neutral formaldehyde solution for histological analysis. The third piece was stored in Eppendorf tubes for dry-wet weight measurement at room temperature. The last piece was frozen in cryomatrix for sectioning and immunofluorescent stainings. Blood samples were centrifuged at 2500 RCF for 15 min at 4 °C, sera were collected and stored at −20 °C until use. After LO administration, animals showed signs of sickness and became sluggish as expected. However, a few of them got depressed and lethargic within 12 h after the LO injection. The core temperature of these animals was monitored with a rectal digital thermometer. Once it decreased to a critical level (27–29 °C), rats were euthanized by pentobarbital overdose (200 mg/kg i.p.) to minimize suffering. The percentage of euthanized rats was 3% in the LO-treated groups.

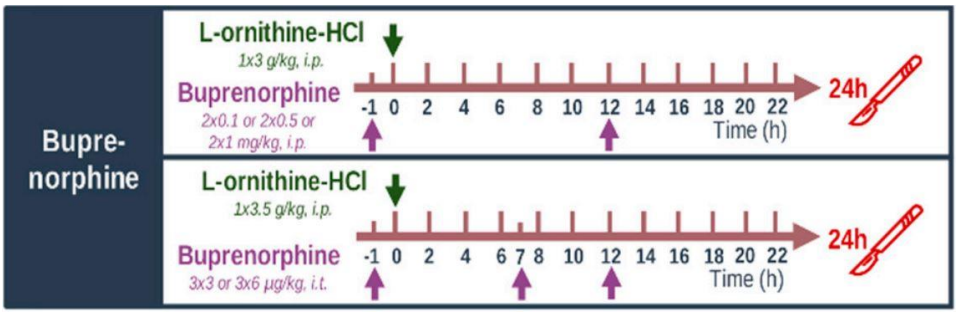

Figure 3. Schematic diagram of the experimental setup. Arrows show the injections respectively. i.p., intraperitoneal; i.t., intrathecal.

Histological analysis

Formalin-fixed pancreatic tissue samples were sectioned to a thickness of 3 µm, then stained with hematoxylin and eosin. Samples were analyzed and scored by two experts blinded to the experimental protocol (Rakonczay et al., 2008). Pancreatic edema was scored from 0-3 points (0: none; 1: patchy interlobular; 2: diffuse interlobular; 3: diffuse interlobular and intra-acinar), leukocyte infiltration from 0-4 points (0: none; 1: patchy interlobular; 2: mild diffuse interlobular; 3: moderate diffuse interlobular; 4: severe diffuse interlobular and intra-acinar). The percentage of acinar cell necrosis, as the most relevant histological feature of AP, was also evaluated.

Laboratory measurements

Serum amylase activity was measured on a Fluorostar Optima plate reader (BMG Labtech, Ortenberg, Germany) with a colorimetric kinetic method using a commercial kit purchased from Diagnosticum Zrt. (Budapest, Hungary). To evaluate tissue water content, wet weight (WW) of the pancreas was measured right after the *in vivo* experiment, then it was dried for 24 h at 100 °C. After that, dry weight (DW) was measured as well. The wet/dry weight ratio was calculated as: [(WW−DW)/WW]×100. Pancreatic MPO activity, a hallmark of leukocytic infiltration, was measured according to Kuebler et al. (1996) and was normalized to total protein content as measured by the Lowry method (1951). To determine the extent of inflammatory response in the pancreata, we measured interleukin-1β (IL-1β) levels by a commercial ELISA kit from R&D Systems (Minneapolis, MN, USA) as described by the manufacturer. Blood pH, HCO_3^-, and partial pressure of CO_2 (pCO_2) from femoral arterial blood samples were measured with a blood gas analyzer (AVL Compact 2, Graz, Austria; (Varga et al., 2010). Pancreatic heat shock protein 72 (HSP72) expression

was measured from tissue homogenate using Western blot analysis (Rakonczay et al., 2003). Briefly, pancreatic tissue was homogenized with sonication (Branson Sonifer 250; Emerson Electric, Brookfield, CT, USA) on ice in a buffer containing 10 mM Na-HEPES, 1μM $MgCl_2$, 10mM KCl, 1mM DL-dithiothreitol, 5mM iodoacetamide, 4 mM benzamidine-HCl, 1mM phenylmethyl-sulfonyl fluoride. The protein concentration of the homogenate was determined by the Bradford protein assay. 40 μg of protein was loaded per lane and samples were electrophoresed on an 8% Na-dodecyl-sulfate-polyacrylamide gel. Gels were either stained with Coomassie brilliant blue (to demonstrate equal loading of proteins for Western blot analysis) or transferred to a nitrocellulose membrane for 1 h at 100V. Membranes were blocked in 5% non-fat dry milk for 1 h and incubated with rabbit anti-HSP72 antibody [1:2500 dilution; a generous gift from István Kurucz, Biorex Laboratories, Veszprém, Hungary, that has been characterized previously (Kurucz et al., 1999)] for an additional 1 h at room temperature. The immunoreactive protein was visualized by enhanced chemiluminescence, using horseradish peroxidase-coupled anti-rabbit immunoglobulin at 1:5000 dilution (Agilent Technologies, Santa Clara, CA, USA). Quantitative analysis of results was achieved using ImageJ software (NIH, Bethesda, MD, USA). The blot images were cropped and only the relevant bands are shown in the figures.

Measurement of hemodynamics and pancreatic microcirculation

Animals were anesthetized with sodium pentobarbital (50 mg/kg) i.p. 24 h after the injection of LO and placed in a supine position on a heating pad. Tracheostomy was performed to facilitate spontaneous breathing, and the right jugular vein was cannulated with PE50 tubing for fluid administration such as Ringer's lactate infusion (10 ml/kg/h) during the experiments. A thermistor-tip catheter (PTH-01; Experimetria Ltd., Budapest, Hungary) was placed into the ascending aorta via the right common carotid artery to measure cardiac output by a thermodilution technique, using a SPEL Advanced Cardiosys 1.4 computer (Experimetria Ltd., Budapest, Hungary). The left common carotid artery was dissected free and an ultrasonic flow probe (1RS; Transonic Systems Inc., Ithaca, NY, USA) was inserted around the exposed artery to measure carotid artery flow. The right femoral artery was cannulated with PE40 tubing to collect arterial blood for pH measurements (Varga et al., 2010). Carotid artery flow (T206 Animal Research Flowmeter; Transonic Systems Inc.) and pressure (BPR-02 transducer; Experimetria Ltd., Budapest, Hungary) were measured continuously and registered with a computerized data acquisition system (Experimetria Ltd.,

Budapest, Hungary). After median laparotomy, the pancreas was carefully placed on the detector from the abdomen without disturbing the circulation. The pancreas was kept moist with wet gauze. The microcirculation of the pancreas was continuously visualized with intravital orthogonal polarization spectral imaging technique (Cytoscan A/R, Cytometrics, Philadelphia, Pennsylvania, USA). This technique utilizes reflected polarized light at the wavelength of the isosbestic point of oxy-and deoxyhaemoglobin (548 nm). As polarization is preserved in reflection, only photons scattered from a depth of 2-300 μm contribute to image formation. A 10× objective was placed onto the serosal surface of the pancreas, and microscopic recordings were made with an S−VHS video recorder 1 (Panasonic AG-TL 700, Matsushita Electric Ind. Co. Ltd, Osaka, Japan). Quantitative assessment of the microcirculatory parameters was performed off-line by frame-to-frame analysis of the videotaped images. Red blood cell velocity (RBCV, mm/s) changes in the postcapillary venules were determined in three separate fields by means of a computer-assisted image analysis system (IVM Pictron, Budapest, Hungary). All microcirculatory evaluations were performed by the same investigator (Érces et al., 2012).

Total RNA isolation and reverse transcription polymerase chain reaction

Total RNA was isolated from the control rat brain cortex and pancreas by using TRI Reagent (Molecular Research Center, Cincinnati, OH, USA) and 1 μg RNA from each sample was transcribed to complementary DNA by Maxima First Strand cDNA Synthesis Kit (Thermo Fisher, Waltham, MA, USA), according to the manufacturer's instructions. Gene-specific and exon/exon junction spanning oligonucleotide primer pairs (Table 1) for *nmdar1* and *gpr35* were designed with The Universal Probe Library Assay Design Center (Merck KGaA, Darmstadt, Germany). Primers for hypoxanthine phosphoribosyltransferase (*hprt*) gene were used as loading control. PCR was performed with DreamTaq DNA Polymerase (Thermo Fisher) in BioRad C1000 ThermalCycler (Bio-Rad Laboratories, Hercules, CA, USA). After heat inactivation for 3 min at 95 °C, cycling conditions were the following: denaturation for 10 s at 95 °C, annealing for 10 s at 50 °C, polymerization for 10 s at 72 °C (40 cycles), final extension for 3 min at 72 °C. Products were analyzed on 3% MetaPhor agarose gel (Lonza, Basel, Switzerland), then isolated fragments were sequence-verified by capillary DNA sequencing.

Primer	Sequence 5' - 3'	Product size (bp)	Gene ID
nmdar1/glun1	fwd tgtcatcccaaatgacagga	108	24408
	rvs ggctcttggtggattgtcac		
gpr35	fwd caacttggccgtgtttatca	60	367315
	rvs acctgcactgtcaggatcaa		
hprt	fwd gaccggttctgtcatgtcg	61	24465
	rvs acctggttcatcatcactaatcac		

Table 1. Primers used in the study.

Immunofluorescent stainings for NMDAR and amylase

Pancreata embedded in cryomatrix were cut into 7 µm thick slices at −20 °C with a Leica Cryostat (Leica Biosystems, Buffalo Grove, IL, United States). Slides were kept at −20 °C until processing. Immunofluorescent staining was performed in a humidified chamber at room temperature. Sections were fixed in 4% paraformaldehyde in phosphate-buffered saline (PBS) for 15 min then washed in 1× Tris-buffered saline (TBS) for 5 min, repeated 3 times. Antigen retrieval was performed in Sodium Citrate-Tween 20 buffer (0.001 M sodium-citrate buffer, pH 6.0 and 0.05% Tween 20) at 90–96 °C for 30 min. After cooling to room temperature in 1× TBS, sections were blocked with 0.01% goat serum and 5× BSA−TBS (bovine serum albumin in Tris Saline Buffer) for 1 h. Thereafter, pancreatic sections were incubated overnight with anti-NMDAR1 rabbit monoclonal antibody (1:100, ThermoFisher Scientific, Waltham, USA) at 4 °C in a humidified chamber. The following day, slides were washed 3 × 5 min in 1× TBS, then Alexa Fluor 568 goat anti-rabbit secondary antibody was added (1:500) and slides were incubated for 3 h at room temperature, covered from light. After that, co-immunostaining was performed with anti-amylase mouse monoclonal antibody (1:200) and Alexa Fluor 488 goat anti-mouse secondary antibody (1:500) as described above. Samples were washed 3 × 5 min with 1× TBS, then nuclei were counterstained with 2.5 µg/ml Hoechst 33342. After washing 3 times in 1× TBS, Fluoromount Aqueous mounting medium was added. Slides were covered, then left to dry in a dark slide box. After mounting, slides were stored at 4 °C until visualizing with confocal microscopy (ZEISS LSM 880, Carl Zeiss Technika Kft., Budapest, Hungary), and images were processed with ImageJ software (NIH, Bethesda, MD, USA). For proper visibility, images were cropped from the raw images and all of them were adjusted

uniformly, brightness was increased by 20% with PowerPoint software (Microsoft, Redmond, WA, USA).

Pancreatic acinar cell isolation and viability measurement

Rat pancreatic acinar cells were isolated with collagenase digestion technique according to Pandol et al. (1982). Briefly, animals were sacrificed, and the pancreas was removed, washed, and placed into ice-cold PS, then the tissue was cleaned from fat and lymph nodes. The extracellular solution, used in the next steps contained (in mM) 120 NaCl, 5 KCl, 25 HEPES, 2 NaH_2PO_4, 2 $CaCl_2$, 1 $MgCl_2$, 5 pyruvate, 4 Na-fumarate, 4 Na-glutamate, 12 D-glucose, as well as 0.02% (wt/vol) soybean trypsin inhibitor, 0.2% (wt/vol) bovine serum albumin, 0.025% (vol/vol) minimal essential amino acids and 0.01% (vol/vol) vitamins eagle. After cleaning, the pancreas was cut into small pieces in 5 ml extracellular solution, containing 80 U/ml type 4 collagenase (Worthington Biochemical Co., Lakewood, USA). The tissue was incubated in a shaking water bath at 37 °C for 2 × 20 min. After 20 min, the supernatant was removed and 5 ml fresh collagenase solution was added to the tissue fragments. After digestion, acinar cells were washed three times with extracellular solution, then resuspended in Medium 199 solution and placed in 37 °C CO_2 incubator for 15 min. Acini were used for experiments immediately thereafter.

Isolated pancreatic acinar cells were placed into a 96-well plate and 1 μM propidium-iodide was added to each well. Fluorescence intensity was measured at excitation and emission wavelengths of 540 nm and 620 nm with a Fluorostar Optima plate reader every 5 min. The 300 mg/kg dose of KYNA, used in the *in vivo* experiments, was converted to an equimolar concentration (250 mM). After intensity stabilized (in approximately 1 h), the cells were treated with 20 mM LO, 25-2500 μM KYNA/SZR-72/NMDA according to the experimental protocol. At the end of the experiment (approximately 10 h), Triton X-100 was added to each well to kill every living cell. The intensity measured at this point was considered to represent 100% toxicity. Data were evaluated by selecting minimum (MIN) and maximum (MAX) intensities in each treatment-group. The percentage of cell death at each time point was calculated using the following formula: [(intensity-MIN)/(MAX-MIN)] ×100. Figures show the values measured at 8 h.

Neutrophil granulocyte isolation and measurement of H_2O_2 production

Neutrophil granulocytes were isolated from rats treated with PS, LO or LO + 300 mg/kg SZR-72 24 h after AP induction using Ficoll-Hypaque density gradient centrifugation. After sacrifice, blood was collected in EDTA coated tubes from each animal. Blood was gently mixed with an equal volume of 3% Dextran solution and left to sediment for 40 min. In a conical tube, the leukocyte-rich plasma was carefully added on top of Ficoll-Hypaque, forming two phases. After centrifugation (250 RCF, 40 min) polymorphonuclear and red blood cell pellet was obtained. Erythrocytes were lysed with 0.2% NaCl solution for no more than 30 sec. Immediately thereafter, lysis was stopped with ice-cold 3% NaCl solution. If red color was still visible after centrifugation, the process was repeated. Granulocytes were resuspended in PBS containing 10 mM glucose, then cells were counted in a Bürker chamber. The cell number was adjusted to 1.5×10^4/100 µl. H_2O_2 production was measured with Fluorostar Optima plate reader (BMG Labtech, Ortenberg, Germany) using Amplex Red Hydrogen Peroxide/Peroxidase Assay Kit described by the manufacturer.

Measurement of IL-1β production in isolated acinar cells

Isolated pancreatic acinar cells were placed into 6-well plates and treated with medium, LO (20 mM), KYNA (250 µM), SZR-72 (250 µM) or with the combination of LO and KYNA/SZR-72 for 6 h. Next, the cells were washed with PBS, then the washing buffer was removed and the cells were frozen at –80 °C until further processes. After adding 200 µL homogenization buffer (10 mM Na-HEPES, 1 µM $MgCl_2$, 10 mM KCl, 5 mM iodoacetamide, 4 mM benzamidine-HCl, 1 mM DL-Dithiothreitol, 1 mM Phenylmethyl sulfonyl fluoride) to the first well, the cells were scratched from the bottom. Further 100 µL homogenization buffer was used to collect the remaining cells. After that, the collected cell suspension was added to the next well (same treated group) and the scratching process was repeated. 50 µL cell-free homogenization buffer was used to wash and collect the remaining cells. With this process, two wells were pooled into one microcentrifuge tube. After 3 × 15 s sonication, the homogenate was incubated for 20 min at 0 °C. Then, the homogenates were centrifuged with 20000 RCF at 4 °C for 20 min and the supernatants were kept for further measurements. To determine the degree of inflammatory response in the acinar cells, IL-1β levels were measured by a commercial ELISA kit from R&D Systems as described by the manufacturer.

Statistical analysis

Data are presented as means ± SEM. Experiments were evaluated by one-way ANOVA followed by Holm-Sidak post hoc test or two-way ANOVA followed by Bonferroni post hoc test (SPSS, IBM, Armonk, NY, USA). $P < 0.05$ was accepted as statistically significant.

RESULTS

Dose-dependent effects of KYNA and SZR-72 on the severity of AP

Three different doses of KYNA were tested to determine its effects on LO-induced AP (Figure 4). Representative histological images show morphological changes of the pancreas in different groups (Figure 4A). Administration of LO alone induced necrotizing AP, whereas 300 mg/kg KYNA significantly reduced LO-induced pancreatic tissue injury. A marked increase of pancreatic edema was detected in the LO-treated group compared to control, while the highest dose of KYNA (300 mg/kg) significantly reduced it (Figures 4B, C). Leukocyte infiltration into the pancreas and tissue MPO activity also significantly increased in the AP group compared to control (Figures 4D, E). As seen in case of edema, the 300 mg/kg dose of KYNA significantly reduced both leukocyte infiltration and MPO activity during AP, whereas lower doses of KYNA were ineffective. The most important measure of pancreatic inflammation is tissue damage (necrosis), which was highly severe as a result of LO treatment (Figure 4F), but was significantly reduced in the 300 mg/kg KYNA group. Serum amylase activity also increased in the LO group, while 150 and 300 mg/kg KYNA significantly reduced the enzyme activity (Figure 4G). Overall, the two lower doses (75 and 150 mg/kg) of KYNA did not significantly influence most of the measured values, but 300 mg/kg KYNA reduced the severity of AP.

Similar results to KYNA were obtained when the effect of different doses of its analogue, SZR-72 was examined (Figure 5). Histological images show the effects of LO and the co-treatment of LO and SZR-72 (Figure 5A). The 300 mg/kg dose of SZR-72 was able to significantly reduce the AP-evoked increases in pancreatic edema and leukocyte infiltration (Figures 5B, D). These results were also supported by measurements of pancreatic water content and MPO activity (Figures 5C, E). The score of pancreatic tissue damage was significantly reduced by the highest dose of SZR-72 in AP (Figure 5F). Serum amylase activity increased in response to LO injection, which was decreased by all SZR-72 doses (Figure 5G). Overall, AP severity parameters were reduced by 300 mg/kg SZR-72 treatment.

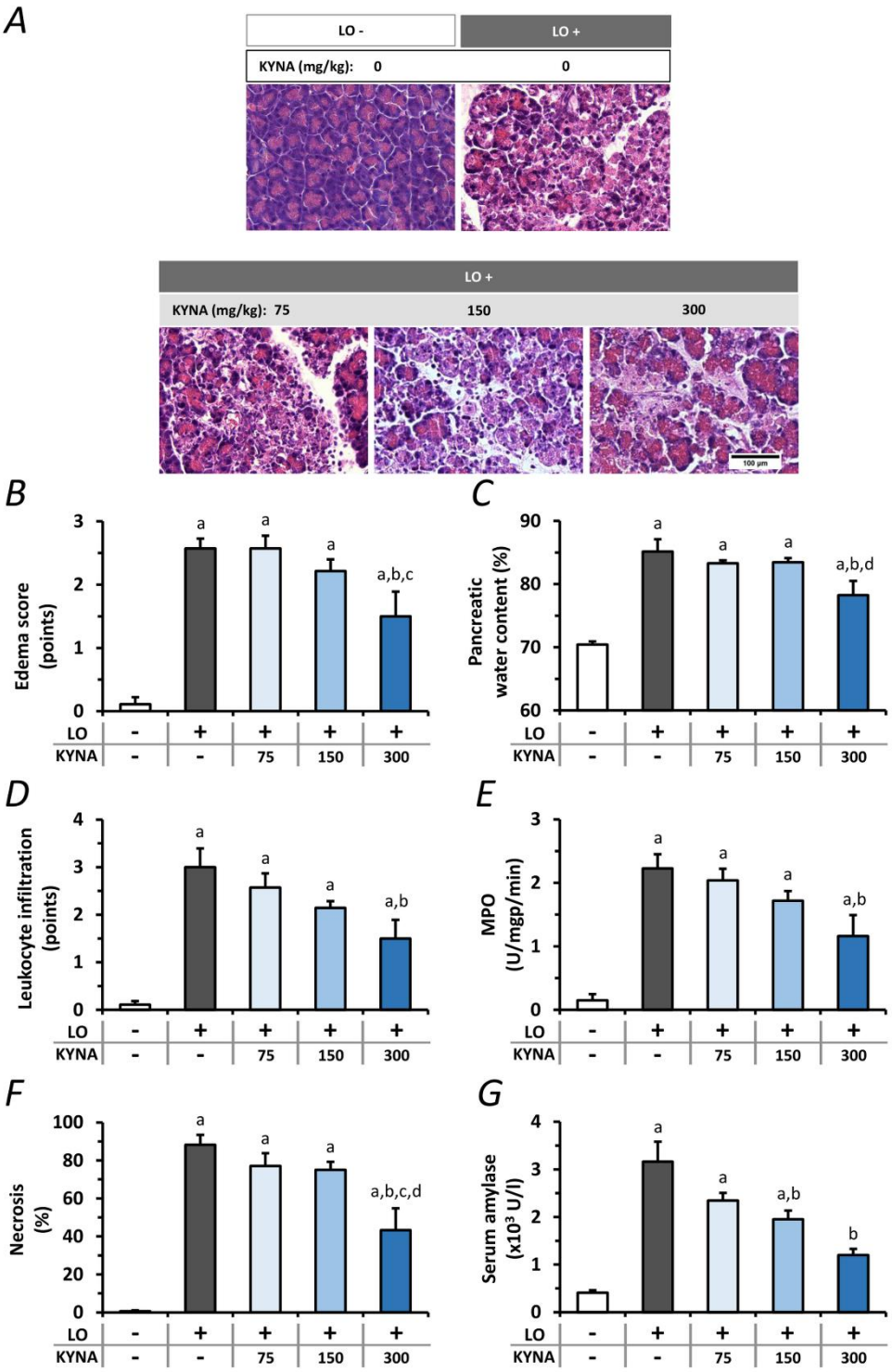

Figure 4. The effects of kynurenic acid (KYNA) on the severity of acute pancreatitis (AP). (A) Representative histopathological images of pancreatic tissues of the treatment groups. Bar charts show the extent of pancreatic **(B)** edema, **(C)** water content, **(D)** leukocyte infiltration, **(E)** myeloperoxidase (MPO) activity, **(F)** necrosis, and **(G)** serum amylase activity measurements. Values represent means with standard error, n=5-14. One-way ANOVA was performed followed by Holm-Sidak post-hoc test. Statistically significant differences ($p<0.05$) were marked with: (a) vs. control; (b) vs. LO; (c) vs. LO+75 mg/kg KYNA; (d) vs. LO+150 mg/kg KYNA. AP, acute pancreatitis; KYNA, kynurenic acid; LO, L-ornithine-HCl; MPO, myeloperoxidase.

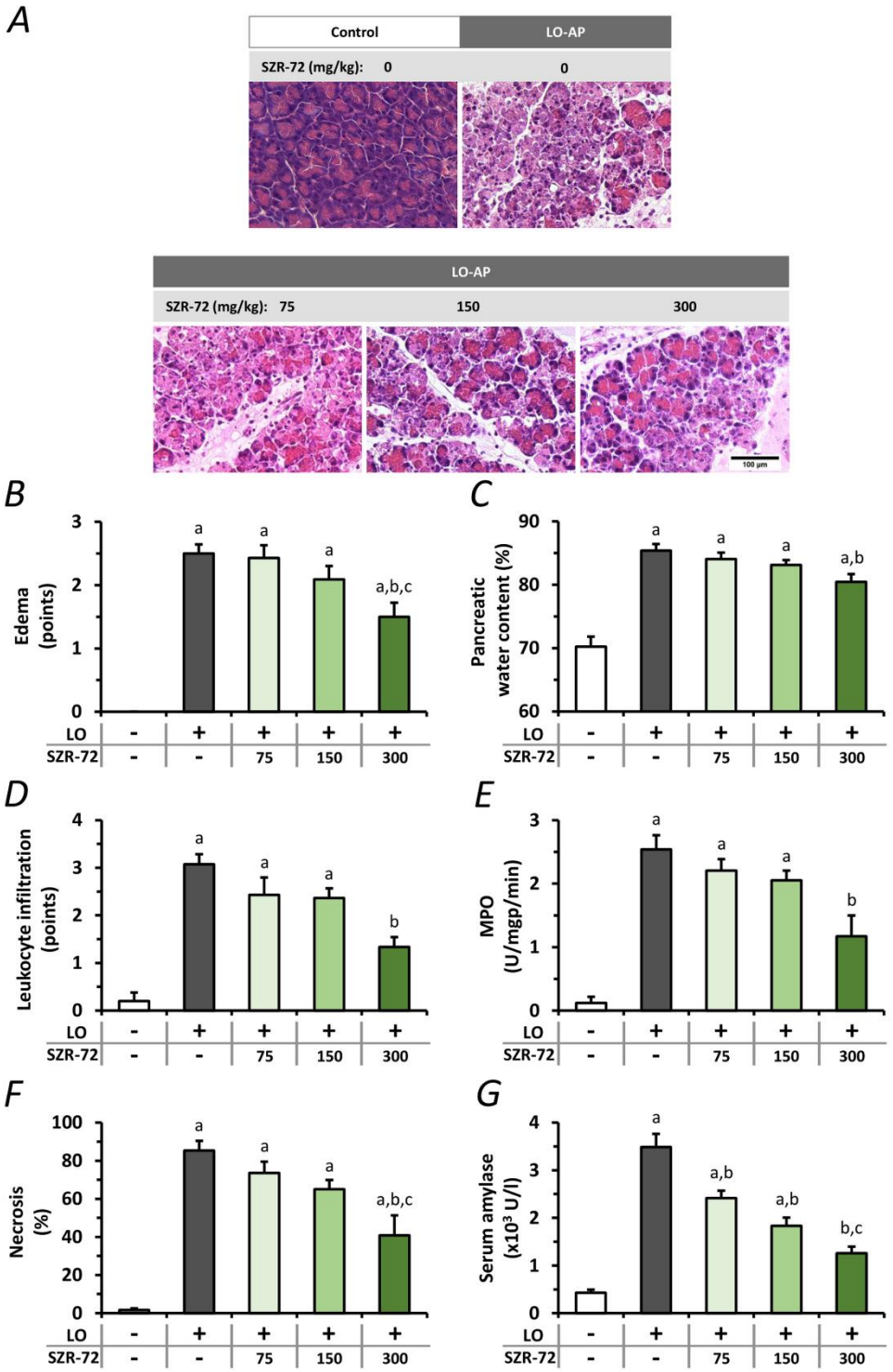

Figure 5. The effects of SZR-72 on the severity of AP. (A) Representative histopathological images of pancreatic tissues of the treatment groups. Bar charts show the extent of pancreatic **(B)** edema, **(C)** water content, **(D)** leukocyte infiltration, **(E)** myeloperoxidase (MPO) activity, **(F)** necrosis, and **(G)** serum amylase activity measurements. Values represent means with standard error, n=5-11. One-way ANOVA was performed followed by HolmSidak post-hoc test. Statistically significant differences ($p<0.05$) were marked with: (a) vs. control; (b) vs. LO; (c) vs. LO+75 mg/kg SZR-72. LO, L-ornithine-HCl; MPO, myeloperoxidase.

The effects of KYNA and SZR-72 treatment on microcirculation and hemodynamic parameters in AP

Microcirculatory and hemodynamic changes during AP and KYNA/SZR-72 treatment (300 mg/kg) were measured (Figure 6). AP significantly increased cardiac output and carotid artery flow compared to the control animals (Figures 6A, B). Cardiac output in rats with AP was reduced to control level by both KYNA and SZR-72, whereas the decrease in carotid artery flow was significant only in the case of SZR-72. Mean arterial blood pressure was similar in all experimental groups (Figure 6C). Pancreatic microcirculation was quantified by measuring serosal RBCV (Figure 6D). Interestingly, microcirculation significantly decreased in LO-induced AP compared to the control group. However, pre-treatment with KYNA or SZR-72 was able to improve microcirculation during AP. AP also caused a significant drop in arterial blood pH and bicarbonate concentration, resulting in metabolic acidosis, which was restored to the control level by KYNA and SZR-72 pre-treatments as well (Figures 7A, B). At the same time, there was no detectable difference in arterial pCO_2 between the examined groups (Figure 7C).

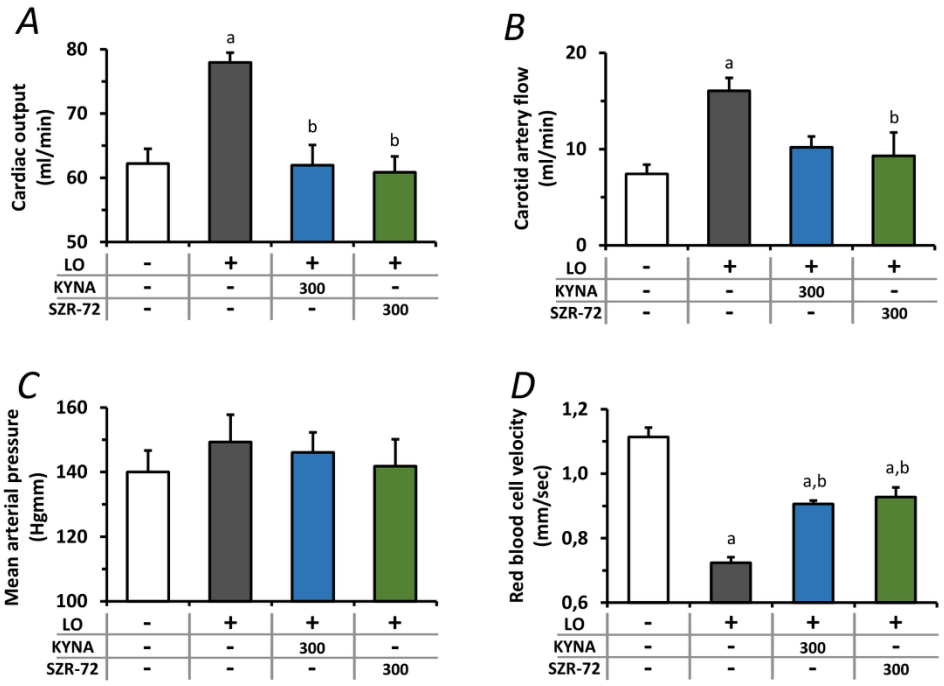

Figure 6. Changes in circulation and haemodynamic parameters during experimental AP and treatments with KYNA and SZR-72. Bar charts show **(A)** cardiac output, **(B)** carotid artery flow **(C)** mean arterial pressure, and **(D)** red blood cell velocity. Values represent means with standard error, (A–C) n=3-6; (D) n=60-98. One-way ANOVA was performed followed by Holm-Sidak post-hoc test. Statistically significant differences ($p<0.05$) were marked with: (a) vs. control; (b) vs. LO. LO, L-ornithine-HCl.

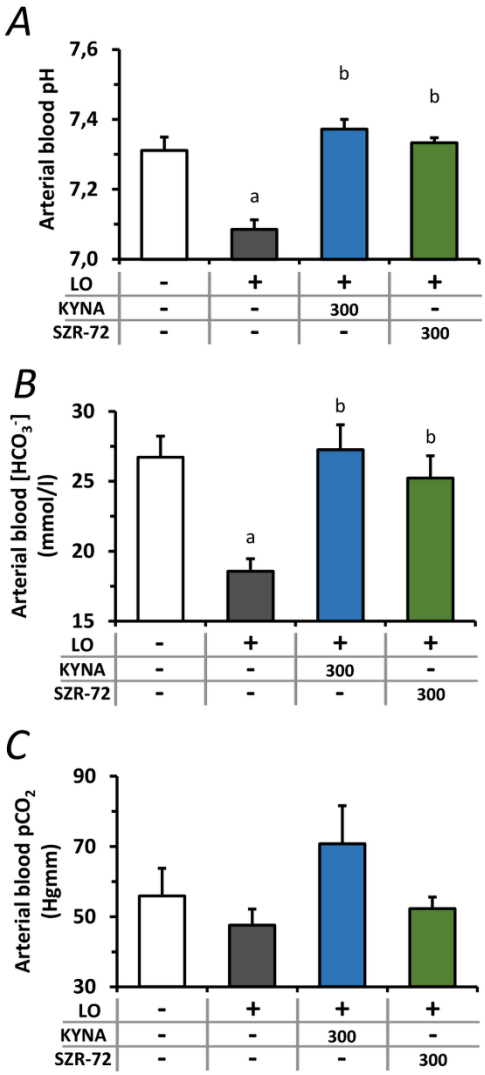

Figure 7. Plasma pH and HCO_3^- and pCO_2 levels during experimental AP and treatments with KYNA and SZR-72. Bar charts show **(A)** arterial blood pH, **(B)** arterial blood HCO_3^- concentration, and **(C)** arterial blood CO_2 pressure. Values represent means with standard error, n=3-6. One-way ANOVA was performed followed by Holm-Sidak post-hoc test. Statistically significant differences ($p<0.05$) were marked with: (a) vs. control; (b) vs. LO. LO, L-ornithine-HCl.

Changes in pancreatic IL-1β and HSP72 expression in AP upon KYNA and SZR-72 treatment

KYNA and SZR-72 alone did not affect the pancreatic IL-1β content (Figure 8A). However, the amount of IL-1β was significantly increased in the LO group compared to controls (Figure 9A). In animals with AP treated with KYNA or SZR-72, the amount of IL-1β was reduced to the level of control. As a member of the HSP70 family, HSP72 is the major stress-induced protective chaperone in mammalian cells. First, we examined how KYNA and SZR-72 treatment affects pancreatic HSP72 levels in physiological conditions

(Figures 8B, C) and during AP (Figures 9B, C). Interestingly, both KYNA and SZR-72 alone significantly increased HSP72 expression compared to the control group, and SZR-72 had a more prominent effect on HSP72 protein expression than KYNA (Figures 8B, C). In our experiments, it was clear that the level of HSP72 was elevated in AP compared to the control group (Figures 9B, C). However, when the animals also received KYNA or SZR-72 pre-treatment, the amount of HSP72 significantly increased even compared to the AP group without KYNA or SZR-72.

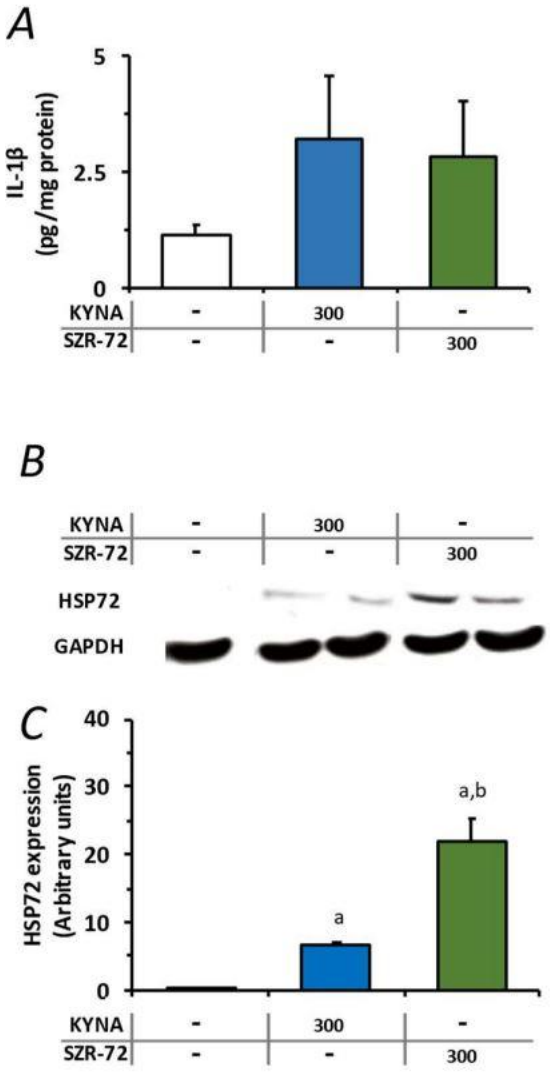

Figure 8. Changes in interleukin 1 beta (IL-1β) and heat shock protein 72 (HSP72) levels during treatments with 300 mg/kg KYNA or SZR-72 in rats. (A) Pancreatic IL-1β level, **(B)** representative Western blot images of pancreatic HSP72 and glicerinaldehide-3-phosphate-dehydrogenase (GAPDH) levels, and **(C)** densitometry of Western Blot images for pancreatic HSP72 level. Values represent means with standard error, n=7-10. One-way ANOVA was performed followed by Holm-Sidak post-hoc test. Statistically significant differences ($p<0.05$) were marked with: (a) vs. control; (b) vs. KYNA.

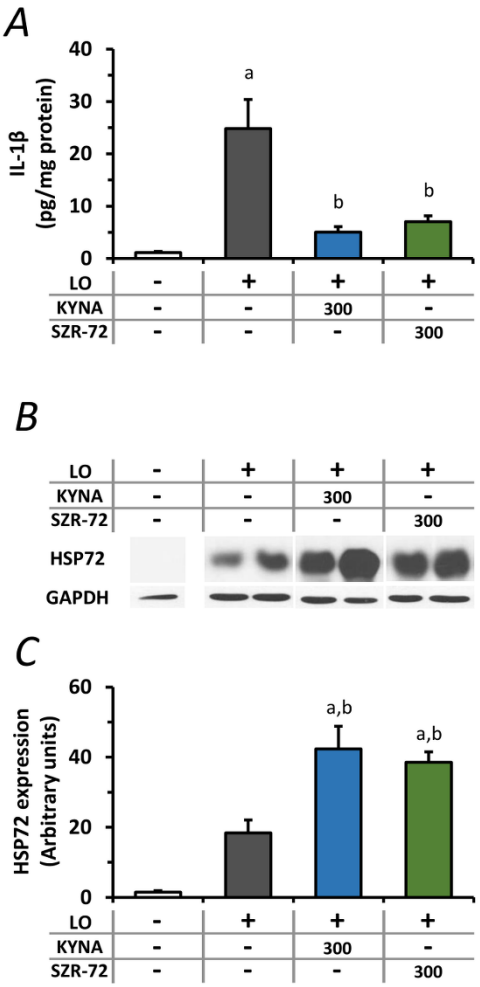

Figure 9. Changes in pancreatic interleukin 1β (IL-1β) and heat shock protein 72 (HSP72) levels in AP in rats treated with 300 mg/kg KYNA or SZR-72. (A) Pancreatic IL-1β level, **(B)** representative Western blot images of pancreatic HSP72 and glycerinaldehyde-3-phosphate-dehydrogenase (GAPDH) levels, and **(C)** densitometry of Western Blot images for pancreatic HSP72 level. Values represent means with standard error, n=7-10. One-way ANOVA was performed followed by Holm-Sidak post-hoc test. Statistically significant differences ($p<0.05$) were marked with: (a) vs. control; (b) vs. LO.

The expression of NMDAR1 and GPR35 in the pancreas

NMDAR1 expression was investigated by RT-PCR and immunohistochemistry, GPR35 expression was examined by RT-PCR (Figure 10). In both methods, brain tissue was used as a positive control. *Gpr35* gene expression was nearly equal in the brain and pancreas, while *nmdar1* expression was much lower in the pancreas than in the brain (Figure 10A). This was also confirmed by immunohistochemistry, where NMDAR1 staining of the brain was clearly visible (Figure 10B). The image of the control pancreas showed low NMDAR1 expression with well-structured amylase staining. The pancreas was sampled 2 and 24 h after

LO administration in order to visualize if there was a difference in NMDAR1 staining depending on how advanced the inflammation was. NMDAR1 staining was found to be more pronounced 2 h after AP induction, however, the strongest staining was observed after 24 h. In parallel, amylase staining lost its structural integrity as the inflammation progressed.

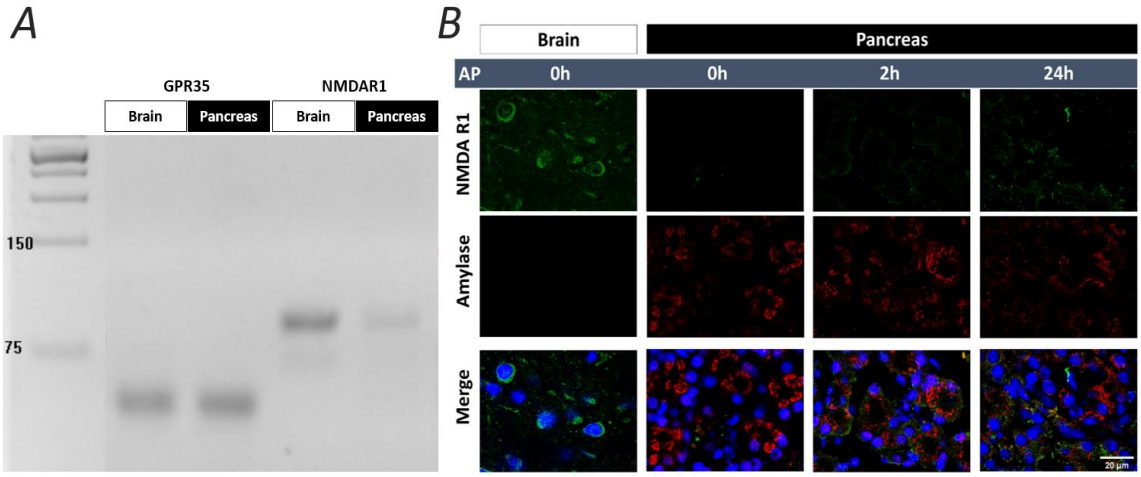

Figure 10. Detection of N-methyl-D-aspartate receptor 1 (NMDAR1) and G-protein coupled receptor 35 (GPR35) expression. (A) *Gpr35* and *nmdar1* gene expression in brain cortex and pancreas, **(B)** representative immunofluorescent images (NMDAR1, amylase, and cellular nuclei stainings) of pancreatic tissue (scale bar: 20 µm). AP, acute pancreatitis.

In vitro effects of KYNA, SZR-72, and NMDA on LO-induced acinar toxicity

The effects of KYNA and SZR-72 were investigated on LO-induced acinar toxicity in *in vitro* experiments. Since both compounds are NMDAR antagonists, NMDA was also applied to reveal whether KYNA or SZR-72 exert their effect on NMDAR. Before testing, the protective properties of KYNA and SZR-72, or their interaction with NMDAR, the safe concentrations of KYNA, SZR-72, and NMDA were determined on isolated pancreatic acinar cells (Figures 11A, 12). SZR-72 can be administered safely up to a concentration of 500 µM, and concentrations above this were toxic to acinar cells (Figure 12). As the 300 mg/kg dose of KYNA proved to be effective *in vivo*, the corresponding, equimolar (250 µM) and ten times higher (2500 µM) concentrations of KYNA and NMDA were tested on acini. In case of SZR-72, only the 250 µM concentration was used in further viability studies because the ten times higher concentration has been already proven to be toxic. Neither KYNA nor NMDA affected pancreatic acinar viability even at a concentration of 2500 µM (Figure 11A). Then we measured the effect of LO treatment on cell viability and

whether it could be affected by KYNA, SZR-72, or NMDA (Figure 11B). LO was shown to be highly toxic to pancreatic acinar cells.

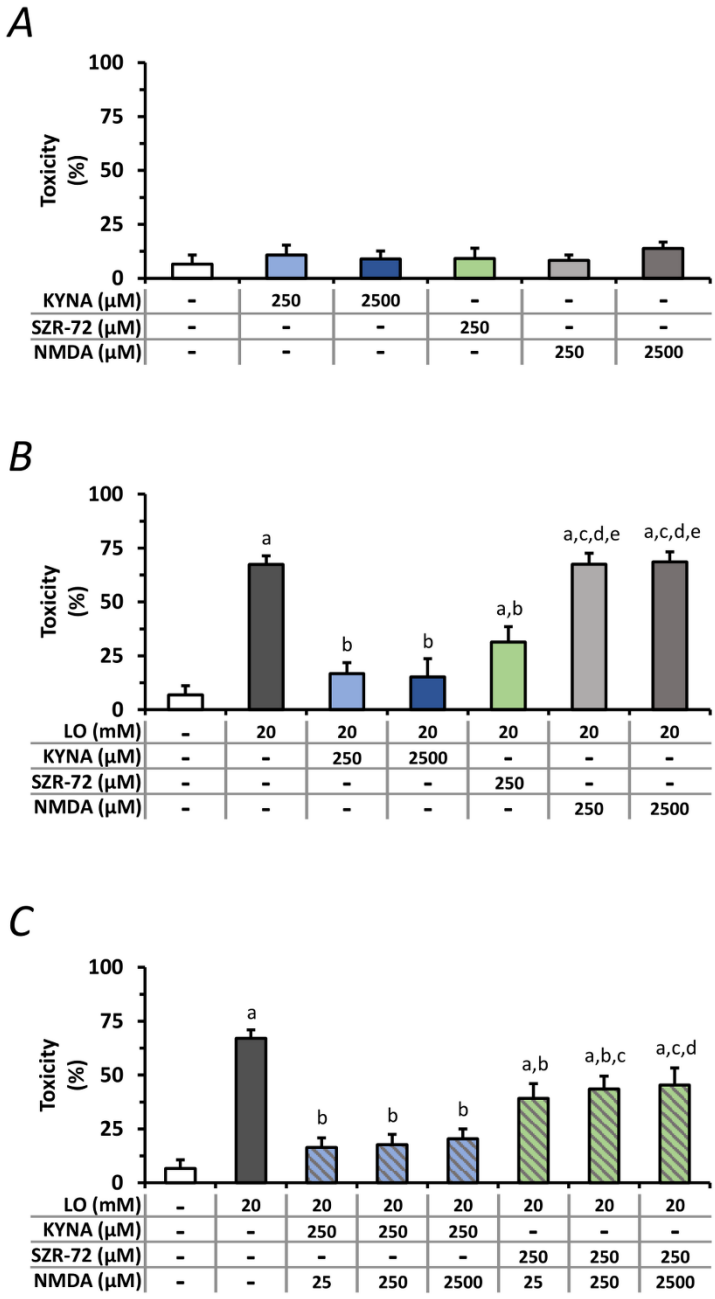

Figure 11. Toxicity measurements on isolated pancreatic acinar cells. (A) Toxicity of KYNA, SZR-72, and N-methyl-D-aspartate (NMDA) in different concentrations. **(B)** Toxic effect of L-ornithine-HCl (LO) combined with KYNA, SZR−72 or NMDA treatments. One-way ANOVA was performed followed by Holm-Sidak post-hoc test. Statistically significant differences ($p<0.05$) were marked with: (a) vs. control; (b) vs. LO; (c) vs. LO+250 µM KYNA; (d) vs. LO+2500 µM KYNA; (e) vs. LO+250 µM SZR72. **(C)** Toxicity of co-treatment of LO (20 µM) and NMDA (25, 250, 2500 µM) combined with 250 µM KYNA or SZR-72. One-way ANOVA was performed followed by Holm-Sidak post-hoc test. Statistically significant differences ($p<0.05$) were marked with: (a) vs. control; (b) vs. LO; (c) vs. LO+250 µM KYNA+25 µM NMDA; (d) vs. LO+250 µM KYNA+250 µM NMDA. Values represent means with standard error, n=4-10.

However, KYNA prevented the toxic effect of LO at both 250 and 2500 µM concentrations and cell viability was comparable to the control group. Treatment with 250 µM SZR-72 also significantly reduced LO-induced toxicity. NMDA did not affect the toxicity of LO at any concentrations. Last, we examined whether the beneficial effects of KYNA and SZR-72 could be suspended by the addition of NMDA (Figure 11C). Besides LO, acinar cells were subjected to 250 µM KYNA or SZR-72 and increasing doses of NMDA (25, 250, 2500 µM). Co-treatment with NMDA had no effect on cell viability. KYNA and SZR-72 were still able to significantly reduce toxicity compared to the LO group. Moreover, KYNA treatment reduced cellular toxicity to a level that was equivalent to the control group.

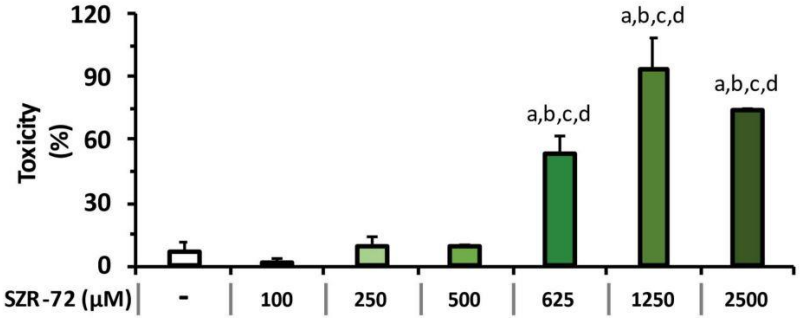

Figure 12. Concentration-dependent toxicity of SZR-72. Values represent means with standard error, n=4-10. One-way ANOVA was performed followed by Holm-Sidak post-hoc test, $p<0.05$. (a) vs. control; (b) vs. 100 µM SZR-72; (d) vs. 250 µM SZR-72; (e) vs. 300 µM SZR-72.

SZR-72 reduces H_2O_2 production in isolated neutrophil granulocytes, but it does not affect the IL-1β expression of pancreatic acinar cells

Neutrophil granulocytes play an important role in the development of AP. Their function is characterized by their H_2O_2 production. The effect of SZR-72 was determined on neutrophil granulocyte function (Figure 13). H_2O_2 production of granulocytes was examined after cell isolation from control, LO-, and LO + SZR-72-treated animals. In case of control granulocytes, H_2O_2 production remained at baseline throughout the experiment. In contrast, neutrophils from AP animals produced increased amounts of H_2O_2, the level of which was significantly higher than the control group from as early as 20 min. However, when neutrophils from LO and SZR-72 co-treated animals were examined, a significant decrease was observed in H_2O_2 production from 70 min compared to LO treatment alone.

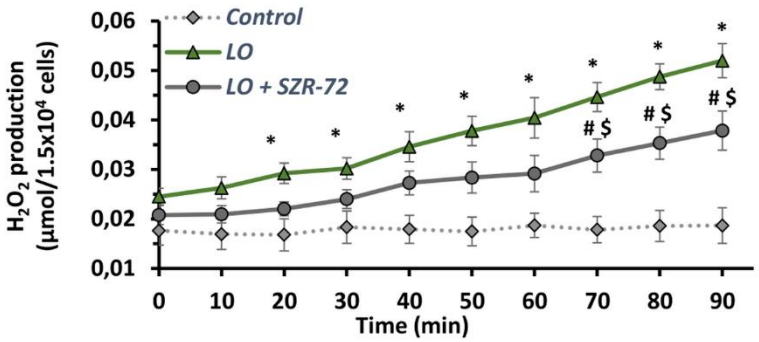

Figure 13. Time course of H_2O_2 production of neutrophil granulocytes isolated from rats treated with physiological saline, LO or LO+300 mg/kg SZR-72. Values represent means with standard error, n=4. Two-way ANOVA was performed followed by Bonferroni post-hoc test. Statistically significant differences ($p<0.05$) were marked with: (*) control vs. LO; (#) LO vs. LO+SZR-72; ($) control vs. LO+SZR-72.

The IL-1β protein expression of isolated acinar cells was measured *in vitro* after 6 h treatment with LO, KYNA, and/or SZR-72 (Figure 14). LO administration did not induce any change in IL-1β expression compared to the control group in acinar cells. Furthermore, KYNA, SZR-72, or their combinations with LO did not affect the proinflammatory cytokine production.

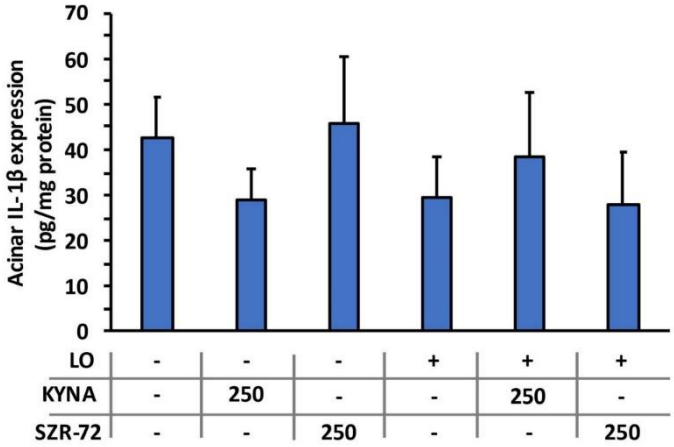

Figure 14. Acinar IL-1β concentrations remain unchanged after treatment with L-ornithine (LO), KYNA, and/or SZR-72. Bar chart shows IL-1β concentrations 6h after the treatments with 20 mM LO, 250 µM KYNA, and/or 250 µM SZR-72 using isolated rat pancreatic acinar cells. Values represent means with standard error, n=7-14. One-way ANOVA was performed followed by Holm-Sidak post-hoc test.

BQ administration has no significant effect on the severity of AP

Two administration routes were investigated for BQ (i.p., i.t.). BQ alone did not cause histological abnormalities in the pancreas. I.p. BQ in the tested doses (2 × 0.1, 2 × 0.5, 2 × 1 mg/kg) did not affect the LO-induced cell damage and leukocyte infiltration in the pancreas, or amylase activity in the serum (Figure 15A–C, E). However, the water content of the pancreas was slightly increased by the 2 × 1 mg/kg dose of BQ (Figure 15D). For the i.t. route of administration, 3 × 3 mg/kg BQ did not affect any of the measured parameters, whereas the higher, 3 × 6 mg/kg dose significantly reduced leukocyte infiltration (Figure 16).

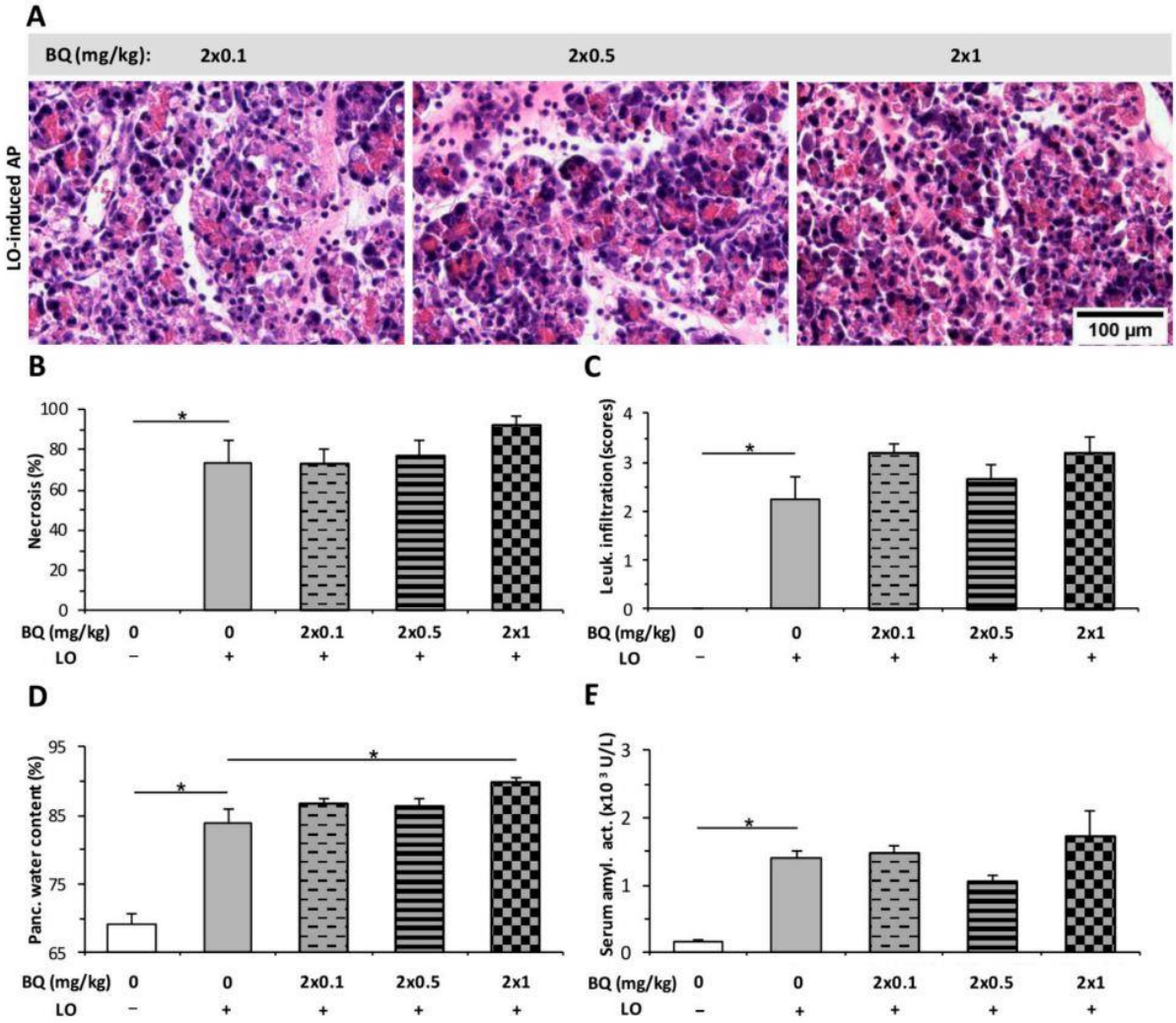

Figure 15. Intraperitoneal (i.p.) buprenorphine (BQ) treatment does not affect the severity of L-ornithine (LO)-induced acute pancreatitis (AP). (A) Representative histopathological images of pancreatic tissue of the treatment groups. Bar charts show the extent of pancreatic **(B)** necrosis, **(C)** leukocyte infiltration, **(D)** water content, and **(E)** serum amylase activity measurements. Values represent mean with standard error, n=6. Two-way ANOVA was performed followed by Holm-Sidak post-hoc test, $p<0.05$.

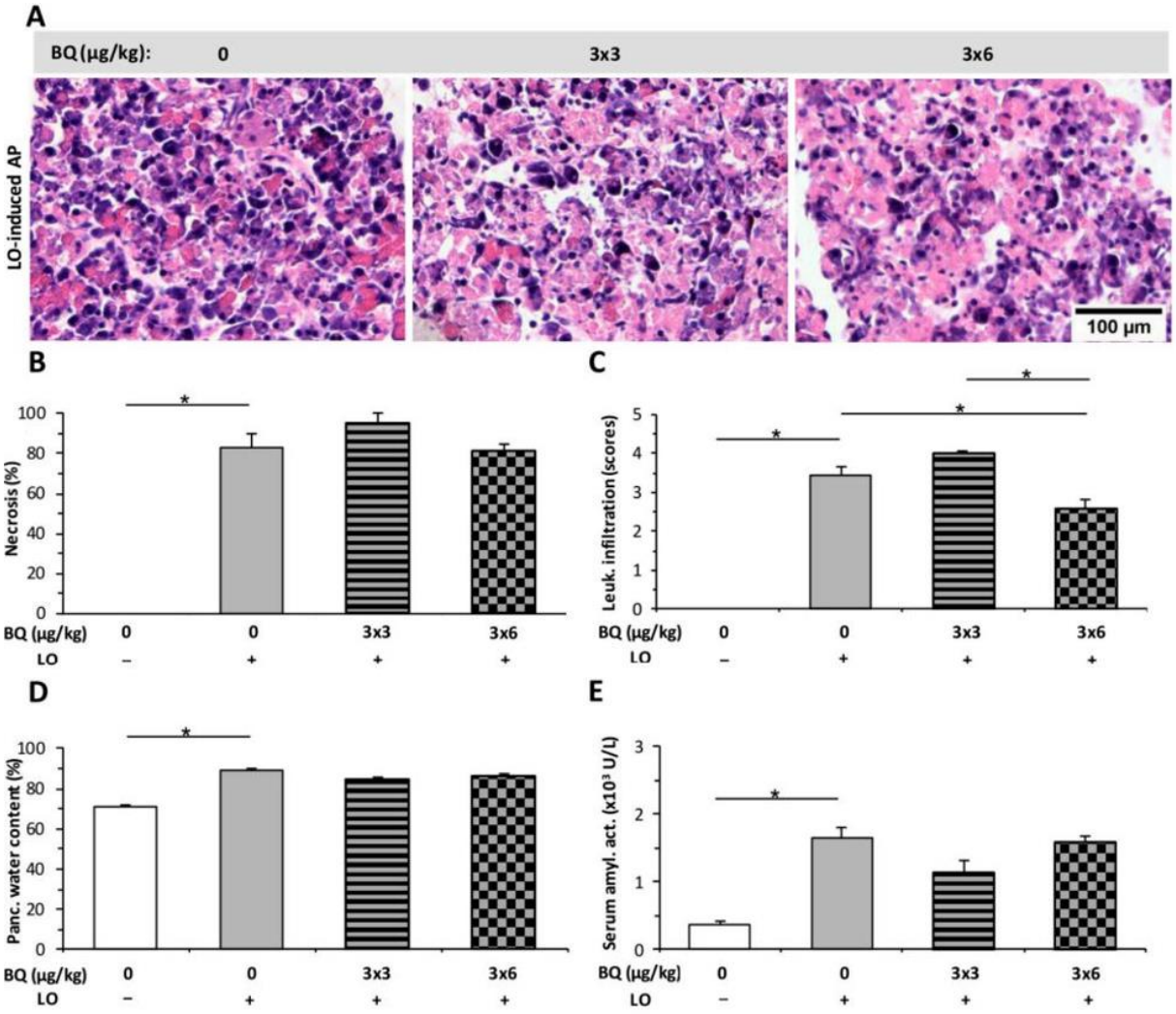

Figure 16. Intrathecal (i.t.) buprenorphine (BQ) treatment does not affect the severity of L-ornithine (LO)-induced acute pancreatitis (AP). (A) Representative histopathological images of pancreatic tissue of the treatment groups. Bar charts show the extent of pancreatic **(B)** necrosis, **(C)** leukocyte infiltration, **(D)** water content, and **(E)** serum amylase activity measurements. Values represent mean with standard error, n=6. One-way ANOVA was performed followed by Holm-Sidak post-hoc test, $p<0.05$.

DISCUSSION

As AP is a disorder without specific therapy, it is important to find possibilities for its management. The pathophysiology of the disease involves multiple cell types and processes (Barreto et al., 2021). The pathway of tryptophan metabolism is unambiguously disturbed during AP, resulting in overactivation of the kynurenine-3-monooxygenase enzyme and excess production of pro-inflammatory 3-HK (Mole et al., 2016; Skouras et al., 2016). In this study, we tested the possible application of endogenous tryptophan pathway metabolite KYNA, and its synthetic derivative SZR-72 for the treatment of experimental AP. Our novel findings with KYNA or SZR-72 administration in experimental AP are the following: They (1) dose-dependently reduced the severity of the disease; (2) reduced the pro-inflammatory cytokine IL-1β expression *in vivo*; (3) increased the synthesis of HSP72; (4) reduced the extent of metabolic acidosis; (5) restored pancreatic microcirculation; (6) suppressed the function of neutrophil granulocytes. (7) In addition, their effect was likely to be independent of acinar NMDAR. SZR-72 can cross the blood-brain barrier, while KYNA is poorly permeable (Fukui et al., 1991; Lukács et al., 2017). Therefore, SZR-72 can exert its effect on the central nervous system as well (Demeter et al., 2013; Kassai et al., 2015). As the results with SZR-72 and KYNA were similar, we do not think that the possible central nervous system effects of SZR-72 play part in the protection against AP. We demonstrated that the 300 mg/kg dose of KYNA and SZR-72 exerted strong anti-inflammatory effects. Csáti et al. (2015) also used the same dose of KYNA or kynurenic acid amide 2 i.p. in rats, and observed successful suppression of inflammation evoked by trigeminal ganglion activation. Similar results were obtained when SZR-72 was administered in a trigeminal nerve activation model at a dose of 300 mg/kg i.p. in rats, which had an anti-inflammatory effect (Lukacs et al., 2016). In the case of experimental colitis in rats, even doses ten times lower have been shown to be effective (Érces et al., 2012; Varga et al., 2010). Furthermore, Juhász et al. (2020) successfully applied KYNA (2 × 15 mg/kg) and SZR-72 (2 × 23.5 mg/kg) in a sepsis model. Based on these results, it appears that the effective dose of KYNA and SZR-72 is also dependent on the disease model itself.

Our results demonstrate that during AP, in order for an animal to be able to maintain the blood supply to vital organs, i.e., mean arterial pressure, it must significantly increase its cardiac output. The most important means to do this is to increase heart rate, as total peripheral resistance cannot be adequately increased due to the inflammatory milieu caused by pancreatitis. However, when the animals were also treated with KYNA or SZR-72 in

addition to LO, mean arterial pressure did not decrease even at normal cardiac output. That is, the autonomic nervous system did not have to intervene to maintain circulation. This suggests that KYNA and SZR-72 prevent life-threatening hemodynamic imbalance caused by pancreatitis. It is likely to provide protection against the release of such an amount of pro-inflammatory mediator and cytokine that would lead to the severe intravascular volume depletion, vasodilation, and hypoperfusion expected in AP. In addition to restoring total peripheral resistance, KYNA/SZR-72 treatment may play a role in reducing heart rate. Similar findings were found by Badzynska et al. (2020) in spontaneously hypertensive rats, where 25 mg/kg/day KYNA treatment reduced heart rate. Pain may serve as an explanation, as pain is an unavoidable symptom of AP and is directly responsible for the increase in heart rate (Tousignant-Laflamme et al., 2005). As NMDA antagonists are a distinct class of analgesics, one obvious explanation for our *in vivo* results may be the analgesic effect of KYNA and SZR-72. GPR35 receptor is considered important for nociceptive transmission (Cosi et al., 2011), and through this receptor, KYNA could reduce pain, which could contribute to the reduced heart rate.

This is partly what gave us the idea to investigate the effect of analgesia in experimental AP (Bálint et al., 2022). Opioids are commonly used for pain management in patients with AP, although their effect on AP progression is not yet fully understood. Our experiments examined the effect of the partial opioid receptor agonist BQ in LO-induced necrotizing AP. No substantial adverse complication was observed as an effect of BQ; only the pancreatic tissue water content was increased after the highest i.p. dose. The lower i.t. dose left all the measured parameters unchanged and did not affect the severity of the disease. However, the higher i.t. dose significantly reduced leukocyte infiltration. We first demonstrated the effect of spinally applied BQ on AP. BQ given intravenously in a Na-taurocholate-induced model did not influence the severity of pancreatitis, and when administered subcutaneously in cerulein-induced AP, it reduced the zymogen content and protein synthesis of pancreatic acini (Ogden et al., 1994). Both our results and literature data support that BQ may be a beneficial analgesic in AP.

AP causes the impairment of both pancreatic and systemic microcirculation (Cuthbertson et al., 2006), which are among the early signs of AP (Dobosz et al., 2004). We showed significantly decreased RBCV in the pancreas during experimental AP, which was remarkably restored by the administration of KYNA and SZR-72 as well. The reduced organ microcirculation contributes to ischemia and organ failure, not just in the pancreas but in other organs like the kidneys or lungs. Therefore, KYNA or SZR-72 can alleviate the

symptoms of multiple and/or persistent organ failure which is present in the severe form of the disease. Furthermore, Zhang et al. (2020) found that a decrease in intestinal microcirculation secondary to severe AP can lead to reduced mucosal barrier integrity and immunity, thus increasing the possibility of infection, sepsis, and mortality. Based on this, the beneficial effect of KYNA and SZR-72 on microcirculation is important and should be further investigated. Interestingly, KYNA was found to improve ileal microcirculation in a sepsis model, whereas SZR-72 was ineffective (Juhász et al., 2020). However, in this model, SZR-72 improved mitochondrial respiration, resulting in better conversion of ADP to ATP. In the present research, the study of mitochondrial function was out of focus. Nevertheless, mitochondrial dysfunction is common in AP and has serious consequences (Barreto et al., 2021), so further studies are needed to explore how KYNA or its derivatives modulate it. AP is often accompanied by acid-base disturbance, and there is an association between the severity of AP and metabolic acidosis (Rumbus et al., 2018). Meta-analysis of clinical trials confirmed that the severity of AP is related to the degree of metabolic acidosis. In addition, experimental AP exacerbated pre-existing acid-base imbalance. Several mechanisms trigger metabolic acidosis during AP: loss of bicarbonate-rich pancreatic juice through pancreatic fistula or drainage; lactic acidosis due to shock or sepsis (Zhan et al., 2015). An important observation in the present study was that both KYNA and SZR-72 were effective in restoring decreased plasma pH and HCO_3^- concentration. The exact mechanism by which they affect acid-base balance is unknown, but this action may also contribute to reducing the severity of the disease. HSP72 is an inducible chaperone that is upregulated in the cell under stressful conditions, such as inflammation. It was found earlier that thermal stress-induced HSP72 increase could protect against AP (Bhagat et al., 2002; Wagner et al., 1996), and pharmacological induction of HSP72 with BRX-220 also significantly improved the outcome of experimental AP (Rakonczay et al., 2002; Rakonczay et al., 2003). Furthermore, overexpression of HSP72 in transgenic mice enhanced recovery from AP (Lunova et al., 2012). In our study, we demonstrated not only LO-induced pancreatitis increased greatly HSP72 expression, but also KYNA and SZR-72 treatment alone without AP. However, when animals with pancreatitis were pretreated with KYNA or SZR-72, HSP72 expression was even far more elevated. SZR-72 was a considerably more potent HSP72-inducer than KYNA. The effect of KYNA and SZR-72 on HSP72 may be one of the mechanisms by which they protect against AP.

NMDAR1 was expressed in pancreatic tissue even under physiological conditions. Surprisingly, NMDAR1 protein expression was increased by the progression of AP. This

phenomenon could be explained by three reasons: (1) pancreatic cells (e.g. acinar, ductal, beta cells) increased their expression of NMDAR1; (2) invading leukocytes express the receptor; (3) the previous two together. Therefore, we examined whether KYNA or SZR-72 exerts its effect through NMDAR. *In vitro* LO-toxicity measurements of acinar cells showed that the observed protection of KYNA or SZR-72 was unlikely to be related to NMDAR1. The receptor agonist NMDA did not suspend the effects of the receptor antagonist KYNA and SZR-72 even at ten times higher concentrations. Consequently, the protection observed in LO-AP may be a direct effect or an indirect one through another receptor, such as GPR35. KYNA is an endogenous antioxidant, and it can decrease ROS release evoked by AP (Lugo-Huitrón et al., 2011). GPR35 receptor is also present in macrophages, eosinophil and basophil granulocytes, mast cells, natural killer T cells, and several cells along the digestive tract (Wirthgen et al., 2018). GPR35 activation will result in decreased intracellular Ca^{2+} and cyclic adenosine monophosphate signals; inhibition of phosphatidylinositol 3-kinase/protein kinase B and mitogen-activated protein kinase pathways. All these effects of KYNA-GPR35 interaction may contribute to immunosuppression. In our experiments, it was not our aim to investigate the GPR35-mediated effects of KYNA and SZR-72 in AP, but this is an issue worth further research.

KYNA or SZR-72 markedly reduced the pancreatic IL-1β expression *in vivo*. However, when isolated acinar cells were tested *in vitro*, KYNA and SZR-72 did not affect IL-1β levels. Therefore, it appears that the IL-1β reducing effect of KYNA and SZR-72 is independent of acinar cells. Therefore, the tested compounds most probably affect leukocytes, and this can result in decreased cytokine release from the pancreatic tissue. Neutrophil granulocytes are the first inflammatory cells reaching the pancreas during AP. ROS such as H_2O_2 is produced in large quantities by neutrophils which reflects the activity of these cells (Winterbourn et al., 2016). Our results showed that SZR-72 treatment reduced the H_2O_2 production of neutrophil granulocytes isolated from animals with LO-induced pancreatitis. Since neutrophils contribute to AP by amplifying the inflammatory cascade, the reduced activity of these cells by KYNA and SZR-72 is also beneficial and can contribute to their mechanism of action.

CONCLUSION

We confirmed the expression of NMDAR in the acini of the exocrine pancreas. We showed that the administartion of the endogenous tryptophan metabolite, KYNA and its synthetic analogue, SZR-72 reduced the severity of experimental AP (Table 2). Both provide dose-dependent protection against LO-induced AP and *in vitro* acinar cell toxicity, which action is most likely independent of pancreatic NMDARs. There may be several mechanisms mediating this protective effect. Both KYNA and SZR-72 improved acid-base balance, cardiovascular parameters and pancreatic microcirculation during AP. SZR-72 also reduced the elevated H_2O_2 production of neutrophil granulocytes isolated from rats with AP suppressing their activation. KYNA and its synthetic derivative affectes the amount of cytokines (reduced the expression of pancreatic IL-1β), the body's self-defense mechanism (enhanced the expression of pancreatic HSP72), and leukocyte function, demonstrating an immunomodulatory role in experimental AP. Overall, the administration of these molecules could be beneficial in AP.

In addition, we have also shown that BQ treatment can slightly reduce the severity of experimental AP, but its effect is greatly dependent on the dose, timing, and route of administration, suggesting that a well-planned strategy of pain management is crucial.

Type of experiment	Target of investigation	Parameter	KYNA	SZR-72
In vivo **experimental AP**	**Pancreatic effects**	**Histological parameters**	↓↓	↓↓
		Pancreatic MPO activity	↓↓	↓↓
		Pancreatic water content	↓↓	↓↓
		Local microcirculation	Partially rest.	Partially rest.
		Pancreatic IL-1β expression	Restored	Restored
		HSP72 expression during AP	↑↑	↑↑
		HSP72 expression without AP	↑	↑↑
	Systemic effects	**Serum amylase activity**	↓↓	↓↓
		Cardiac output	Restored	Restored
		Metabolic acidosis	Restored	Restored
In vitro **experiments**	**Pancreatic acinar cells**	**Cell protection**	++	+
		IL-1β expression	no effect	no effect
	Neutrophil granulocytes	**Suppression of ROS production**	N.A.	++

Table 2. Summarizing the effects (*in vivo*: 300 mg/kg; *in vitro*: 250 µM) of KYNA and SZR-72 in AP. Explanation of symbols and phrases: ↓, decrease; ↑, increase; +, positive effect; restored/partially rest., the measured condition during AP was restored/partially restored to control levels after KYNA or SZR-72 treatment. AP, acute pancreatitis; HSP72, heat shock protein 72; IL-1β, interleukin-1β; KYNA, kynurenic acid; N.A., not available; MPO, myeloperoxidase; ROS, reactive oxygen species; SZR-72, 2-(2-N,N-dimethylaminoethyl-amine-1carbonyl)-1H-quinolin-4-one hydrochloride.

SUMMARIES

Summary of the thesis

Introduction: Despite its high incidence the exact pathophysiology of AP remains unclear, thus there is still no specific cure. The L-tryptophan metabolite KYNA is known to have several physiological roles, including being an NMDAR antagonist and a ligand for the GPR35 receptor. KYNA and its synthetic analogue, SZR-72, have been shown to play an immunomodulatory role in various inflammatory diseases. Therefore, we aimed to investigate the effect of KYNA and SZR-72 in experimental acute pancreatitis and whether it is mediated through the NMDAR. Since the most common symptom of AP is abdominal pain, which is likely to affect the outcome of the disease, we also aimed to investigate the effects of analgesia.

Methods: AP was induced by i.p. injection of LO in SPRD rats. Animals were pretreated with 75-300 mg/kg KYNA or SZR-72. BQ was administered either i.p. (0.1, 0.5, 1 mg/kg) 1 h before and 12 h after LO injection; or i.t. (3, 6 μg/kg) 1 h before and 7, 12 h after LO. Laboratory (serum amylase activity, tissue water content, pancreatic MPO activity) and histological parameters (pancreatic edema, leukocyte infiltration, cell damage) were measured to evaluate AP severity. Pancreatic HSP-72 and IL-1β expression was measured by western blot analysis and ELISA, respectively. Systemic circulation and hemodynamics were quantified by determining cardiac output, carotid artery flow, and mean arterial pressure. Blood gas analysis included arterial blood pH, partial pressure of CO_2, and HCO_3^- concentration. Microcirculation of the pancreas was characterized by measuring serosal RBCV. Expression of pancreatic NMDAR1 and GPR35 was examined by RT-PCR and immunohistochemistry. In the *in vitro* experimental setup, we investigated the effect of LO, KYNA, SZR-72, and NMDA on the viability of isolated pancreatic acinar cells applying propidium-iodide assay. Neutrophil granulocytes were also treated with LO and/or SZR-72 and changes in their H_2O_2 production were measured.

Results: Treatment with 300 mg/kg KYNA or SZR-72 significantly reduced almost all laboratory and histological parameters of AP, while lower doses (150, 75 mg/kg) were less effective. Decreased pancreatic microcirculation in AP groups was improved by 300 mg/kg KYNA or SZR-72 treatment. Moreover, both KYNA and SZR-72 significantly reduced high IL-1β levels in animals with AP. Interestingly, elevated HSP72 levels due to LO-induced pancreatitis were further increased by KYNA and SZR-72 treatment as well. Expression of

NMDAR1 mRNA and protein was detected in pancreatic acinar cells. 250 μM KYNA or SZR-72 reversed LO-induced acinar cell toxicity *in vitro*, and this effect could not be blocked by the addition of NMDA. Furthermore, SZR-72 reduced LO-stimulated H_2O_2 production of neutrophil granulocytes. Analgesia with BQ improved some aspects of AP when administered intrathecally.

Conclusions: KYNA and SZR-72 dose-dependently protect against LO-induced AP and *in vitro* acinar cell toxicity, which action is most likely independent of pancreatic NMDARs. KYNA and its synthetic derivative affect the expression of cytokines (IL-1β), the body's self-defense mechanism (HSP72), and neutrophil granulocyte function, demonstrating an immunomodulatory role in experimental AP.

We have also shown that BQ treatment can slightly reduce the severity of experimental AP, but this effect is greatly dependent on the dose, timing, and route of administration.

Summary of new findings

- KYNA and SZR-72 administration dose-dependently reduce the severity of LO-induced experimental AP
- KYNA and SZR-72 restored hemodynamic parameters and pancreatis microcirculation during LO-induced experimental AP
- NMDAR1 protein and mRNA expression was detected in pancreatic acinar cells
- KYNA and SZR-72 reduce LO-induced toxicity in isolated pancreatic acinar cells *in vitro*
- SZR-72 reduce *in vitro* H_2O_2 production of neutrophil granulocytes isolated from rats with AP
- The beneficial effects of KYNA and SZR-72 are probably independent of pancreatic NMDARs
- I.t. administration of BQ significantly reduced pancreatic leukocyte infiltration during LO-induced experimental AP

FUNDING

This work was supported by EFOP-3.6.2–16–2017–00006, GINOP-2.3.2-15-2016-00034, János Bólyai Research Grant (BO/00866/20/5), ÚNKP Grant (ÚNKP-20-5-SZTE-163), NKFIH PD129114 and NKFIH K119938, and the University of Szeged Open Access Fund (Grant No. 5304).

ACKNOWLEDGEMENTS

First of all, I would like to thank my supervisors, **Prof. Dr. Zoltán Rakonczay** and **Dr. Lóránd Kiss** (Department of Pathophysiology, University of Szeged). Without their guidance and support, this Ph.D. thesis would not have been possible.

I am grateful to **Prof. Dr. Péter Hegyi** (Semmelweis University and University of Pécs), **Prof. Dr. Tamás Takács** (Department of Medicine, University of Szeged) and **Prof. Dr. László Vécsei** (Department of Neurology, University of Szeged) whose knowledge and diligence were exemplary for me. I would also like to thank **Prof. Dr. Gyula Szabó** the former head of the Department of Pathophysiology, and **Prof. Dr. Csaba Lengyel, Prof. Dr. György Ábrahám** and **Prof. Dr. Tibor Wittmann**, the current and former heads of the (First) Department of Medicine, who provided me with the opportunity to work in their institutions.

Special thanks for **Dr. Zsolt Balla**, who has been there for me since my first day in the lab. Thank you to all my colleagues and friends, **Gabriella Fűr, Emese Réka Bálint, Dr. Balázs Kui, Erik Márk Orján, Dr. József Maléth, Dr. Viktória Venglovecz, Dr. Petra Pallagi, Dr. Eszter Teréz Végh, Dr. Emese Tóth, Dr. Júlia Fanczal, Tamara Madácsy, Dr. Máté Katona, Dr. Eszter Hegyi, Dr. Andrea Szentesi, Dr. Krisztina Csabafi, Dr. Júlia Szakács, Dr. Katalin Ibos, Dr. Miklós Jászberényi, Dr. Zsolt Bagosi, Dr. Zsófia Mezei, Dr. Imre Pataki, Dr. Árpád Gecse, Sándor Váczi** who helped me so much over the years with their advice and encouragement.

This thesis would not have been possible to accomplish without the assistance and help of **Edit Magyarné Pálfi, Tünde Pritz, Rea Fritz, Miklósné Árva, Zoltánné Fuksz†, Zoltán Kocsispéter, Zsolt Tóth, Magdolna Laurinyecz, Gusztáv Kiss, Ágnes Pál, Veronika Romhányi**. I would like to highlight **Kitti Ancsányi** and **Erzsébet Dallos-Szilágyi**, and I thank them for their precise and kind help.

Finally, the ones to whom I owe the most. Thank you to my husband, **László Budai** for his endless patience and support. Without him, I would have given up on research a long time ago. Thank you to my children, **Richárd, Erik** and **Ottó** for all the love and happy moments, they inspired me day after day. I will always be grateful to my brother **Zénó** for his unfailing encouragement. Lastly, I thank my mother, **Sára**. I know how happy and proud she would be. I dedicate this thesis to her.

"If we knew what we were doing, it would not be called research, would it?" – Albert Einstein

REFERENCES

Agudelo LZ, Ferreira DMS, Cervenka I, Bryzgalova G, Dadvar S, Jannig PR, Pettersson-Klein AT, Lakshmikanth T, Sustarsic EG, Porsmyr-Palmertz M, Correia JC, Izadi M, Martínez-Redondo V, Ueland PM, Midttun Ø, Gerhart-Hines Z, Brodin P, Pereira T, Berggren PO, Ruas JL. (2018). Kynurenic acid and Gpr35 regulate adipose tissue energy homeostasis and inflammation. *Cell Metab* 27(2), 378-392.

Bądzyńska B, Zakrocka I, Turski WA, Olszyński KH, Sadowski J, Kompanowska-Jezierska E. (2020). Kynurenic acid selectively reduces heart rate in spontaneously hypertensive rats. *Naunyn Schmiedebergs Arch Pharmacol* 393(4), 673-679.

Bálint ER, Fűr G, Kui B, Balla Z, Kormányos ES, Orján EM, Tóth B, Horváth G, Szűcs E, Benyhe S, Ducza E, Pallagi P, Maléth J, Venglovecz V, Hegyi P, Kiss L, Rakonczay Z Jr. (2022). Fentanyl but Not Morphine or Buprenorphine Improves the Severity of Necrotizing Acute Pancreatitis in Rats. *Int J Mol Sci* 23(3), 1192.

Banks PA, Bollen TL, Dervenis C, Gooszen HG, Johnson CD, Sarr MG, Tsiotos GG, Vege SS. (2013). Acute Pancreatitis Classification Working Group. Classification of acute pancreatitis--2012: revision of the Atlanta classification and definitions by international consensus. *Gut* 62(1), 102-111.

Barreto SG, Habtezion A, Gukovskaya A, Lugea A, Jeon C, Yadav D, Hegyi P, Venglovecz V, Sutton R, Pandol SJ. (2021). Critical thresholds: key to unlocking the door to the prevention and specific treatments for acute pancreatitis. *Gut* 70(1), 194-203.

Bhagat L, Singh VP, Song AM, van Acker GJ, Agrawal S, Steer ML, Saluja AK. (2002). Thermal stress-induced HSP70 mediates protection against intrapancreatic trypsinogen activation and acute pancreatitis in rats. *Gastroenterology* 122(1), 156-165.

Biczó G, Hegyi P, Dósa S, Shalbuyeva N, Berczi S, Sinervirta R, Hracskó Z, Siska A, Kukor Z, Jármay K, Venglovecz V, Varga IS, Iványi B, Alhonen L, Wittmann T, Gukovskaya A, Takács T, Rakonczay Z Jr. (2011). The crucial role of early mitochondrial injury in L-lysine-induced acute pancreatitis. *Antioxid Redox Signal* 15(10), 2669-2681.

Biczo G, Vegh ET, Shalbueva N, Mareninova OA, Elperin J, Lotshaw E, Gretler S, Lugea A, Malla SR, Dawson D, Ruchala P, Whitelegge J, French SW, Wen L, Husain SZ, Gorelick FS, Hegyi P, Rakonczay Z Jr, Gukovsky I, Gukovskaya AS. (2018). Mitochondrial dysfunction, through impaired autophagy, leads to endoplasmic reticulum

stress, deregulated lipid metabolism, and pancreatitis in animal models. *Gastroenterology* 154(3), 689-703.

Cai W, Liu F, Wen Y, Han C, Prasad M, Xia Q, Singh VK, Sutton R, Huang W. (2021). Pain Management in Acute Pancreatitis: A systematic review and meta-analysis of randomised controlled trials. *Front Med (Lausanne)* 8, 782151.

Cosi C, Mannaioni G, Cozzi A, Carlà V, Sili M, Cavone L, Maratea D, Moroni F. (2011). G-protein coupled receptor 35 (GPR35) activation and inflammatory pain: Studies on the antinociceptive effects of kynurenic acid and zaprinast. *Neuropharmacology* 60(7-8), 1227-1231.

Criddle DN. (2016). Reactive oxygen species, Ca(2+) stores and acute pancreatitis; a step closer to therapy? *Cell Calcium* 60(3), 180-189.

Cruz-Santamaría DM, Taxonera C, Giner M. (2012). Update on pathogenesis and clinical management of acute pancreatitis. *World J Gastrointest Pathophysiol* 3(3), 60-70.

Cuthbertson CM, Christophi C. (2006). Disturbances of the microcirculation in acute pancreatitis. *Br J Surg* 93(5), 518-530.

Czakó L, Hegyi P, Rakonczay Z Jr, Wittmann T, Otsuki M. (2009). Interactions between the endocrine and exocrine pancreas and their clinical relevance. Pancreatology 9(4), 351-359.

Csáti A, Edvinsson L, Vécsei L, Toldi J, Fülöp F, Tajti J, Warfvinge K. (2015). Kynurenic acid modulates experimentally induced inflammation in the trigeminal ganglion. *J Headache Pain* 16, 99.

Dawra R, Sah RP, Dudeja V, Rishi L, Talukdar R, Garg P, Saluja AK. (2011). Intra-acinar trypsinogen activation mediates early stages of pancreatic injury but not inflammation in mice with acute pancreatitis. *Gastroenterology* 141(6), 2210-2217.

Demeter I, Nagy K, Farkas T, Kis Z, Kocsis K, Knapp L, Gellert L, Fülöp F, Vecsei L, Toldi J. (2013). Paradox effects of kynurenines on LTP induction in the Wistar rat. An in vivo study. *Neurosci Lett* 553, 138-141.

Divorty N, Mackenzie AE, Nicklin SA, Milligan G. (2015). G protein-coupled receptor 35: an emerging target in inflammatory and cardiovascular disease. *Front Pharmacol* 6, 41.

Dobos I, Toth K, Kekesi G, Joo G, Csullog E, Klimscha W, Benedek G, Horvath G. (2003). The significance of intrathecal catheter location in rats. *Anesth Analg* 96(2), 487-492.

Dobosz M, Mionskowska L, Hac S, Dobrowolski S, Dymecki D, Wajda Z. (2004). Heparin improves organ microcirculatory disturbances in caeruleinInduced acute pancreatitis in rats. *World J Gastroenterol* 10, 2553-2556.

Érces D, Varga G, Fazekas B, Kovács T, Tőkés T, Tiszlavicz L, Fülöp F, Vécsei L, Boros M, Kaszaki J. (2012). N-methyl-D-aspartate receptor antagonist therapy suppresses colon motility and inflammatory activation six days after the onset of experimental colitis in rats. *Eur J Pharmacol* 691(1-3), 225-234.

Fallarini S, Magliulo L, Paoletti T, de Lalla C, Lombardi G. (2010). Expression of functional GPR35 in human iNKT cells. *Biochem Biophys Res Commun* 398(3), 420-425.

Foley PL, Kendall LV, Turner PV. (2019). Clinical management of pain in rodents. *Comp Med* 69(6), 468-489.

Forsmark CE, Vege SS, Wilcox CM. (2016). Acute pancreatitis. *N Engl J Med* 375(20), 1972-1981.

Fukui S, Schwarcz R, Rapoport SI, Takada Y, Smith QR. (1991). Blood-brain barrier transport of kynurenines: implications for brain synthesis and metabolism. *J Neurochem* 56(6), 2007-2017.

Guarnieri M, Brayton C, DeTolla L, Forbes-McBean N, Sarabia-Estrada R, Zadnik P. (2012). Safety and efficacy of buprenorphine for analgesia in laboratory mice and rats. *Lab Anim (NY)* 41(11), 337-343.

Gukovskaya AS, Vaquero E, Zaninovic V, Gorelick FS, Lusis AJ, Brennan ML, Holland S, Pandol SJ. (2002). Neutrophils and NADPH oxidase mediate intrapancreatic trypsin activation in murine experimental acute pancreatitis. *Gastroenterology* 122(4), 974-984.

Hegyi P, Rakonczay Z Jr. (2015). The role of pancreatic ducts in the pathogenesis of acute pancreatitis. *Pancreatology* 15(4Suppl), S13-17.

Juhász L, Rutai A, Fejes R, Tallósy SP, Poles MZ, Szabó A, Szatmári I, Fülöp F, Vécsei L, Boros M, Kaszaki J. (2020). Divergent effects of the N-methyl-D-aspartate receptor antagonist kynurenic acid and the synthetic analog SZR-72 on microcirculatory and mitochondrial dysfunction in experimental sepsis. *Front Med (Lausanne)* 27, 566582.

Kassai F, Kedves R, Gyertyán I, Tuka B, Fülöp F, Toldi J, Lendvai B, Vécsei L. (2015). Effect of a kynurenic acid analog on home-cage activity and body temperature in rats. *Pharmacol Rep* 67(6), 1188-1192.

Kaya B, Melhem H, Niess JH. (2021). GPR35 in intestinal diseases: from risk gene to function. *Front Immunol* 12, 717392.

Keszthelyi D, Troost FJ, Jonkers DM, Kruimel JW, Leue C, Masclee AA. (2013). Decreased levels of kynurenic acid in the intestinal mucosa of IBS patients: relation to serotonin and psychological state. *J Psychosom Res* 74(6), 501-504.

Kuebler WM, Abels C, Schuerer L, Goetz AE. (1996). Measurement of neutrophil content in brain and lung tissue by a modified myeloperoxidase assay. *Int J Microcirc Clin Exp* 16(2), 89-97.

Kurucz I, Tombor B, Prechl J, Erdö F, Hegedüs E, Nagy Z, Vitai M, Korányi L, László L. (1999). Ultrastructural localization of Hsp-72 examined with a new polyclonal antibody raised against the truncated variable domain of the heat shock protein. *Cell Stress Chaperones* 4(2), 139-152.

Lowry OH, Rosebrough NJ, Farr AL, Randall RJ. (1951). Protein measurement with the Folin phenol reagent. *J Biol Chem* 193(1), 265-275.

Lugo-Huitrón R, Blanco-Ayala T, Ugalde-Muñiz P, Carrillo-Mora P, Pedraza-Chaverrí J, Silva-Adaya D, Maldonado PD, Torres I, Pinzón E, Ortiz-Islas E, López T, García E, Pineda B, Torres-Ramos M, Santamaría A, La Cruz VP. (2011). On the antioxidant properties of kynurenic acid: free radical scavenging activity and inhibition of oxidative stress. *Neurotoxicol Teratol* 33(5), 538-547.

Lukacs M, Warfvinge K, Kruse LS, Tajti J, Fülöp F, Toldi J, Vécsei L, Edvinsson L. (2016). KYNA analogue SZR72 modifies CFA-induced dural inflammation- regarding expression of pERK1/2 and IL-1β in the rat trigeminal ganglion. *J Headache Pain* 17(1), 64.

Lukács M, Warfvinge K, Tajti J, Fülöp F, Toldi J, Vécsei L, Edvinsson L. (2017). Topical dura mater application of CFA induces enhanced expression of c-fos and glutamate in rat trigeminal nucleus caudalis: attenuated by KYNA derivate (SZR72). *J Headache Pain* 18(1), 39.

Lunova M, Zizer E, Kucukoglu O, Schwarz C, Dillmann WH, Wagner M, Strnad P. (2012). Hsp72 overexpression accelerates the recovery from caerulein-induced pancreatitis. *PLoS One* 7(7), e39972.

Mackenzie AE, Lappin JE, Taylor DL, Nicklin SA, Milligan G. (2011). GPR35 as a novel therapeutic target. *Front Endocrinol (Lausanne)* 2, 68.

Maléth J, Venglovecz V, Rázga Z, Tiszlavicz L, Rakonczay Z Jr, Hegyi P. (2011). Non-conjugated chenodeoxycholate induces severe mitochondrial damage and inhibits bicarbonate transport in pancreatic duct cells. *Gut* 60(1), 136-138.

Mándi Y, Vécsei L. (2012). The kynurenine system and immunoregulation. *J Neural Transm (Vienna)* 119(2), 197-209.

Marquard J, Otter S, Welters A, Stirban A, Fischer A, Eglinger J, Herebian D, Kletke O, Klemen MS, Stožer A, Wnendt S, Piemonti L, Köhler M, Ferrer J, Thorens B, Schliess F, Rupnik MS, Heise T, Berggren PO, Klöcker N, Meissner T, Mayatepek E, Eberhard D, Kragl M, Lammert E. (2015). Characterization of pancreatic NMDA receptors as possible drug targets for diabetes treatment. *Nat Med* 21(4), 363-372.

Mayerle J, Sendler M, Hegyi E, Beyer G, Lerch MM, Sahin-Tóth M. (2019). Genetics, cell biology, and pathophysiology of pancreatitis. *Gastroenterology* 156(7), 1951-1968.

Mole DJ, Webster SP, Uings I, Zheng X, Binnie M, Wilson K, Hutchinson JP, Mirguet O, Walker A, Beaufils B, Ancellin N, Trottet L, Bénéton V, Mowat CG, Wilkinson M, Rowland P, Haslam C, McBride A, Homer NZ, Baily JE, Sharp MG, Garden OJ, Hughes J, Howie SE, Holmes DS, Liddle J, Iredale JP. (2016). Kynurenine-3-monooxygenase inhibition prevents multiple organ failure in rodent models of acute pancreatitis. *Nat Med* 22(2), 202-209.

Mukherjee R, Mareninova OA, Odinokova IV, Huang W, Murphy J, Chvanov M, Javed MA, Wen L, Booth DM, Cane MC, Awais M, Gavillet B, Pruss RM, Schaller S, Molkentin JD, Tepikin AV, Petersen OH, Pandol SJ, Gukovsky I, Criddle DN, Gukovskaya AS, Sutton R. (2016). Mechanism of mitochondrial permeability transition pore induction and damage in the pancreas: inhibition prevents acute pancreatitis by protecting production of ATP. *Gut* 65(8), 1333-1346.

Nahomi RB, Nam MH, Rankenberg J, Rakete S, Houck JA, Johnson GC, Stankowska DL, Pantcheva MB, MacLean PS, Nagaraj RH. (2020). Kynurenic acid protects against ischemia/reperfusion-induced retinal ganglion cell death in mice. *Int J Mol Sci* 21(5), 1795.

O'Dowd BF, Nguyen T, Marchese A, Cheng R, Lynch KR, Heng HH, Kolakowski LF Jr, George SR. (1998). Discovery of three novel G-protein-coupled receptor genes. *Genomics* 47(2), 310-313.

Ogden JM, Modlin IM, Gorelick FS, Marks IN. (1994). Effect of buprenorphine on pancreatic enzyme synthesis and secretion in normal rats and rats with acute edematous pancreatitis. *Dig Dis Sci* 39(11), 2407-2415.

Pallagi P, Balla Z, Singh AK, Dósa S, Iványi B, Kukor Z, Tóth A, Riederer B, Liu Y, Engelhardt R, Jármay K, Szabó A, Janovszky A, Perides G, Venglovecz V, Maléth J, Wittmann T, Takács T, Gray MA, Gácser A, Hegyi P, Seidler U, Rakonczay Z Jr. (2014). The role of pancreatic ductal secretion in protection against acute pancreatitis in mice. *Crit Care Med* 42(3), 177-188.

Paluszkiewicz P, Zgrajka W, Saran T, Schabowski J, Piedra JL, Fedkiv O, Rengman S, Pierzynowski SG, Turski WA. (2009). High concentration of kynurenic acid in bile and pancreatic juice. *Amino Acids* 37, 637-641.

Pandol SJ, Jensen RT, Gardner JD. (1982). Mechanism of [Tyr4]bombesin-induced desensitization in dispersed acini from guinea pig pancreas. *J Biol Chem* 257(20), 12024-12029.

Pandol SJ, Saluja AK, Imrie CW, Banks PA. (2007). Acute pancreatitis: bench to the bedside. *Gastroenterology* 132(3), 1127-51.

Párniczky A, Kui B, Szentesi A, Balázs A, Szűcs Á, Mosztbacher D, Czimmer J, Sarlós P, Bajor J, Gódi S, Vincze Á, Illés A, Szabó I, Pár G, Takács T, Czakó L, Szepes Z, Rakonczay Z, Izbéki F, Gervain J, Halász A, Novák J, Crai S, Hritz I, Góg C, Sümegi J, Golovics P, Varga M, Bod B, Hamvas J, Varga-Müller M, Papp Z, Sahin-Tóth M, Hegyi P. (2016). Hungarian Pancreatic Study Group. Prospective, multicentre, nationwide clinical data from 600 cases of acute pancreatitis. *PLoS One* 11(10), e0165309.

Peery AF, Crockett SD, Murphy CC, Jensen ET, Kim HP, Egberg MD, Lund JL, Moon AM, Pate V, Barnes EL, Schlusser CL, Baron TH, Shaheen NJ, Sandler RS. (2022). Burden and cost of gastrointestinal, liver, and pancreatic diseases in the United States: update 2021. *Gastroenterology* 162(2), 621-644.

Petrov MS, van Santvoort HC, Besselink MG, van der Heijden GJ, Windsor JA, Gooszen HG. (2008). Enteral nutrition and the risk of mortality and infectious complications in patients with severe acute pancreatitis: a meta-analysis of randomized trials. *Arch Surg* 143(11), 1111-1117.

Rakonczay Z Jr, Hegyi P, Dósa S, Iványi B, Jármay K, Biczó G, Hracskó Z, Varga IS, Karg E, Kaszaki J, Varró A, Lonovics J, Boros I, Gukovsky I, Gukovskaya AS, Pandol SJ, Takács T. (2008). A new severe acute necrotizing pancreatitis model induced by L-ornithine in rats. *Crit Care Med* 36(7), 2117-2127.

Rakonczay Z Jr, Hegyi P, Takács T, McCarroll J, Saluja AK. (2008). The role of NF-kappaB activation in the pathogenesis of acute pancreatitis. *Gut* 57(2), 259-67.

Rakonczay Z Jr, Takács T, Boros I, Lonovics J. (2003). Heat shock proteins and the pancreas. *J Cell Physiol* 195(3), 383-391.

Rakonczay Z Jr, Iványi B, Varga I, Boros I, Jednákovits A, Németh I, Lonovics J, Takács T. (2002). Nontoxic heat shock protein coinducer BRX-220 protects against acute pancreatitis in rats. *Free Radic Biol Med* 32(12), 1283-1292.

Rakonczay Z Jr, Boros I, Jármay K, Hegyi P, Lonovics J, Takacs T. (2003). Ethanol administration generates oxidative stress in the pancreas and liver, but fails to induce heat-shock proteins in rats. *J Gastroenterol Hepatol* 18(7), 858-867.

Roberts SE, Morrison-Rees S, John A, Williams JG, Brown TH, Samuel DG. (2017). The incidence and aetiology of acute pancreatitis across Europe. *Pancreatology* 17(2), 155-165.

Roth W, Zadeh K, Vekariya R, Ge Y, Mohamadzadeh M. (2021). Tryptophan metabolism and gut-brain homeostasis. *Int J Mol Sci* 22(6), 2973.

Rumbus Z, Toth E, Poto L, Vincze A, Veres G, Czako L, Olah E, Marta K, Miko A, Rakonczay Z Jr, Balla Z, Kaszaki J, Foldesi I, Maleth J, Hegyi P, Garami A. (2018). Bidirectional relationship between reduced blood pH and acute pancreatitis: a translational study of their noxious combination. *Front Physiol* 9, 1360.

Sadowski SM, Andres A, Morel P, Schiffer E, Frossard JL, Platon A, Poletti PA, Bühler L. (2015). Epidural anesthesia improves pancreatic perfusion and decreases the severity of acute pancreatitis. *World J Gastroenterol* 21(43), 12448-12456.

Schepers NJ, Bakker OJ, Besselink MG, Ahmed Ali U, Bollen TL, Gooszen HG, van Santvoort HC, Bruno MJ. (2019). Impact of characteristics of organ failure and infected necrosis on mortality in necrotising pancreatitis. *Gut* 68(6), 1044-1051.

Sendler M, Weiss FU, Golchert J, Homuth G, van den Brandt C, Mahajan UM, Partecke LI, Döring P, Gukovsky I, Gukovskaya AS, Wagh PR, Lerch MM, Mayerle J. (2018).

Cathepsin B-mediated activation of trypsinogen in endocytosing macrophages increases severity of pancreatitis in mice. *Gastroenterology* 154(3), 704-718.

Skouras C, Zheng X, Binnie M, Homer NZ, Murray TB, Robertson D, Briody L, Paterson F, Spence H, Derr L, Hayes AJ, Tsoumanis A, Lyster D, Parks RW, Garden OJ, Iredale JP, Uings IJ, Liddle J, Wright WL, Dukes G, Webster SP, Mole DJ. (2016). Increased levels of 3-hydroxykynurenine parallel disease severity in human acute pancreatitis. *Sci Rep* 6, 33951.

Stone TW. (2020). Does kynurenic acid act on nicotinic receptors? An assessment of the evidence. *J Neurochem* 152(6), 627-649.

Tanaka M, Bohár Z, Vécsei L. (2020). Are Kynurenines Accomplices or Principal Villains in Dementia? Maintenance of Kynurenine Metabolism. *Molecules* 25(3), 564.

Tejwani GA, Rattan AK. (2002). The role of spinal opioid receptors in antinociceptive effects produced by intrathecal administration of hydromorphone and buprenorphine in the rat. *Anesth Analg* 94(6), 1542-1546.

Tenner S, Baillie J, DeWitt J, Vege SS. (2013). American College of Gastroenterology guideline: management of acute pancreatitis. *Am J Gastroenterol* 108(9), 1400-1415.

Thompson DR. (2001). Narcotic analgesic effects on the sphincter of Oddi: a review of the data and therapeutic implications in treating pancreatitis. *Am J Gastroenterol* 96(4), 1266-1272.

Tiszlavicz Z, Németh B, Fülöp F, Vécsei L, Tápai K, Ocsovszky I, Mándi Y. (2011). Different inhibitory effects of kynurenic acid and a novel kynurenic acid analogue on tumour necrosis factor-α (TNF-α) production by mononuclear cells, HMGB1 production by monocytes and HNP1-3 secretion by neutrophils. *Naunyn Schmiedebergs Arch Pharmacol* 383(5), 447-455.

Tousignant-Laflamme Y, Rainville P, Marchand S. (2005). Establishing a link between heart rate and pain in healthy subjects: a gender effect. *J Pain* 6(6), 341-347.

Varga G, Erces D, Fazekas B, Fülöp M, Kovács T, Kaszaki J, Fülöp F, Vécsei L, Boros M. (2010). N-Methyl-D-aspartate receptor antagonism decreases motility and inflammatory activation in the early phase of acute experimental colitis in the rat. *Neurogastroenterol Motil* 22(2), 217-225.

Vécsei L, Szalárdy L, Fülöp F, Toldi J. (2013). Kynurenines in the CNS: recent advances and new questions. *Nat Rev Drug Discov* 12(1), 64-82.

Wagner AC, Weber H, Jonas L, Nizze H, Strowski M, Fiedler F, Printz H, Steffen H, Göke B. (1996). Hyperthermia induces heat shock protein expression and protection against cerulein-induced pancreatitis in rats. *Gastroenterology* 111(5), 1333-1342.

Wang J, Simonavicius N, Wu X, Swaminath G, Reagan J, Tian H, Ling L. (2006). Kynurenic acid as a ligand for orphan G protein-coupled receptor GPR35. *J Biol Chem* 281(31), 22021-22028.

Wang Q, Fu B, Su D, Fu X. (2022). Impact of early thoracic epidural analgesia in patients with severe acute pancreatitis. *Eur J Clin Invest*, 13740.

Wang Q, Liu D, Song P, Zou MH. (2015). Tryptophan-kynurenine pathway is dysregulated in inflammation, and immune activation. *Front Biosci (Landmark Ed)* 20(7), 1116-1143.

Weber CK, Adler G. (2001). From acinar cell damage to systemic inflammatory response: current concepts in pancreatitis. *Pancreatology* 1(4), 356-362.

Winterbourn CC, Kettle AJ, Hampton MB. (2016). Reactive oxygen species and neutrophil function. *Annu Rev Biochem* 85, 765-792.

Wirthgen E, Hoeflich A, Rebl A, Günther J. (2018). Kynurenic acid: the Janus-faced role of an immunomodulatory tryptophan metabolite and its link to pathological conditions. *Front Immunol* 8, 1957.

Yadav D, Lowenfels AB. (2013). The epidemiology of pancreatitis and pancreatic cancer. *Gastroenterology* 144(6), 1252-1261.

Yaksh TL, Rudy TA. (1976). Chronic catheterization of the spinal subarachnoid space. *Physiol Behav* 17(6), 1031-1036.

Zhan XB, Guo XR, Yang J, Li J, Li ZS. (2015). Prevalence and risk factors for clinically significant upper gastrointestinal bleeding in patients with severe acute pancreatitis. *J Dig Dis* 16(1), 37-42.

Zhang J, Yu WQ, Wei T, Zhang C, Wen L, Chen Q, Chen W, Qiu JY, Zhang Y, Liang TB. (2020). Effects of short-peptide-based enteral nutrition on the intestinal microcirculation and mucosal barrier in mice with severe acute Pancreatitis. *Mol Nutr Food Res* 64(5), e1901191.

Zhou Q, Shi Y, Chen C, Wu F, Chen Z. (2021). A narrative review of the roles of indoleamine 2,3-dioxygenase and tryptophan-2,3-dioxygenase in liver diseases. *Ann Transl Med* 9(2), 174.

ANNEX

frontiers in Immunology

ORIGINAL RESEARCH
published: 21 October 2021
doi: 10.3389/fimmu.2021.702764

Kynurenic Acid and Its Analogue SZR-72 Ameliorate the Severity of Experimental Acute Necrotizing Pancreatitis

Zsolt Balla[1†‡], Eszter Sára Kormányos[1‡], Balázs Kui[2], Emese Réka Bálint[1], Gabriella Fűr[1], Erik Márk Orján[1], Béla Iványi[3], László Vécsei[4,5], Ferenc Fülöp[6,7§], Gabriella Varga[8], András Harazin[9], Vilmos Tubak[10], Mária A. Deli[9], Csaba Papp[11,12], Attila Gácser[11,12], Tamara Madácsy[2], Viktória Venglovecz[13], József Maléth[2], Péter Hegyi[2,14,15], Lóránd Kiss[1] and Zoltán Rakonczay Jr.[1*]*

[1] Department of Pathophysiology, University of Szeged, Szeged, Hungary, [2] Department of Medicine, University of Szeged, Szeged, Hungary, [3] Department of Pathology, University of Szeged, Szeged, Hungary, [4] Department of Neurology, Interdisciplinary Excellence Centre, University of Szeged, Szeged, Hungary, [5] Hungarian Academy of Sciences-University of Szeged Neuroscience Research Group, Hungarian Academy of Sciences – University of Szeged, Szeged, Hungary, [6] Institute of Pharmaceutical Chemistry, University of Szeged, Szeged, Hungary, [7] Stereochemistry Research Team, Hungarian Academy of Sciences – University of Szeged, Szeged, Hungary, [8] Institute of Surgical Research, University of Szeged, Szeged, Hungary, [9] Institute of Biophysics, Biological Research Centre, Szeged, Hungary, [10] Creative Laboratory Ltd., Szeged, Hungary, [11] Department of Microbiology, University of Szeged, Szeged, Hungary, [12] Hungarian Academy of Sciences-University of Szeged Lendület Mycobiome Research Group, University of Szeged, Szeged, Hungary, [13] Department of Pharmacology and Pharmacotherapy, University of Szeged, Szeged, Hungary, [14] Hungarian Academy of Sciences-University of Szeged Translational Gastroenterology Research Group, Szeged, Hungary, [15] Institute for Translational Medicine, University of Pécs, Pécs, Hungary

The pathophysiology of acute pancreatitis (AP) is not well understood, and the disease does not have specific therapy. Tryptophan metabolite L-kynurenic acid (KYNA) and its synthetic analogue SZR-72 are antagonists of the N-methyl-D-aspartate receptor (NMDAR) and have immune modulatory roles in several inflammatory diseases. Our aims were to investigate the effects of KYNA and SZR-72 on experimental AP and to reveal their possible mode of action. AP was induced by intraperitoneal (i.p.) injection of L-ornithine-HCl (LO) in SPRD rats. Animals were pretreated with 75-300 mg/kg KYNA or SZR-72. Control animals were injected with physiological saline instead of LO, KYNA and/or SZR-72. Laboratory and histological parameters, as well as pancreatic and systemic circulation were measured to evaluate AP severity. Pancreatic heat shock protein-72 and IL-1β were measured by western blot and ELISA, respectively. Pancreatic expression of NMDAR1 was investigated by RT-PCR and immunohistochemistry. Viability of isolated pancreatic acinar cells in response to LO, KYNA, SZR-72 and/or NMDA administration was assessed by propidium-iodide assay. The effects of LO and/or SZR-72 on neutrophil granulocyte function was also studied. Almost all investigated laboratory and histological parameters of AP were significantly reduced by administration of 300 mg/kg KYNA or SZR-72, whereas the 150 mg/kg or 75 mg/kg doses were less or not effective, respectively. The decreased pancreatic microcirculation was also improved in the AP groups treated with 300 mg/kg KYNA or SZR-72. Interestingly, pancreatic heat shock protein-72 expression was significantly increased by administration of SZR-72, KYNA

OPEN ACCESS

Edited by:
Jean-Pierre Routy,
McGill University, Canada

Reviewed by:
Amir Rashidian,
Tehran University of Medical Sciences, Iran
Xuanjun Wang,
Yunnan Agricultural University, China

***Correspondence:**
Zoltán Rakonczay Jr.
rakonczay.zoltan@med.u-szeged.hu
Lóránd Kiss
lorand.kiss.work@gmail.com

[†]Present address:
Zsolt Balla,
Institute of Applied Sciences, Department of Environmental Biology and Education, Juhász Gyula Faculty of Education, University of Szeged, Szeged, Hungary

[‡]These authors have contributed equally to this work

[§]Deceased

Specialty section:
This article was submitted to Inflammation, a section of the journal Frontiers in Immunology

Received: 29 April 2021
Accepted: 29 September 2021
Published: 21 October 2021

Citation:
Balla Z, Kormányos ES, Kui B, Bálint ER, Fűr G, Orján EM, Iványi B, Vécsei L, Fülöp F, Varga G, Harazin A, Tubak V, Deli MA, Papp C, Gácser A, Madácsy T, Venglovecz V, Maléth J, Hegyi P, Kiss L and Rakonczay Z Jr. (2021) Kynurenic Acid and Its Analogue SZR-72 Ameliorate the Severity of Experimental Acute Necrotizing Pancreatitis. Front. Immunol. 12:702764. doi: 10.3389/fimmu.2021.702764

and/or LO. mRNA and protein expression of NMDAR1 was detected in pancreatic tissue. LO treatment caused acinar cell toxicity which was reversed by 250 μM KYNA or SZR-72. Treatment of acini with NMDA (25, 250, 2000 μM) did not influence the effects of KYNA or SZR-72. Moreover, SZR-72 reduced LO-induced H_2O_2 production of neutrophil granulocytes. KYNA and SZR-72 have dose-dependent protective effects on LO-induced AP or acinar toxicity which seem to be independent of pancreatic NMDA receptors. Furthermore, SZR-72 treatment suppressed AP-induced activation of neutrophil granulocytes. This study suggests that administration of KYNA and its derivative could be beneficial in AP.

Keywords: acute pancreatitis, kynurenic acid, SZR-72, NMDA receptor-1, NMDA, tryptophan pathway, N-methyl-D-aspartate

INTRODUCTION

Acute pancreatitis (AP) is a relatively common disease among gastrointestinal disorders (1) with increasing incidence over time (2). Its overall mortality is about 2%, but in severe cases this can reach 30% (3). AP may appear in mild, moderately severe or severe forms based on the Revised Atlanta Classification (4). The pathomechanism of AP is complex and not fully understood. It involves toxic cellular Ca^{2+} overload causing nuclear factor-κB activation in pancreatic acinar cells, impaired autophagy, mitochondrial dysfunction, release of reactive oxygen species (ROS), as well as premature activation of digestive enzymes like trypsinogen (5–8). These events lead to release of tumor necrosis factor α (TNF-α), cytokines (e.g. interleukin 1) and chemokines, which participate in leukocyte recruitment. Neutrophils are the first immune cells reaching pancreatic parenchyma. These cells also activate trypsinogen in acinar cells (9), release inflammatory cytokines or chemokines, secrete myeloperoxidase and reactive oxygen species e.g. hydrogen peroxide (H_2O_2), which all contribute to further aggravation of AP (10). Unfortunately, AP management is still based on supportive therapy without specific drugs available.

Tryptophan and its metabolites are important participants of cellular processes, especially in neuronal cells. L-tryptophan is metabolized to N-formyl-L-kynurenine and L-kynurenine (KYN). KYN is further converted to kynurenic acid (KYNA, **Figure 1**), 3-hydroxy-L-kynurenine (3-HK), or anthranilic acid depending on the enzymes (11). Metabolites of the tryptophan-KYN pathway have several effects on both innate and adaptive immune responses (12). KYNA acts as an antagonist on N-methyl-D-aspartate receptor (NMDAR) and has neuroprotective effects (11). It also reduces ischemia/reperfusion-induced retinal ganglion cell death (13). Recently, SZR-72, a promising derivative of KYNA, was also investigated by different research groups (**Figure 1**). SZR-72 readily crosses the blood-brain barrier but KYNA is poorly permeable (14, 15). SZR-72 effectively modulated mitochondrial respiration, while KYNA could restore microcirculation in sepsis (16). KYNA and SZR-72 suppressed pro-inflammatory factors released by mononuclear cells and neutrophils e.g. TNF-α, high mobility group box protein 1, and human neutrophil peptide 1–3 (17). Furthermore, in that study SZR-72 showed more potent effects than KYNA. SZR-72 could also suppress inflammation in the colon through antagonism of NMDAR (18).

AP severity was shown to be influenced by metabolites of the tryptophan pathway or by disturbance of this pathway. Overall, 3-HK generates free radicals and causes cytotoxicity, while KYNA inhibits inflammation, prevents lipid peroxidation and ROS generation (19). 3-HK concentration is increased during AP in human samples and its plasma levels correlated with the progression of systemic inflammation and the severity of AP (20). The inhibitors of kynurenine-3-monoxigenase reduce the production of 3-HK. Application of such an inhibitor prevented multiple organ failure in experimental AP in rodents (21). In contrast to 3-HK, the effect of endogenous KYNA or its synthetic derivate SZR-72 is unknown during AP.

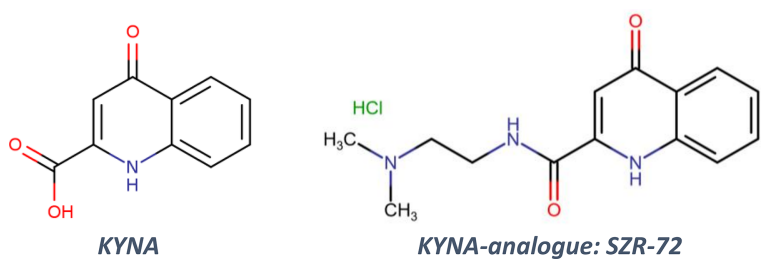

FIGURE 1 | The structure of kynurenic acid (KYNA) and its analogue SZR-72 (2-(2-*N*,*N*-dimethylaminoethylamine-1-carbonyl)-1*H*-quinolin-4-one hydrochloride).

Based on the previously detected promising anti-inflammatory roles of KYNA and SZR-72, our aim was to investigate the effects of these molecules on the severity of experimental AP. Furthermore, we wanted to reveal whether they act *via* NMDAR.

MATERIALS AND METHODS

Materials

All chemicals were purchased from Sigma-Aldrich (Budapest, Hungary) unless indicated otherwise. SZR-72 [2-(2-N,N-dimethylaminoethyl-amine-1carbonyl)-1H-quinolin-4-one hydrochloride] was synthesized by the Institute of Pharmaceutical Chemistry (University of Szeged, Hungary).

The solutions used for *in vivo* measurements were freshly prepared before each experiment. L–ornithine-HCl (LO, 300 mg/ml), kynurenic acid (KYNA, 50 mg/ml), and SZR–72 (50 mg/ml) were dissolved in physiological saline (PS) and the pH of the solutions was adjusted to 7.35-7.4 (KYNA and SZR-72 precipitate above pH 7.4).

Animals

Male Sprague-Dawley (SPRD) rats weighing 200-250 g were used for the experiments. The animals were kept at a constant room temperature of 23°C with a 12-hour light–dark cycle and were allowed free access to water and standard laboratory chow for rodents (Biofarm, Zagyvaszántó, Hungary). Our experiments were executed according to the European Union Directive 2010/63/EU and the Hungarian Government Decree 40/2013 (II.14.). Experiments were approved by both local (University of Szeged) and national ethics committees (X/3353/2017.) for investigations involving animals.

In Vivo Experiments: Acute Pancreatitis Induction, Treatment With Kynurenic Acid or SZR–72, and Tissue Harvesting

Necrotizing AP was induced by intraperitoneal (i.p.) injection of 3 g/kg LO administered in the morning. A single i.p. injection of kynurenic acid (KYNA) or SZR-72 (75, 150, or 300 mg/kg) was administered 1 hour prior to the induction of AP. Control animals were treated with physiological saline (PS) instead of LO, KYNA and/or SZR-72. Animals were sacrificed 24 h after the LO injection (at the peak of pancreatic inflammation) by deep anesthesia with 45 mg/kg i.p. pentobarbital (Bimeda MTC, Cambridge, Canada). Blood was collected *via* cardiac puncture, then the pancreas was rapidly removed. Pancreatic tissue was cleaned from fat and lymph nodes on ice, then cut into pieces. One large piece was immediately frozen in liquid nitrogen and stored at –80°C until biochemical assays were performed. Another piece of the pancreas was fixed in 8% neutral formaldehyde solution for histological analysis. The third piece was stored in Eppendorf tubes at room temperature for dry-wet weight measurement. The last piece was frozen in cryomatrix for sectioning and immunofluorescent stainings. Blood samples were centrifuged at 2500 RCF for 15 mins at 4°C, sera were collected and stored at –20°C until use.

After LO administration, animals showed signs of sickness and became sluggish as expected. However, a few of them got depressed and lethargic within 12 h after the LO injection. The core temperature of these animals was monitored with a rectal digital thermometer. Once it decreased to a critical level (27-29°C), rats were euthanized by pentobarbital overdose (200 mg/kg i.p.) to minimize suffering. The percentage of euthanized rats was 3% in the LO treated groups. Surviving animals either developed necrotizing AP or remained AP–free by the time the experiment was terminated (24 h).

Histological Analysis

Formalin-fixed pancreatic tissues were sectioned to 3 μm. These sections were prepared and stained with hematoxylin and eosin and were analyzed and scored by a pathologist blinded to the experimental protocol (22). Edema was scored from 0–3 points (0: none; 1: patchy interlobular; 2: diffuse interlobular; 3: diffuse interlobular and intra-acinar), leukocyte infiltration from 0–4 points (0: none; 1: patchy interlobular; 2: moderate diffuse interlobular; 3: mild diffuse interlobular; 4: diffuse interlobular and intra-acinar). Percentage of acinar cell necrosis was also evaluated.

Laboratory Measurements

Serum amylase activity was measured on a Fluorostar Optima plate reader (BMG Labtech, Ortenberg, Germany) with a colorimetric kinetic method using a commercial kit purchased from Diagnosticum Zrt. (Budapest, Hungary). To evaluate tissue water content, wet weight (WW) of the pancreas was measured right after the *in vivo* experiment, then it was dried for 24 h at 100°C. After that, dry weight (DW) was measured as well. The wet/dry weight ratio was calculated as: [(WW-DW)/WW]×100. Pancreatic myeloperoxidase (MPO) activity, a hallmark of leukocytic infiltration, was measured according to Kuebler et al. (23) and was normalized to total protein content as measured by the Lowry method (24). To determine the extent of inflammatory response in the pancreata, we measured interleukin-1β (IL-1β) levels by a commercial ELISA kit from R&D Systems (Minneapolis, MN, USA) as described by the manufacturer. Blood pH, HCO_3^-, and partial pressure of CO_2 (pCO_2) in femoral arterial blood samples were measured with a blood gas analyzer (AVL Compact 2, Graz, Austria; (25).

Pancreatic HSP72 expression was measured from tissue homogenate using Western blot analysis (26). Briefly, pancreatic tissue was homogenized with sonication (Branson Sonifer 250; Emerson Electric, Brookfield, CT, USA) on ice in a buffer containing: 10 mM Na-HEPES, 1μM $MgCl_2$, 10mM KCl, 1mM DL-dithiothreitol, 5mM iodoacetamide, 4 mM benzamidine-HCl, 1mM phenylmethyl sulfonylfluoride. Protein concentration of the homogenate was determined by the Bradford protein assay. Forty micrograms of protein were loaded per lane. Samples were electrophoresed on an 8% sodium dodecyl sulfate-polyacrylamide gel. The gels were either stained with Coomassie brilliant blue (to demonstrate equal loading of proteins for Western blot analysis) or transferred to a nitrocellulose membrane for 1h at 100V. Membranes were blocked in 5% non-fat dry milk for 1 h and incubated with

rabbit anti-HSP72 (1:2500 dilution; a generous gift from István Kurucz, Biorex Laboratories, Veszprém, Hungary, that has been characterized previously; (27) antibody for an additional 1h at room temperature. The immunoreactive protein was visualized by enhanced chemiluminescence, using horseradish peroxidase-coupled anti-rabbit immunoglobulin at 1:5000 dilution (Agilent Technologies, Santa Clara, CA, USA). Quantitative analysis of results was achieved using ImageJ software (NIH, Bethesda, MD, USA). The blot images were cropped, and only the relevant bands are shown in the figures (the raw blot images are presented in the **Supplementary Materials**).

Measurement of Circulation (Hemodynamics and Pancreatic Microcirculation)

Animals were anaesthetized with sodium pentobarbital (50 mg/kg) i.p. 24 h after the injection of LO and placed in a supine position on a heating pad. Tracheostomy was performed to facilitate spontaneous breathing, and the right jugular vein was cannulated with PE50 tubing for fluid administration such as Ringer's lactate infusion (10 ml kg^{-1} h^{-1}) during the experiments. A thermistor-tip catheter (PTH-01; Experimetria Ltd., Budapest, Hungary) was positioned into the ascending aorta through the right common carotid artery to measure cardiac output (CO) by a thermodilution technique, using a SPEL Advanced Cardiosys 1.4 computer (Experimetria Ltd., Budapest, Hungary). The left common carotid artery was dissected free and an ultrasonic flow-probe (1RS; Transonic Systems Inc., Ithaca, NY, USA) was placed around the exposed artery to measure carotid artery flow. The right femoral artery was cannulated with PE40 tubing to collect arterial blood for pH measurements (25). Carotid artery flow (T206 Animal Research Flowmeter; Transonic Systems Inc.) and pressure (BPR-02 transducer; Experimetria Ltd., Budapest, Hungary) were measured continuously and registered with a computerized data-acquisition system (Experimetria Ltd., Budapest, Hungary).

After median laparotomy, the pancreas was carefully placed on the detector from the abdomen without disturbing the circulation. The pancreas was kept moist with wet gauze. The microcirculation of the pancreas was continuously visualized with intravital orthogonal polarization spectral imaging technique (Cytoscan A/R, Cytometrics, Philadelphia, Pennsylvania, USA). This technique utilizes reflected polarized light at the wavelength of the isobestic point of oxy-and deoxyhaemoglobin (548 nm). As polarization is preserved in reflection, only photons scattered from a depth of 2–300 μm contribute to image formation. A 10x objective was placed onto the serosal surface of the pancreas, and microscopic recordings were made with an S–VHS video recorder 1 (Panasonic AG–TL 700, Matsushita Electric Ind. Co. Ltd, Osaka, Japan). Quantitative assessment of the microcirculatory parameters was performed off-line by frame-to-frame analysis of the videotaped images. Red blood cell velocity (RBCV, mm/s) changes in the postcapillary venules were determined in three separate fields by means of a computer-assisted image analysis system (IVM Pictron, Budapest, Hungary). All microcirculatory evaluations were performed by the same investigator (18).

Total RNA Isolation and Reverse Transcription Polymerase Chain Reaction

Total RNA was isolated from the control rat brain cortex and pancreas by using TRI Reagent (Molecular Research Center, USA) and 1 μg RNA from each sample was transcribed to complementary DNA by Maxima First Strand cDNA Synthesis Kit (Thermo Fisher, Waltham, MA, USA), according to the manufacturer's instructions. Gene-specific and exon/exon junction spanning oligonucleotide primer pairs (**Table 1**) were designed with The Universal Probe Library Assay Design Center (Merck KGaA, Darmstadt, Germany). Primers for hypoxanthine phosphoribosyltransferase (HPRT) gene were used as loading control (**Table 1**). PCR was performed with DreamTaq DNA Polymerase (Thermo Fisher) in BioRad C1000 ThermalCycler (Bio-Rad Laboratories, Hercules, CA, USA). After heat inactivation for 3 min at 95°C, cycling conditions were the following: denaturation for 10 s at 95°C, annealing for 10 s at 50°C, polymerization for 10 s at 72°C (40 cycles), final extension for 3 min at 72°C. Products were analyzed on 3% MetaPhor agarose gel (Lonza, Basel, Switzerland), then isolated fragments were sequence verified by capillary DNA sequencing.

Immunofluorescent Stainings for N-Methyl-D-Aspartate Receptor and Amylase

Pancreata embedded in cryomatrix were cut into 7 μm thick slices at −20°C with a Leica Cryostat (Leica Biosystems, Buffalo Grove, IL, United States). Slides were kept at −20°C until processing. Immunofluorescent staining was performed in a humidified chamber at room temperature. Sections were fixed in 4% PFA–PBS for 15 min then washed in 1x Tris buffered saline (TBS) for 5 mins, repeated 3 times. Antigen retrieval was performed in Sodium Citrate - Tween 20 buffer (0.001 M Sodium Citrate Buffer, pH 6.0 and 0.05% Tween 20) at 90-96°C for 30 min. After cooling to room temperature in 1x TBS, sections were blocked with 0.01% goat serum and 5x BSA–TBS (bovine serum albumin in Tris Saline Buffer) for 1 h. Thereafter, pancreatic sections were incubated with anti-NMDAR1 rabbit monoclonal antibody (1:100, ThermoFisher Scientific, Waltham, USA) overnight at 4°C in a humidified chamber. The following day slides were washed 3 x 5 min in 1x TBS, then Alexa Fluor 568 goat anti-rabbit secondary antibody was added (1:500) and slides were incubated for 3 h at room temperature, covered from light. After that, co-immunostaining was performed with anti-amylase mouse monoclonal antibody (1:200) and Alexa Fluor 488 goat anti-mouse secondary antibody (1:500) as described above. Samples were washed 3 x 5 min with 1x TBS, then nuclei were counterstained with 2.5 μg/ml Hoechst 33342. After washing 3

TABLE 1 | Primers used in this study.

Primer		Sequence	Product size (bp)	Gene ID
GluN1/ NMDAR1	fwd	tgtcatcccaaatgacagga	108	24408
	rvs	ggctcttggtggattgtcac		
HPRT	fwd	gaccggttctgtcatgtcg	61	24465
	rvs	acctggttcatcatcactaatcac		

times in 1x TBS, Fluoromount Aqueous mounting medium was added. Slides were covered, then left to dry in a dark slide box. After drying, slides were stored at 4°C until visualizing with confocal microscopy (ZEISS LSM 880), and images were processed with ImageJ software (NIH, Bethesda, MD, USA). For proper visibility images were cropped from the raw images and all of them were adjusted uniformly, brightness was increased by 20% with PowerPoint software (Microsoft, Redmond, WA, US). Raw images are shown in **Supplementary Materials**.

Pancreatic Acinar Cell Isolation

Rat pancreatic acinar cells were isolated with collagenase digestion technique according to Pandol et al. (28). Briefly, animals were sacrificed, and the pancreas was removed, washed, and placed into ice-cold PS, then the tissue was cleaned from fat and lymph nodes. The extracellular solution, used in the next steps contained (in mM) 120 NaCl, 5 KCl, 25 HEPES, 2 NaH_2PO_4, 2 $CaCl_2$, 1 $MgCl_2$, 5 pyruvate, 4 Na-fumarate, 4 Na-glutamate, 12 D-glucose, as well as 0.02% (wt/vol) soybean trypsin inhibitor, 0.2% (wt/vol) bovine serum albumin, 0.025% (vol/vol) minimal essential amino acids and 0.01% (vol/vol) vitamins eagle. After cleaning, the pancreas was cut into small pieces in 5 ml extracellular solution, containing 80 U/ml type 4 collagenase (Worthington Biochemical Co., Lakewood, USA). The tissue was incubated in a shaking water bath at 37°C for 2 x 20 min. After 20 min, the supernatant was removed and 5 ml fresh collagenase solution was added to the tissue fragments. After digestion, acinar cells were washed three times with extracellular solution, then resuspended in Medium 199 solution and placed in 37°C CO_2 incubator for 15 min. Acini were used for experiments immediately thereafter.

Acinar Viability

Isolated pancreatic acinar cells were placed into a 96-well plate and 1 μM propidium-iodide (PI) was added to each well. Fluorescence intensity was measured at excitation and emission wavelengths of 540 nm and 620 nm with Fluorostar Optima plate reader every 5 min. The 300 mg/kg dose of KYNA used in the *in vivo* experiments was converted to an equimolar concentration (250 μM). After intensity stabilized (in approximately 1 h), the cells were treated with 20 mM LO, 25-2500 μM KYNA/SZR-72/NMDA according to the experimental protocol. At the end of the experiment (approximately 10 h), Triton X-100 was added to each well to kill every living cells. Intensity measured at this point was considered to represent 100% toxicity. Data were evaluated by selecting minimum (MIN) and maximum (MAX) intensities in each treatment-group. The percentage of cell death at each time point was calculated using the following formula: [(intensity-MIN)/(MAX-MIN)]*100. Figures show the values measured at 8 h.

Neutrophil Granulocyte Isolation and Measurement of H_2O_2 Production

Neutrophil granulocytes were isolated from rats treated with PS, LO or LO+300 mg/kg SZR-72 24 h prior to AP induction using Ficoll-Hypaque density gradient centrifugation. After sacrifice, blood was collected in EDTA coated tubes from each animal. Blood was gently mixed with equal volume of 3% Dextran solution and left to sediment for 40 min. In a conical tube, the leukocyte-rich plasma was carefully added on top of Ficoll-Hypaque, forming two phases. After centrifugation (250 RCF, 40 min) polymorphonuclear and red blood cell pellet was obtained. Erythrocytes were lysed with 0.2 % NaCl solution for no more than 30 sec. Immediately thereafter, lysis was stopped with ice-cold 3% NaCl solution. If red color was still visible after centrifugation, the process was repeated. Granulocytes were resuspended in phosphate buffered saline (PBS) containing 10 mM glucose, then cells were counted in a Bürker chamber. Cell number was adjusted to $1.5x10^4$/100μl. H_2O_2 production was measured with Fluorostar Optima plate reader (BMG Labtech, Ortenberg, Germany) using Amplex Red Hydrogen Peroxide/Peroxidase Assay Kit described by the manufacturer.

Measurement of IL-1β Production in Isolated Acinar Cells

Isolated pancreatic acinar cells were placed into 6-well plates and treated with medium, LO (20mM), KYNA (250μM), SZR-72 (250μM) or with the combination of LO and KYNA/SZR-72 for 6 h. Then cells were washed with PBS, then the washing buffer was removed and cells were frozen at -80°C until further processes. Then 200 μL homogenization buffer (Na-HEPES 10 mM, $MgCl_2$ 1μM, KCl 10mM, iodoacetamide 5mM, benzamidine-HCl 4 mM, DL-Dithiothreitol 1mM, Phenylmethyl sulfonylfluoride 1mM) was added to the first well and cells were scratch from the bottom. Further 100 μL homogenization buffer was used to collect the remaining cells. After that the collected suspension of cells was added to the next well (same treated group) and scratching process were repeated. 50 μL cell free homogenization buffer was used to wash and collect the remaining cells. With this process two wells were pooled into one microcentrifuge tube. Following this, 3x15s homogenization with sonication was carried out, and homogenate was incubated for 20 min at 0°C. Then homogenates were centrifuged with 20000 rcf at 4°C for 20 min and supernatants were kept for further measurements. To determine the extent of inflammatory response in the acinar cells interleukin-1β (IL-1β) levels were measured by a commercial ELISA kit from R&D Systems as described by the manufacturer.

Statistical Analysis

Data are presented as means ± SEM. Experiments were evaluated by one-way ANOVA followed by Holm-Sidak *post hoc* test or two-way ANOVA followed by Bonferroni *post hoc* test (SPSS, IBM, Armonk, NY, USA). $P<0.05$ was accepted as statistically significant.

RESULTS

Dose-Dependent Effects of KYNA and Its Analog SZR-72 on the Severity of AP

Three different doses of KYNA were tested to determine its effects on LO-induced AP (**Figure 2**). Representative histological images show morphological changes of the pancreas in different

groups (**Figure 2A**). LO administration alone induced necrotizing AP, while 300 mg/kg KYNA significantly reduced pancreatic tissue injury observed in AP. Marked increase of pancreatic edema was detected in the LO-treated groups compared to control, while the highest dose of KYNA (300 mg/kg) significantly reduced it (**Figures 2B, C**). Leukocyte infiltration into the pancreas and tissue MPO activity also significantly increased in AP groups compared to control (**Figures 2D, E**). As seen in case of edema, the 300 mg/kg dose of KYNA significantly reduced both leukocyte infiltration and MPO activity during AP, while smaller doses of KYNA were ineffective. The most important measure of inflammation is tissue damage, which was remarkable in response to a single LO-treatment (**Figure 2F**), but it significantly decreased in the 300 mg/kg KYNA group. Serum amylase activity also increased in the LO group, while 150 and 300 mg/kg KYNA significantly reduced the enzyme activity (**Figure 2G**). Overall, the two lower doses (75 and 150 mg/kg) of KYNA did not significantly influence most of the measured values, but 300 mg/kg KYNA reduced the severity of AP.

Similar results to KYNA were obtained when the effects of different doses of its analog, SZR-72 were examined (**Figure 3**). Histological images show the effects of LO and the co-treatment of LO and SZR-72 (**Figure 3A**). The signs of AP could be observed in tissue sections and 300 mg/kg SZR-72 reduced tissue damage. The 300 mg/kg dose of SZR-72 was able to significantly reduce the AP-evoked increases in pancreatic edema and leukocyte infiltration (**Figures 3B, D**). These results were supported by measurements of pancreatic water content and MPO activity (**Figures 3C, E**). The scores of pancreatic damage could be significantly reduced by the highest dose of SZR-72 in AP (**Figure 3F**). Serum amylase activity increased in response to LO injection, which was decreased by all SZR-72 doses (**Figure 3G**). Overall, AP severity parameters were reduced by 300 mg/kg SZR-72 treatment.

The Effects of KYNA and SZR-72 Treatment on Microcirculation and Hemodynamic Changes in AP

Hemodynamic parameters were determined during AP and KYNA/SZR-72 treatments (**Figure 4**). AP significantly increased cardiac output and carotid artery flow compared to the control animals (**Figures 4A, B**). Cardiac output in rats with AP was reduced to the level of the control group by both KYNA and SZR-72 compounds, whereas the decrease in carotid artery flow was significant only in case of SZR−72. Mean arterial blood pressure was comparable in each experimental group (**Figure 4C**). Pancreatic microcirculation was quantified by measuring serosal RBCV (**Figure 4D**). Interestingly, microcirculation significant decreased in LO−induced AP compared to the control group. However, pre-treatment with KYNA or SZR-72 (300 mg/kg) was able to improve microcirculation during AP.

LO−induced AP caused a significant drop in arterial blood pH and bicarbonate concentration resulting in metabolic acidosis, which was restored to the level of the control group by KYNA and SZR-72 pre-treatments (**Figures 5A, B**). At the same time, there was no detectable difference in arterial pCO_2 between the examined groups (**Figure 5C**).

Changes in Pancreatic IL-1β and HSP72 Expression in AP Upon KYNA and SZR-72 Treatment

KYNA and SZR-72 alone did not affect pancreatic IL-1β content of the pancreas (**Supplementary Figure 1A**). However, IL-1β levels significantly increased in the LO groups compared to control animals (**Figure 6A**). In the AP groups that received KYNA or SZR-72, IL-1β levels were significantly reduced and reached the level of control.

As a member of the HSP70 family, HSP72 is the major stress-induced protective chaperone in mammalian cells. First, we examined how KYNA and SZR-72 treatment affected pancreatic HSP72 levels in physiological conditions (**Supplementary Figures 1B, C**) and during AP (**Figures 6B, C**; the corresponding raw blot image is shown in **Supplementary Figure 2**). KYNA and SZR-72 alone significantly increased HSP72 expression compared to the control group, and SZR-72 had more prominent effect on HSP72 protein expression than KYNA (**Supplementary Figures 1B, C**). In our experiments, it was clear that the level of HSP72 was elevated in AP compared to the control group (**Figures 6B, C**). However, when the animals also received KYNA or SZR-72 pre-treatment, the amount of HSP72 significantly increased even compared to the AP group without KYNA or SZR-72.

The Detection of NMDA Receptor-1 in the Pancreas

NMDAR1 expression was examined by RT-PCR and immunohistochemistry (**Figure 7**). In both methods, brain tissue was used as a positive control. mRNA expression was much lower in the pancreas than in the brain (**Figure 7A**; full scan of the original gel is shown in **Supplementary Figure 3**). This was also confirmed by immunohistochemistry, where NMDAR1 staining of the brain was clearly visible (**Figure 7B**; raw images are presented in **Supplementary Figure 4**). The image of the control pancreas showed low NMDAR1 expression with well-structured amylase staining. The pancreas was sampled 2 and 24 h after LO administration in order to visualize if there was a difference in NMDAR1 staining depending on how advanced the inflammation was. NMDAR1 staining was found to be more pronounced 2 h after AP induction, however, the strongest staining was observed after 24 h. In parallel, amylase staining lost its structural integrity as the inflammation progressed.

In Vitro Protective Effects of KYNA, SZR-72, and NMDA on LO-Induced Cellular Toxicity

The effects of KYNA and SZR-72 were measured on LO-induced cellular toxicity in *in vitro* experiments. Since both compounds are NMDAR antagonists, NMDA was also applied to reveal whether KYNA or SZR-72 exert their effect on NMDAR. Before testing the protective properties of KYNA and SZR-72, or their interaction

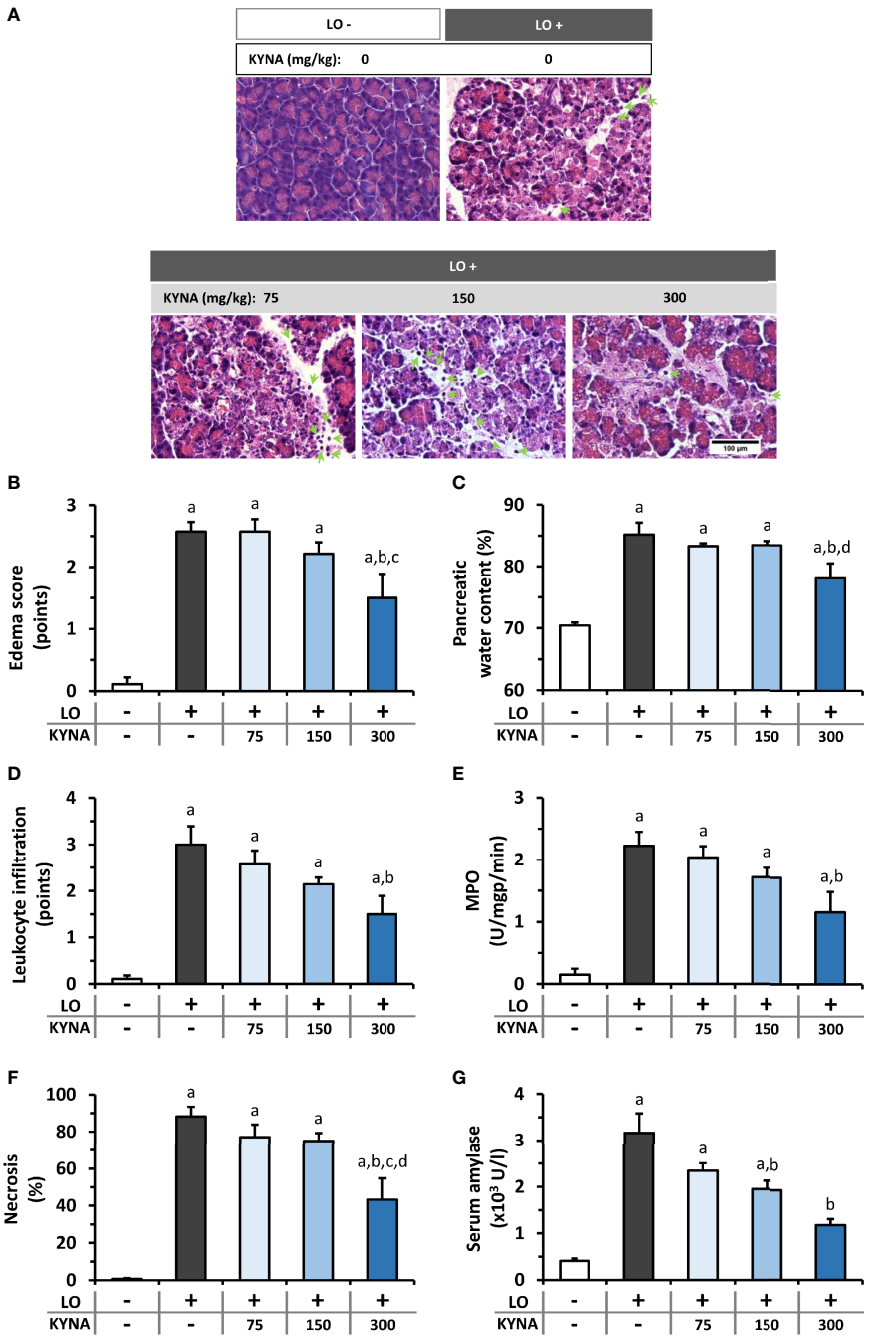

FIGURE 2 | The effects of kynurenic acid (KYNA) on the severity of acute pancreatitis (AP). **(A)** Representative histopathological images of pancreatic tissues of the treatment groups, arrows indicate neutrophil granulocytes. Bar charts show the extent of pancreatic **(B)** edema, **(C)** water content, **(D)** leukocyte infiltration, **(E)** myeloperoxidase (MPO) activity, **(F)** necrosis, and **(G)** serum amylase activity measurements. Values represent means with standard error, n=5-14. One-way ANOVA was performed followed by Holm-Sidak post-hoc test. Statistically significant differences ($p<0.05$) were marked with: (a) *vs*. control; (b) *vs*. LO; (c) *vs*. LO+75 mg/kg KYNA; (d) *vs*. LO+150 mg/kg KYNA. AP, acute pancreatitis; KYNA, kynurenic acid; LO, L-ornithine-HCl; MPO, myeloperoxidase.

with NMDAR, the safe concentrations of KYNA, SZR-72, and NMDA were determined on isolated pancreatic acinar cells (**Figure 8A** and **Supplementary Figure 5**). SZR-72 could be safely administered until 625 µM, higher concentrations were toxic to acinar cells (**Supplementary Figure 5**). As the 300 mg/kg dose of KYNA proved to be effective *in vivo*, the corresponding, equimolar (250µM) and ten times higher concentrations (2500 µM) of KYNA and NMDA were tested on acini. In case of SZR-72, only the 250 µM concentration was used in further viability studies because the ten times higher concentration has been already

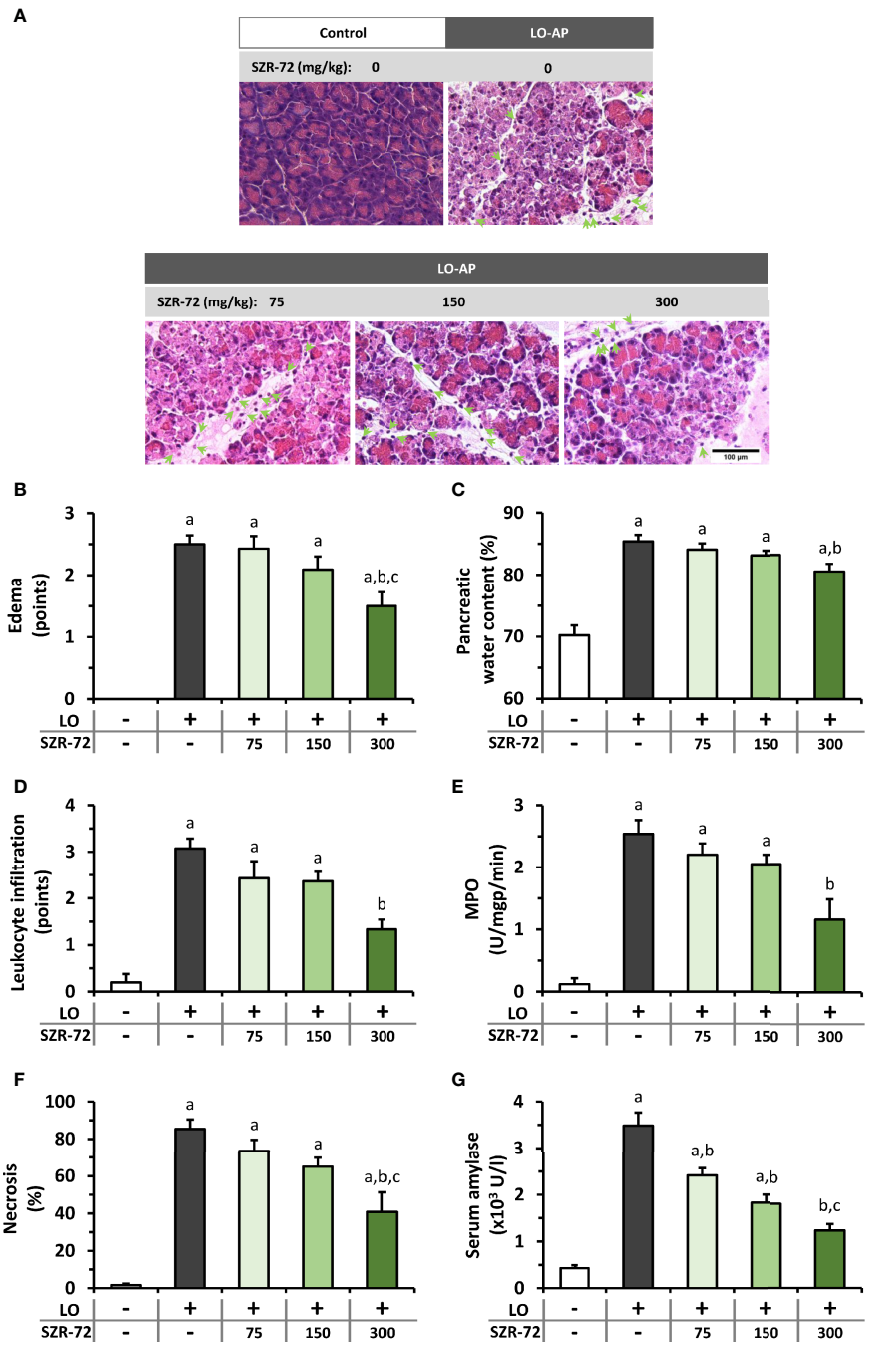

FIGURE 3 | The effects of SZR-72 on the severity of AP. **(A)** Representative histopathological images of pancreatic tissues of the treatment groups, arrows indicate neutrophil granulocytes. Bar charts show the extent of pancreatic **(B)** edema, **(C)** water content, **(D)** leukocyte infiltration, **(E)** myeloperoxidase (MPO) activity, **(F)** necrosis, and **(G)** serum amylase activity measurements. Values represent means with standard error, n=5-11. One-way ANOVA was performed followed by Holm-Sidak post-hoc test. Statistically significant differences ($p<0.05$) were marked with: (a) *vs*. control; (b) *vs*. LO; (c) *vs*. LO+75 mg/kg SZR-72. LO, L-ornithine-HCl; MPO, myeloperoxidase.

proved to be toxic. Neither KYNA nor NMDA affected pancreatic acinar viability even at a concentration of 2500 µM (**Figure 8A**). We then measured the effect of LO treatment on cell viability and whether it could be affected by KYNA, SZR-72, or NMDA (**Figure 8B**). LO was shown to be highly toxic to pancreatic acinar cells. However, KYNA prevented the toxic effect of LO at both 250 and 2500 µM concentrations and cell viability was comparable to the control group. Treatment with 250 µM SZR-

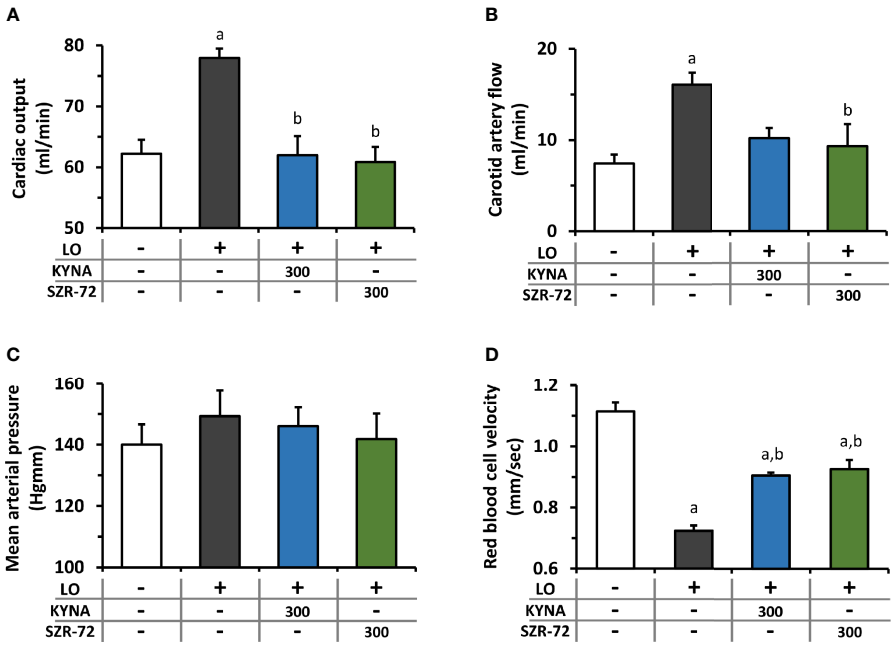

FIGURE 4 | Changes in circulation and haemodynamic parameters during experimental AP and treatments with KYNA and SZR-72. Bar charts show **(A)** cardiac output, **(B)** carotid artery flow **(C)** mean arterial pressure, and **(D)** red blood cell velocity. Values represent means with standard error, **(A–C)** n=3-6; **(D)** n=60-98. One-way ANOVA was performed followed by Holm-Sidak post-hoc test. Statistically significant differences ($p<0.05$) were marked with: (a) *vs*. control; (b) *vs*. LO. LO, L-ornithine-HCl.

72 also significantly reduced LO-induced toxicity. NMDA did not affect the toxicity of LO at any concentrations. Last, we examined whether the beneficial effects of KYNA and SZR-72 could be suspended by the addition of NMDA (**Figure 8C**). Beside LO, acinar cells received 250 μM KYNA or SZR-72 and increasing doses of NMDA (25, 250, 2500 μM). Co-treatment with NMDA had no effect on cell viability. KYNA and SZR-72 were still able to significantly reduce toxicity compared to the LO group. Moreover, KYNA treatment resulted in decreased cellular toxicity which was comparable to the control group.

SZR-72 Reduces the Activity of H_2O_2 Production in Isolated Neutrophil Granulocytes, But Has No Effect on IL-1β Expression of Pancreatic Acinar Cells

Neutrophil granulocytes play an important role in the development of AP. H_2O_2 production corresponds to their function. The effect of SZR-72 was determined on neutrophil granulocyte function (**Figure 9**). H_2O_2 production of granulocytes was examined after cell isolation from control, LO- and LO + SZR-72-treated animals. In case of control granulocytes, H_2O_2 production remained at baseline throughout the experiment. In contrast, neutrophils from AP animals produced increased amounts of H_2O_2, the level of which was significantly different from the control group from as early as 20 min. However, when neutrophils from LO and SZR-72 co-treated animals were examined, a significant decrease was observed in H_2O_2 production from 70 min compared to LO treatment alone.

The IL-1β protein expression of isolated acinar cells was measured *in vitro* after 6h treatment with LO, KYNA, and/or SZR-72 (**Supplementary Figure 6**). LO administration did not induce any change in IL-1β expression compared to the control group in acinar cells. Furthermore, KYNA, SZR-72 or their combinations with LO did not affect the proinflammatory cytokine production, these were comparable with the control group.

DISCUSSION

As AP is a disorder without specific therapy, it is important to find possibilities for its management. The pathophysiology of the disease involves multiple cell types and processes (6). The pathway of tryptophan metabolism is unambiguously disturbed during AP, resulting in overactivation of kynurenine-3-monooxygenase enzyme and excess production of pro-inflammatory 3-HK (20, 21). In this study, we tested the possible application of endogenous tryptophan pathway metabolite KYNA, and its synthetic derivative SZR-72 for the treatment of experimental AP. Our novel findings with KYNA or SZR-72 administration in experimental AP are the following: They (1) dose-dependently reduced the severity of the disease; (2) reduced the proinflammatory cytokine IL-1β expression

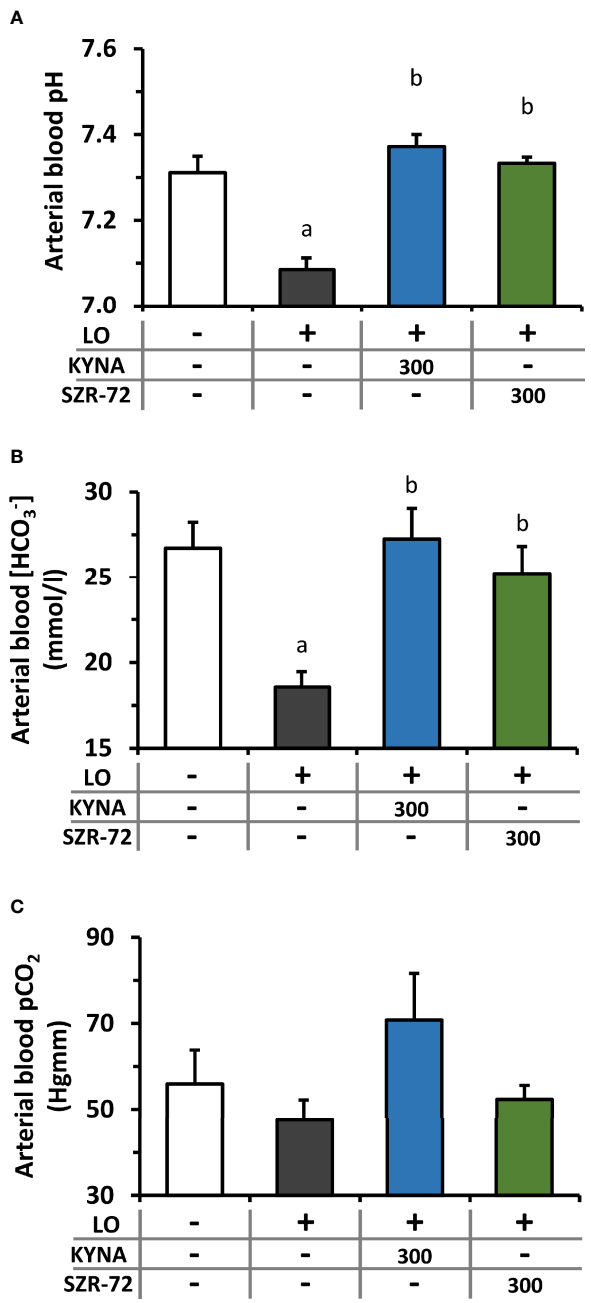

FIGURE 5 | Plasma pH and HCO_3^- and pCO_2 levels during experimental AP and treatments with KYNA and SZR-72. Bar charts show **(A)** arterial blood pH, **(B)** arterial blood HCO_3^- concentration, and **(C)** arterial blood CO_2 pressure. Values represent means with standard error, n=3-6. One-way ANOVA was performed followed by Holm-Sidak post-hoc test. Statistically significant differences ($p<0.05$) were marked with: (a) *vs*. control; (b) *vs*. LO. LO, L-ornithine-HCl.

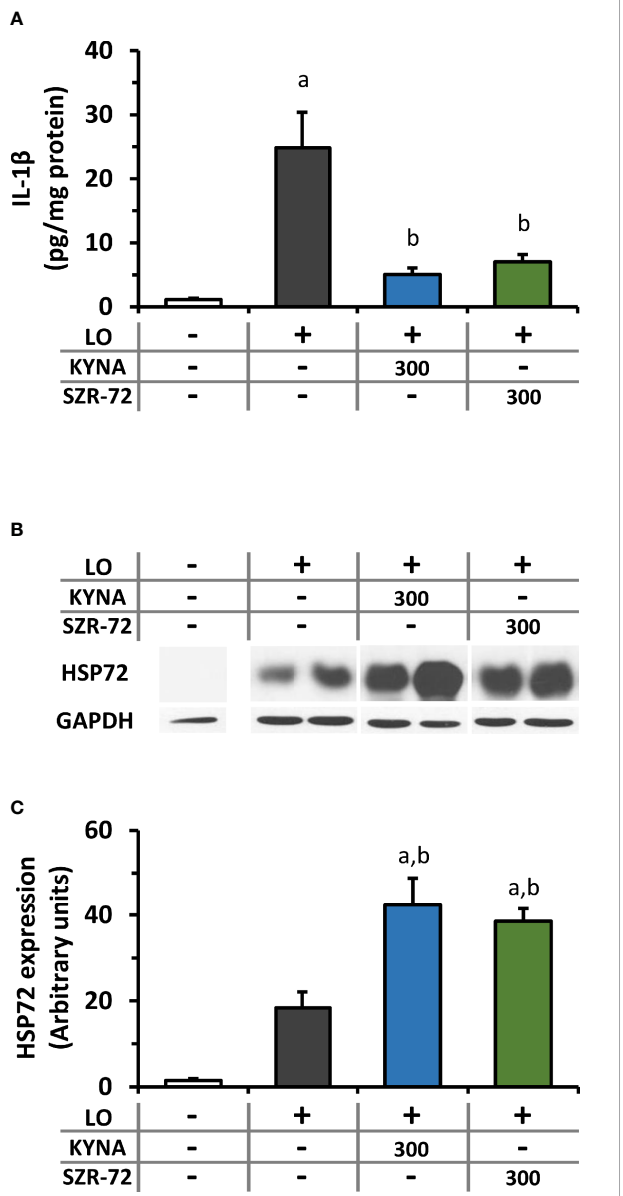

FIGURE 6 | Changes in interleukin 1 beta (IL-1β) and heat shock protein 72 (HSP72) levels in AP in rats treated with 300 mg/kg KYNA or SZR-72. **(A)** Pancreatic IL-1β level, **(B)** representative Western blot images of pancreatic HSP72 and glicerinaldehide-3-phosphate-dehydrogenase (GAPDH) levels, and **(C)** densitometry of Western Blot images for pancreatic HSP72 level. Values represent means with standard error, n=7-10. One-way ANOVA was performed followed by Holm-Sidak post-hoc test. Statistically significant differences ($p<0.05$) were marked with: (a) *vs*. control; (b) *vs*. LO.

invivo; (3) increased the synthesis of HSP72; (4) reduced the extent of metabolic acidosis; (5) restored pancreatic microcirculation; (6) suppressed the function of neutrophil granulocytes. (7) In addition, their effect was likely to be independent of acinar NMDAR1.

SZR-72 can cross the blood-brain barrier, while KYNA is poorly permeable (14, 15). Therefore, SZR-72 can exert its effect in the central nervous system as well (29, 30). As the results with SZR-72 and KYNA were similar, we do not think that the possible central nervous system effects of SZR-72 play part in the protection of AP.

We demonstrated that the 300 mg/kg dose of KYNA and SZR-72 exerted strong anti-inflammatory effects. Csáti et al. (31)

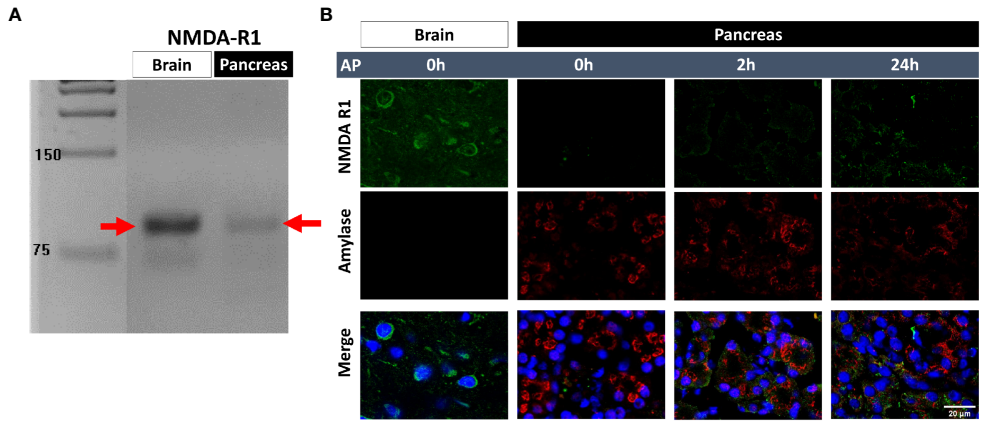

FIGURE 7 | Detection of N-methyl-D-aspartate receptor 1 (NMDAR1) expression. **(A)** NMDAR1 mRNA expression in brain cortex and pancreas, **(B)** representative immunofluorescent images (NMDAR1, amylase, and cellular nuclei stainings) of pancreatic tissue (scale bar: 20 µm). Panc, pancreas.

also applied the same dose of KYNA or kynurenic acid amide 2 in rats i.p., and they observed successful suppression of inflammation evoked by trigeminal ganglion activation. Similar results were obtained when SZR-72 was applied at 300 mg/kg dose i.p. in rats, the KYNA analogue exerted anti-inflammatory response in a model of trigeminal nerve activation (32). In case of rat experimental colitis, more than ten times smaller doses could be used effectively (18, 25). Furthermore, Juhász et al. (16) successfully applied KYNA or SZR-72 in a sepsis model at 2 x 15 or 2 x 23.5 mg/kg respectively. Based on these results, it seems that the effective dose of KYNA and SZR-72 also depends on the disease model.

Hemodynamic parameters like cardiac output and arterial blood flow were increased by AP. Interestingly, this was reduced by KYNA/SZR-72 administration. Blood pressure was unchanged; thus, it is likely that the increase in heart rate contribute to the increased cardiac output. The exact mechanism how KYNA and SZR-72 may affect heart rate is unknown, but most probably this effect is indirect. Similar findings were seen by Badzynska et al. (33) in spontaneously hypertensive rats, where treatment with 25 mg/kg/day KYNA decreased heart rate. An explanation can be the effect of pain, as pain is one of the symptoms of AP and it positively relates to heart rate (34). GPR35 receptor was considered important for nociceptive transmission, and through this receptor KYNA can reduce the pain, which can contribute to the reduced heart rate. However, these speculations should be tested in the future.

AP causes the impairment of both pancreatic and systemic microcirculation (35), which are among the early signs of AP (36). We showed significantly decreased RBCV in the pancreas during experimental AP, which was remarkably restored by the administration of KYNA or SZR-72. The reduced organ microcirculation contributes to ischemia and organ failure, not just in the pancreas but in other organs like the kidneys or lungs. Therefore, KYNA or SZR-72 can alleviate the symptoms of multiple and/or persistent organ failure which is present in the severe form of the disease. Furthermore, Zhang et al. (37) found that decrease in intestinal microcirculation secondary to severe AP can lead to reduced mucosal barrier integrity and immunity, thus increased possibility of infection, sepsis, and mortality. Based on this, the beneficial effect of KYNA and SZR-72 on microcirculation is important and should be further investigated. Interestingly, in our earlier work, KYNA improved ileal microcirculation in a sepsis model, while SZR-72 was ineffective (16). However, in that model SZR-72 could improve mitochondrial respiration, resulting in improved conversion of ADP to ATP. In the present research, the investigation of mitochondrial function was not in focus. However, mitochondrial dysfunction is common in AP and has serious effects (6), therefore further studies are also needed to reveal how KYNA or its derivatives modulate that.

AP is often accompanied by acid-base disturbance. Our earlier work showed the relationship between AP severity and metabolic acidosis (38). Meta-analyses of clinical studies confirmed that the severity of AP relates to the extent of metabolic acidosis. Furthermore, experimental AP aggravated the pre-existing acid-base imbalance. There are several mechanisms that trigger metabolic acidosis during AP, e.g. loss of bicarbonate-rich pancreatic juice through pancreatic fistula or drainage, lactic acidosis due to shock or sepsis which can develop in AP (39). An important observation was that both KYNA and SZR-72 effectively restored the decreased pH and HCO_3^- concentration in the plasma. The exact mechanism how they affect the acid-base balance is unknown, but this effect could also contribute to the reduced disease severity.

HSP72 is an inducible chaperon which is upregulated in different conditions of stress like inflammation. It was found earlier that thermal stress-induced HSP72 increase could protect against AP (40, 41), and pharmacological induction of HSP72 by BRX-220 was also effective in treatment of experimental AP (42, 43). Furthermore, overexpression of HSP72 in transgenic mice enhanced recovery from AP (44). In our study, we showed that both KYNA and SZR-72 significantly increased pancreatic HSP72 expression in rats. Pancreatic HSP72 expression was

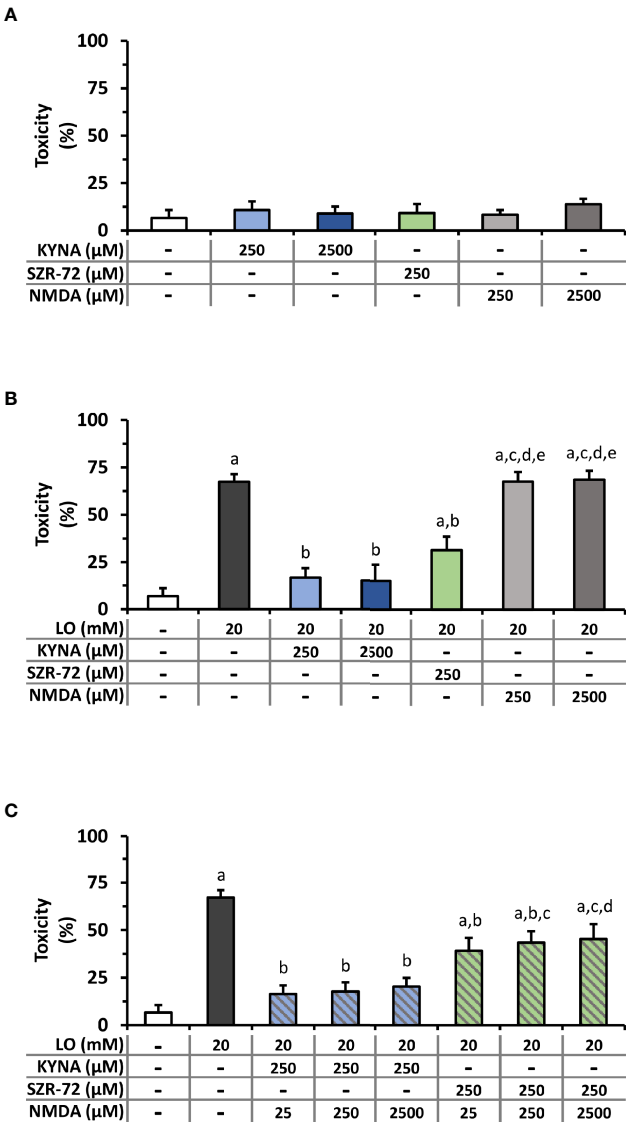

FIGURE 8 | Toxicity measurements on isolated pancreatic acinar cells. **(A)** Toxicity of KYNA, SZR-72, and N-methyl-D-aspartate (NMDA) in different concentrations. **(B)** Toxic effect of L-ornithine-HCl (LO) combined with KYNA, SZR–72 or NMDA treatments. One-way ANOVA was performed followed by Holm-Sidak post-hoc test. Statistically significant differences ($p<0.05$) were marked with: (a) *vs*. control; (b) *vs*. LO; (c) *vs*. LO+250 μM KYNA; (d) *vs*. LO+2500 μM KYNA; (e) *vs*. LO+250 μM SZR-72. **(C)** Toxicity of co-treatment of LO (20 μM) and NMDA (25, 250, 2500 μM) combined with 250 μM KYNA or SZR-72. One-way ANOVA was performed followed by Holm-Sidak post-hoc test. Statistically significant differences ($p<0.05$) were marked with: (a) *vs*. control; (b) *vs*. LO; (c) *vs*. LO+250 μM KYNA+25 μM NMDA; (d) *vs*. LO+250 μM KYNA+250 μM NMDA. Values represent means with standard error, n=4-10.

also increased in AP, KYNA or SZR-72 treatment further upregulated protein expression. SZR-72 was significantly more potent HSP72-inducer than KYNA. The effects of KYNA or SZR-72 on HSP72 can be one of the mechanisms how they exert protection in AP.

NMDAR1 receptor expression was present in pancreatic tissue even in physiological conditions. Surprisingly, NMDAR1 protein expression was increased by the progression of AP. This phenomenon could be explained by three reasons (1): pancreatic cells (e.g. acinar, ductal, beta cells) increased their expression of NMDAR1 (2); invading leukocytes express the receptor (3); the previous two together. We tested whether KYNA or SZR-72 exert their effects *via* NMDAR1. *In vitro* acinar cell LO toxicity measurements demonstrated that the observed protection of KYNA or SZR-72 was unlikely to be related to NMDAR1. Receptor agonist NMDA did not influence the effects of receptor antagonists KYNA or SZR-72 even at ten times the concentration. Therefore, the observed protection against LO-AP could be a direct effect or could be mediated by another receptor like GPR35. KYNA is an endogenous

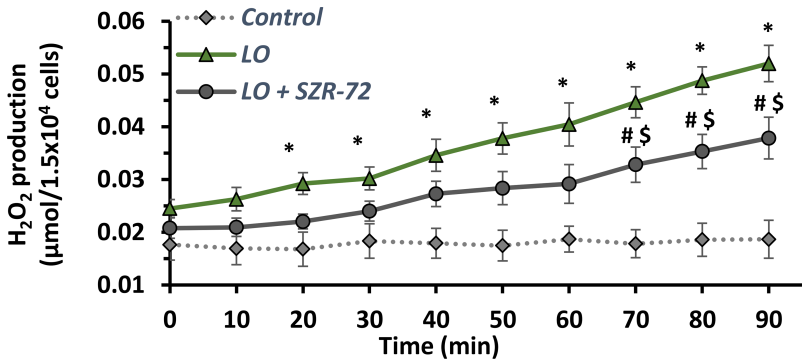

FIGURE 9 | Time course of H_2O_2 production of neutrophil granulocytes isolated from rats treated with physiological saline, LO or LO+300 mg/kg SZR-72. Values represent means with standard error, n=4. Two-way ANOVA was performed followed by Bonferroni post-hoc test. Statistically significant differences ($p<0.05$) were marked with: (*) control *vs*. LO; (#) LO *vs*. LO+SZR-72; ($) control *vs*. LO+SZR-72.

antioxidant, and it can decrease ROS release evoked by AP (45). GPR35 receptor is present in macrophages, eosinophil and basophil granulocytes, mast cells, natural killer T cells, and several cells along the digestive tract (46). GPR35 activation will result in decreased intracellular Ca^{2+} and cAMP signals, inhibition of phosphoinositide 3-kinase/protein kinase B and mitogen-activated protein kinase (MAPK) pathways. All these effects of KYNA-GPR35 interactions contribute to immunosuppression. Our goal was not to investigate the GPR35-mediated effect of KYNA or SZR-72 in AP, but further studies can focus on it.

KYNA or SZR-72 markedly reduced the pancreatic IL-1β expression *in vivo*. However, this effect seems to be independent of acinar cells. Therefore, the tested agents most probably affect leukocytes, and this can result in decreased cytokine release from the pancreatic tissue. Neutrophil granulocytes are the first inflammatory cells reaching the pancreas during AP. ROS such as H_2O_2 is produced in large quantities by neutrophils which reflects the activity of these cells (47). Our measurements showed that *in vivo* administration of SZR-72 reduced H_2O_2 production in neutrophil granulocytes isolated from AP rats. Since neutrophils contribute to AP by amplifying the inflammatory cascade, the reduced activity of these cells by KYNA or SZR-72 is also beneficial and can contribute to their mechanism of action.

In conclusion, we showed that treatment with endogenous tryptophan metabolite KYNA and its synthetic analog SZR-72 dose dependently reduced the severity of experimental AP (**Table 2**). There may be several mechanisms mediating this protective effect. Both molecules reduce the pancreatic expression of the proinflammatory cytokine IL-1β and increase the expression of HSP72 protein. These compounds also ameliorate metabolic acidosis, and restore hemodynamic parameters including pancreatic microcirculation. Their action seems to be independent of acinar NMDAR1 in AP. SZR-72 also suppresses the activation of neutrophil granulocytes. Overall, these molecules could be beneficial in AP.

TABLE 2 | Summarizing the effects (*in vivo*: 300 mg/kg; *in vitro*: 250 µM) of KYNA and SZR-72 in AP.

			KYNA	SZR-72
Experimental AP (*in vivo*)	**Pancreatic effects**	**Histological parameters**	↓↓	↓↓
		MPO	↓↓	↓↓
		Water content	↓↓	↓↓
		Local microcirculation	Partially restored	Partially restored
		IL-1β expression	Restored	Restored
		HSP72 expression during AP	↑↑	↑↑
		HSP72 expression in physiological conditions	↑	↑↑
	Systemic effects	**Serum amylase**	↓↓	↓↓
		Cardiac output	Restored	Restored
		Metabolic acidosis	Restored	Restored
***In vitro* experiments**	**Pancreatic acinar cells**	**Cell protection**	++	+
		IL-1β expression	no effect	no effect
	Neutrophil granulocytes	**Suppression of ROS production**	N.A.	++

Explanation of symbols and phrases: ↓, decrease; ↑, increase; +, positive effect; restored/partially restored, the measured condition during AP was restored/partially restored to control levels after KYNA or SZR-72 treatment. AP, acute pancreatitis; HSP72, heat shock protein 72; IL-1β, interleukin-1β; KYNA, kynurenic acid; N.A., not available; MPO, myeloperoxidase; ROS, reactive oxygen species; SZR-72, 2-(2-N,N-dimethylaminoethyl-amine-1carbonyl)-1H-quinolin-4-one hydrochloride.

DATA AVAILABILITY STATEMENT

The raw data supporting the conclusions of this article will be made available by the authors, without undue reservation.

ETHICS STATEMENT

The animal study was reviewed and approved by Hungarian National Food Chain Safety Office 1024 Budapest, Keleti Károly u. 24. (1525 Budapest, Pf. 30).

AUTHOR CONTRIBUTIONS

ZR had the original idea, initiated the study, obtained funding, and supervised the experimental procedures. Most protocols were designed by ZB, EK, LK, and ZR. Animal experiments were performed by ZB, EK, BK, EB, GF, LK (*in vivo* AP experiments), and GV (microcirculation, haemodynamic measurements). *In vitro* measurements were fulfilled by ZB, EK, EO, GF (pancreatic acinar cell isolation, acinar viability, acinar IL-1β measurement), AH (total RNA isolation, RT-PCR) and CP (neutrophil granulocyte isolation, H_2O_2 production measurement). BI, LV, FF, AG, VT, MD, TM, VV, JM, and PH provided conceptual advice on experimental design and protocol. ZB and EK performed data analysis, ZB, EK, GF, and LK worked on statistical analysis, ZB, EK, EB, GF, and LK produced the figures. ZB, EK, LK, and ZR wrote the manuscript. All authors reviewed the manuscript and approved the final version.

FUNDING

This work was supported by EFOP-3.6.2–16–2017–00006, GINOP-2.3.2-15-2016-00034, János Bólyai Research Grant (BO/00866/20/5), ÚNKP Grant (ÚNKP-20-5-SZTE-163), NKFIH PD129114 and NKFIH K119938, University of Szeged Open Access Fund (Grant No. 5304). The funders did not influence the interpretation of results in any way.

ACKNOWLEDGMENTS

Authors would like to thank Kitti Ancsányi and Erzsébet Dallos-Szilágyi for the technical assistance.

SUPPLEMENTARY MATERIAL

The Supplementary Material for this article can be found online at: https://www.frontiersin.org/articles/10.3389/fimmu.2021.702764/full#supplementary-material

REFERENCES

1. Peery AF, Crockett SD, Barritt AS, Dellon ES, Eluri S, Gangarosa LM, et al. Burden of Gastrointestinal, Liver, and Pancreatic Diseases in the United States. *Gastroenterology* (2015) 149:1731–41.e3. doi: 10.1053/j.gastro.2015.08.045
2. Roberts SE, Morrison-Rees S, John A, Williams JG, Brown TH, Samuel DG. The Incidence and Aetiology of Acute Pancreatitis Across Europe. *Pancreatology* (2017) 17:155–65. doi: 10.1016/j.pan.2017.01.005
3. Forsmark CE, Vege SS, Wilcox CM. Acute Pancreatitis. *N Engl J Med* (2016) 375:1972–81. doi: 10.1056/NEJMra1505202
4. Banks PA, Bollen TL, Dervenis C, Gooszen HG, Johnson CD, Sarr MG, et al. Classification of Acute Pancreatitis–2012: Revision of the Atlanta Classification and Definitions by International Consensus. *Gut* (2013) 62:102–11. doi: 10.1136/gutjnl-2012-302779
5. Abu-El-Haija M, Gukovskaya AS, Andersen DK, Gardner TB, Hegyi P, Pandol SJ, et al. Accelerating the Drug Delivery Pipeline for Acute and Chronic Pancreatitis: Summary of the Working Group on Drug Development and Trials in Acute Pancreatitis at the National Institute of Diabetes and Digestive and Kidney Diseases Workshop. *Pancreas* (2018) 47:1185–92. doi: 10.1097/MPA.0000000000001175
6. Barreto SG, Habtezion A, Gukovskaya A, Lugea A, Jeon C, Yadav D, et al. Critical Thresholds: Key to Unlocking the Door to the Prevention and Specific Treatments for Acute Pancreatitis. *Gut* (2021) 70:194–203. doi: 10.1136/gutjnl-2020-322163
7. Pallagi P, Balla Z, Singh AK, Dósa S, Iványi B, Kukor Z, et al. The Role of Pancreatic Ductal Secretion in Protection Against Acute Pancreatitis in Mice*. *Crit Care Med* (2014) 42:177–88. doi: 10.1097/CCM.0000000000000101
8. Pallagi P, Madácsy T, Varga Á, Maléth J. Intracellular Ca^{2+} Signalling in the Pathogenesis of Acute Pancreatitis: Recent Advances and Translational Perspectives. *Int J Mol Sci* (2020) 21:1–18. doi: 10.3390/ijms21114005
9. Gukovskaya AS, Vaquero E, Zaninovic V, Gorelick FS, Lusis AJ, Brennan ML, et al. Neutrophils and NADPH Oxidase Mediate Intrapancreatic Trypsin Activation in Murine Experimental Acute Pancreatitis. *Gastroenterology* (2002) 122:974–84. doi: 10.1053/gast.2002.32409
10. Sendler M, Weiss FU, Golchert J, Homuth G, van den Brandt C, Mahajan UM, et al. Cathepsin B-Mediated Activation of Trypsinogen in Endocytosing Macrophages Increases Severity of Pancreatitis in Mice. *Gastroenterology* (2018) 154:704–18.e10. doi: 10.1053/j.gastro.2017.10.018
11. Vécsei L, Szalárdy L, Fülöp F, Toldi J. Kynurenines in the CNS: Recent Advances and New Questions. *Nat Rev Drug Discov* (2013) 12:64–82. doi: 10.1038/nrd3793
12. Mándi Y, Vécsei L. The Kynurenine System and Immunoregulation. *J Neural Transm (Vienna)* (2012) 119:197–209. doi: 10.1007/s00702-011-0681-y
13. Nahomi RB, Nam MH, Rankenberg J, Rakete S, Houck JA, Johnson GC, et al. Kynurenic Acid Protects Against Ischemia/Reperfusion-Induced Retinal Ganglion Cell Death in Mice. *Int J Mol Sci* (2020) 21:1795. doi: 10.3390/ijms21051795
14. Fukui S, Schwarcz R, Rapoport SI, Takada Y, Smith QR. Blood-Brain Barrier Transport of Kynurenines: Implications for Brain Synthesis and Metabolism. *J Neurochem* (1991) 56:2007–17. doi: 10.1111/j.1471-4159.1991.tb03460.x
15. Lukács M, Warfvinge K, Tajti J, Fülöp F, Toldi J, Vécsei L, et al. Topical Dura Mater Application of CFA Induces Enhanced Expression of C-Fos and Glutamate in Rat Trigeminal Nucleus Caudalis: Attenuated by KYNA Derivate (SZR72). *J Headache Pain* (2017) 18:39. doi: 10.1186/s10194-017-0746-x
16. Juhász L, Rutai A, Fejes R, Tallósy SP, Poles MZ, Szabó A, et al. Divergent Effects of the N-Methyl-D-Aspartate Receptor Antagonist Kynurenic Acid and the Synthetic Analog SZR-72 on Microcirculatory and Mitochondrial Dysfunction in Experimental Sepsis. *Front Med (Lausanne)* (2020) 7:566582. doi: 10.3389/fmed.2020.566582
17. Tiszlavicz Z, Németh B, Fülöp F, Vécsei L, Tápai K, Ocsovszky I, et al. Different Inhibitory Effects of Kynurenic Acid and a Novel Kynurenic Acid Analogue on Tumour Necrosis Factor-α (TNF-α) Production by Mononuclear Cells, HMGB1 Production by Monocytes and HNP1-3 Secretion by Neutrophils. *Naunyn Schmiedebergs Arch Pharmacol* (2011) 383:447–55. doi: 10.1007/s00210-011-0605-2
18. Érces D, Varga G, Fazekas B, Kovács T, Tőkés T, Tiszlavicz L, et al. N-Methyl-D-Aspartate Receptor Antagonist Therapy Suppresses Colon Motility and

Inflammatory Activation Six Days After the Onset of Experimental Colitis in Rats. *Eur J Pharmacol* (2012) 691:225–34. doi: 10.1016/j.ejphar.2012.06.044
19. Wang Q, Liu D, Song P, Zou MH. Tryptophan-Kynurenine Pathway Is Dysregulated in Inflammation, and Immune Activation. *Front Biosci (Landmark Ed)* (2015) 20:1116–43. doi: 10.2741/4363
20. Skouras C, Zheng X, Binnie M, Homer NZ, Murray TB, Robertson D, et al. Increased Levels of 3-Hydroxykynurenine Parallel Disease Severity in Human Acute Pancreatitis. *Sci Rep* (2016) 6:33951. doi: 10.1038/srep33951
21. Mole DJ, Webster SP, Uings I, Zheng X, Binnie M, Wilson K, et al. Kynurenine-3-Monooxygenase Inhibition Prevents Multiple Organ Failure in Rodent Models of Acute Pancreatitis. *Nat Med* (2016) 22:202–9. doi: 10.1038/nm.4020
22. Rakonczay ZJr, Hegyi P, Dósa S, Iványi B, Jármay K, Biczó G, et al. A New Severe Acute Necrotizing Pancreatitis Model Induced by L-Ornithine in Rats. *Crit Care Med* (2008) 36:2117–27. doi: 10.1097/CCM.0b013e31817d7f5c
23. Kuebler WM, Abels C, Schuerer L, Goetz AE. Measurement of Neutrophil Content in Brain and Lung Tissue by a Modified Myeloperoxidase Assay. *Int J Microcirc Clin Exp* (1996) 16:89–97. doi: 10.1159/000179155
24. Lowry OH, Rosebrough NJ, Farr AL, Randall RJ. Protein Measurement With the Folin Phenol Reagent. *J Biol Chem* (1951) 193:265–75. doi: 10.1016/S0021-9258(19)52451-6
25. Varga G, Erces D, Fazekas B, Fülöp M, Kovács T, Kaszaki J, et al. N-Methyl-D-Aspartate Receptor Antagonism Decreases Motility and Inflammatory Activation in the Early Phase of Acute Experimental Colitis in the Rat. *Neurogastroenterol Motil* (2010) 22:217–25.e68. doi: 10.1111/j.1365-2982.2009.01390.x
26. Rakonczay ZJr, Boros I, Jármay K, Hegyi P, Lonovics J, Takacs T. Ethanol Administration Generates Oxidative Stress in the Pancreas and Liver, But Fails to Induce Heat-Shock Proteins in Rats. *J Gastroenterol Hepatol* (2003) 18:858–67. doi: 10.1046/j.1440-1746.2003.03076.x
27. Kurucz I, Tombor B, Prechl J, Erdö F, Hegedüs E, Nagy Z, et al. Ultrastructural Localization of Hsp-72 Examined With a New Polyclonal Antibody Raised Against the Truncated Variable Domain of the Heat Shock Protein. *Cell Stress Chaperones* (1999) 4:139–52. doi: 10.1379/1466-1268(1999)004<0139:ULOHEW>2.3.CO;2
28. Pandol SJ, Jensen RT, Gardner JD. Mechanism of [Tyr4]bombesin-Induced Desensitization in Dispersed Acini From Guinea Pig Pancreas. *J Biol Chem* (1982) 257:12024–9. doi: 10.1016/S0021-9258(18)33671-8
29. Demeter I, Nagy K, Farkas T, Kis Z, Kocsis K, Knapp L, et al. Paradox Effects of Kynurenines on LTP Induction in the Wistar Rat. *Vivo study. Neurosci Lett* (2013) 553:138–41. doi: 10.1016/j.neulet.2013.08.028
30. Kassai F, Kedves R, Gyertyán I, Tuka B, Fülöp F, Toldi J, et al. Effect of a Kynurenic Acid Analog on Home-Cage Activity and Body Temperature in Rats. *Pharmacol Rep* (2015) 67:1188–92. doi: 10.1016/j.pharep.2015.04.015
31. Csáti A, Edvinsson L, Vécsei L, Toldi J, Fülöp F, Tajti J, et al. Kynurenic Acid Modulates Experimentally Induced Inflammation in the Trigeminal Ganglion. *J Headache Pain* (2015) 16:99. doi: 10.1186/s10194-015-0581-x
32. Lukács M, Warfvinge K, Kruse LS, Tajti J, Fülöp F, Toldi J, et al. KYNA Analogue SZR72 Modifies CFA-Induced Dural Inflammation- Regarding Expression of Perk1/2 and IL-1β in the Rat Trigeminal Ganglion. *J Headache Pain* (2016) 17:64. doi: 10.1186/s10194-016-0654-5
33. Bądzyńska B, Zakrocka I, Turski WA, Olszyński KH, Sadowski J, Kompanowska-Jezierska E. Kynurenic Acid Selectively Reduces Heart Rate in Spontaneously Hypertensive Rats. *Naunyn Schmiedebergs Arch Pharmacol* (2020) 393:673–9. doi: 10.1007/s00210-019-01771-7
34. Tousignant-Laflamme Y, Rainville P, Marchand S. Establishing a Link Between Heart Rate and Pain in Healthy Subjects: A Gender Effect. *J Pain* (2005) 6:341–7. doi: 10.1016/j.jpain.2005.01.351
35. Cuthbertson CM, Christophi C. Disturbances of the Microcirculation in Acute Pancreatitis. *Br J Surg* (2006) 93:518–30. doi: 10.1002/bjs.5316
36. Dobosz M, Mionskowska L, Hac S, Dobrowolski S, Dymecki D, Wajda Z. Heparin Improves Organ Microcirculatory Disturbances in Caerulein-Induced Acute Pancreatitis in Rats. *World J Gastroenterol* (2004) 10:2553–6. doi: 10.3748/wjg.v10.i17.2553
37. Zhang J, Yu WQ, Wei T, Zhang C, Wen L, Chen Q, et al. Effects of Short-Peptide-Based Enteral Nutrition on the Intestinal Microcirculation and Mucosal Barrier in Mice With Severe Acute Pancreatitis. *Mol Nutr Food Res* (2020) 64:e1901191. doi: 10.1002/mnfr.201901191
38. Rumbus Z, Toth E, Poto L, Vincze A, Veres G, Czako L, et al. Bidirectional Relationship Between Reduced Blood pH and Acute Pancreatitis: A Translational Study of Their Noxious Combination. *Front Physiol* (2018) 9:1360. doi: 10.3389/fphys.2018.01360
39. Zhan XB, Guo XR, Yang J, Li J, Li ZS. Prevalence and Risk Factors for Clinically Significant Upper Gastrointestinal Bleeding in Patients With Severe Acute Pancreatitis. *J Dig Dis* (2015) 16:37–42. doi: 10.1111/1751-2980.12206
40. Wagner AC, Weber H, Jonas L, Nizze H, Strowski M, Fiedler F, et al. Hyperthermia Induces Heat Shock Protein Expression and Protection Against Cerulein-Induced Pancreatitis in Rats. *Gastroenterology* (1996) 111:1333–42. doi: 10.1053/gast.1996.v111.pm8898648
41. Bhagat L, Singh VP, Song AM, van Acker GJ, Agrawal S, Steer ML, et al. Thermal Stress-Induced HSP70 Mediates Protection Against Intrapancreatic Trypsinogen Activation and Acute Pancreatitis in Rats. *Gastroenterology* (2002) 122:156–65. doi: 10.1053/gast.2002.30314
42. Rakonczay ZJr, Iványi B, Varga I, Boros I, Jednákovits A, Németh I, et al. Nontoxic Heat Shock Protein Coinducer BRX-220 Protects Against Acute Pancreatitis in Rats. *Free Radic Biol Med* (2002) 32:1283–92. doi: 10.1016/S0891-5849(02)00833-X
43. Rakonczay ZJr, Takács T, Boros I, Lonovics J. Heat Shock Proteins and the Pancreas. *J Cell Physiol* (2003) 195:383–91. doi: 10.1002/jcp.10268
44. Lunova M, Zizer E, Kucukoglu O, Schwarz C, Dillmann WH, Wagner M, et al. Hsp72 Overexpression Accelerates the Recovery From Caerulein-Induced Pancreatitis. *PloS One* (2012) 7:e39972. doi: 10.1371/journal.pone.0039972
45. Lugo-Huitrón R, Blanco-Ayala T, Ugalde-Muñiz P, Carrillo-Mora P, Pedraza-Chaverrí J, Silva-Adaya D, et al. On the Antioxidant Properties of Kynurenic Acid: Free Radical Scavenging Activity and Inhibition of Oxidative Stress. *Neurotoxicol Teratol* (2011) 33:538–47. doi: 10.1016/j.ntt.2011.07.002
46. Wirthgen E, Hoeflich A, Rebl A, Günther J. Kynurenic Acid: The Janus-Faced Role of an Immunomodulatory Tryptophan Metabolite and Its Link to Pathological Conditions. *Front Immunol* (2018) 8:1957. doi: 10.3389/fimmu.2017.01957
47. Winterbourn CC, Kettle AJ, Hampton MB. Reactive Oxygen Species and Neutrophil Function. *Annu Rev Biochem* (2016) 85:765–92. doi: 10.1146/annurev-biochem-060815-014442

Conflict of Interest: Author VT is employed by the company Creative Laboratory Ltd., Szeged, Hungary.

The remaining authors declare that the research was conducted in the absence of any commercial or financial relationships that could be construed as a potential conflict of interest.

Publisher's Note: All claims expressed in this article are solely those of the authors and do not necessarily represent those of their affiliated organizations, or those of the publisher, the editors and the reviewers. Any product that may be evaluated in this article, or claim that may be made by its manufacturer, is not guaranteed or endorsed by the publisher.

International Journal of
Molecular Sciences

MDPI

Article

Fentanyl but Not Morphine or Buprenorphine Improves the Severity of Necrotizing Acute Pancreatitis in Rats

Emese Réka Bálint [1], Gabriella Fűr [1], Balázs Kui [2], Zsolt Balla [1,†], Eszter Sára Kormányos [1], Erik Márk Orján [1], Brigitta Tóth [1], Gyöngyi Horváth [3], Edina Szűcs [4], Sándor Benyhe [4], Eszter Ducza [5], Petra Pallagi [2], József Maléth [2], Viktória Venglovecz [6], Péter Hegyi [2,7,‡], Lóránd Kiss [1,*] and Zoltán Rakonczay, Jr. [1,*]

1 Department of Pathophysiology, University of Szeged, 6725 Szeged, Hungary; bioemese@gmail.com (E.R.B.); gabriella.fur@gmail.com (G.F.); ballatanar@gmail.com (Z.B.); kormanyoseszter@gmail.com (E.S.K.); eorjan@gmail.com (E.M.O.); tothxbrigi@gmail.com (B.T.)
2 Department of Medicine, University of Szeged, 6725 Szeged, Hungary; k.kubali@gmail.com (B.K.); pallagi.petra@gmail.com (P.P.); jozsefmaleth1@gmail.com (J.M.); hegyi2009@gmail.com (P.H.)
3 Department of Physiology, University of Szeged, 6725 Szeged, Hungary; horvath.gyongyi@med.u-szeged.hu
4 Institute of Biochemistry, Biological Research Center, 6726 Szeged, Hungary; szucs.edina@brc.hu (E.S.); benyhe.sandor@brc.hu (S.B.)
5 Department of Pharmacodynamics and Biopharmacy, Faculty of Pharmacy, University of Szeged, 6725 Szeged, Hungary; ducza@pharm.u-szeged.hu
6 Department of Pharmacology and Pharmacotherapy, University of Szeged, 6725 Szeged, Hungary; vviki3@gmail.com
7 Institute for Translational Medicine, Medical School, University of Pecs, 7624 Pecs, Hungary
* Correspondence: lorand.kiss.work@gmail.com (L.K.); rakonczay.zoltan@med.u-szeged.hu (Z.R.J.); Tel.: +36-62-545-994 (Z.R.J.)
† Current address: Department of Environmental Biology and Education, Institute of Applied Sciences, Juhász Gyula Faculty of Education, University of Szeged, 6725 Szeged, Hungary.
‡ Current address: Centre for Translational Medicine and Division for Pancreatic Disorders, CVC, Semmelweis University, 1085 Budapest, Hungary.

Abstract: Opioids are widely used for the pain management of acute pancreatitis (AP), but their impact on disease progression is unclear. Therefore, our aim was to study the effects of clinically relevant opioids on the severity of experimental AP. Various doses of fentanyl, morphine, or buprenorphine were administered as pre- and/or post-treatments in rats. Necrotizing AP was induced by the intraperitoneal injection of L-ornithine-HCl or intra-ductal injection of Na-taurocholate, while intraperitoneal caerulein administration caused edematous AP. Disease severity was determined by laboratory and histological measurements. Mu opioid receptor (MOR) expression and function was assessed in control and AP animals. MOR was expressed in both the pancreas and brain. The pancreatic expression and function of MOR were reduced in AP. Fentanyl post-treatment reduced necrotizing AP severity, whereas pre-treatment exacerbated it. Fentanyl did not affect the outcome of edematous AP. Morphine decreased vacuolization in edematous AP, while buprenorphine pre-treatment increased pancreatic edema during AP. The overall effects of morphine on disease severity were negligible. In conclusion, the type, dosing, administration route, and timing of opioid treatment can influence the effects of opioids on AP severity. Fentanyl post-treatment proved to be beneficial in AP. Clinical studies are needed to determine which opioids are best in AP.

Keywords: acute pancreatitis; fentanyl; morphine; buprenorphine; opioids; analgesia

Citation: Bálint, E.R.; Fűr, G.; Kui, B.; Balla, Z.; Kormányos, E.S.; Orján, E.M.; Tóth, B.; Horváth, G.; Szűcs, E.; Benyhe, S.; et al. Fentanyl but Not Morphine or Buprenorphine Improves the Severity of Necrotizing Acute Pancreatitis in Rats. *Int. J. Mol. Sci.* **2022**, *23*, 1192. https://doi.org/10.3390/ijms23031192

Academic Editor: Daniela Basso

Received: 27 July 2021
Accepted: 18 January 2022
Published: 21 January 2022

1. Introduction

Acute pancreatitis (AP) is one of the most common causes for hospitalization within gastrointestinal diseases [1], which has an overall mortality of about 2% [2]. This death proportion in severe cases can increase to 30%. The incidence of the disease is more than 30 per 100,000 population in Europe, and this number has increased over time [3,4].

Excessive alcohol consumption and gallstone diseases account for approximately 70% of cases [2,5]. AP can present in mild, moderately severe, and severe forms based on the Revised Atlanta Classification [6]. The pathomechanism of AP is rather complex, and our understanding of the disease is far from complete, but it involves toxic cellular Ca^{2+} overload causing NF-κB activation, impaired autophagy, mitochondrial dysfunction, and the early intra-acinar and intra-ductal activation of digestive enzymes [7–10]. The clinical symptoms of AP include severe abdominal pain (which can radiate to the back), fever, nausea, and vomiting. The diagnostic criteria for AP include the presentation at least two of the following: (i) upper abdominal pain, (ii) >3× elevated serum amylase or lipase, and/or (iii) imaging (CT, MRI, ultrasonography) [6,11]. Notably, pain is present in 95% of AP patients [5]. The therapy of AP is only supportive, and there is no specific drug against this disease. Recent AP management guidelines highlight the importance of (a) early intravenous (i.v.) fluid resuscitation; (b) analgesics; (c) enteral nutrition [12–15].

As pain is the most prominent symptom of AP, its relief is a priority in clinical settings. Unfortunately, recent guidelines for AP treatment do not have clear recommendations for the types of analgesics to be used [12,13,16]. Most commonly, the WHO pain management guideline is utilized, and treatment ranges from nonsteroidal anti-inflammatory drugs (NSAID) to high potent opioids. The latter are applied in cases of severe AP and include fentanyl (FE), buprenorphine (BQ), pethidine, pentazocine, morphine (MO), etc. [17]. Although opioids are the most effective pain killers, which makes them valuable in clinical settings, there is a scientific debate on their use due to their side effects such as constipation or immunosuppression [18,19]. Actually, Meng et al. (2013) attempted to collect all randomized controlled trials that investigated the side effects of analgesics (opioids and non-opioids) in AP, but the included studies were of low quality, without clear outcome. However, the use of MO is often not preferred in humans due to the spasm of sphincter of Oddi, which might worsen the outcome of AP [20]. Even more importantly, Barlass et al. [21] have also shown the drawbacks of MO use in AP and the pathological processes of its side effects in a mouse model.

Despite the dubious benefits of opioid use, their impact on the progression of AP is unclear. Therefore, our aim was to investigate opioid receptor function, the effects of FE, MO, and BQ on the severity of AP in rats. We utilized different AP models with opioid pre- and/or post-treatments.

2. Results

2.1. The Effect of Fentanyl Pre-Treatment on AP Severity

The pancreata of the control group displayed normal morphology (Figure 1A), and intraperitoneal (i.p.) FE alone did not induce any structural changes in the pancreas (Figure S1A). L-ornithine (LO)-induced AP resulted in about 60% pancreatic necrosis and intensive leukocyte infiltration (Figure 1A–C). These signs even worsened due to FE pre-treatment. The extent of tissue necrosis significantly increased when the higher dose (3 × 0.2 mg/kg) of FE was applied, whereas the level of leukocyte infiltration was higher in the 3 × 0.1 mg/kg FE and AP group compared to the AP group not receiving FE. FE treatment did not cause any change in pancreatic water content in the AP groups (Figure 1D). Serum amylase activity markedly increased in the AP groups versus the control group (Figure 1G). Importantly, 3 × 0.1 mg/kg FE significantly increased serum amylase activity during AP. MPO activity was greatly elevated in the AP groups compared to the control group (Figure 1F), and the dose of 3 × 0.2 mg/kg FE further increased MPO activity in AP. Interestingly, the concentration of pancreatic IL-1β significantly decreased due to 3 × 0.1 mg/kg FE in the AP group.

I.p. injections of CER induced mild AP and increased the extent of pancreatic vacuolization, leukocyte infiltration, and water content (Figure 2A–D) compared to the control group (histology of control is shown in Figure S1). FE pre-treatment did not cause any change during AP progression in histological parameters or water content (Figure 2A–D). CER-induced AP resulted in elevated pancreatic IL-1β content and serum amylase activity,

whereas it did not significantly affect MPO activity (Figure 2E–G). FE pre-treatment did not alter IL-1β level, MPO, or serum amylase activity in the AP groups.

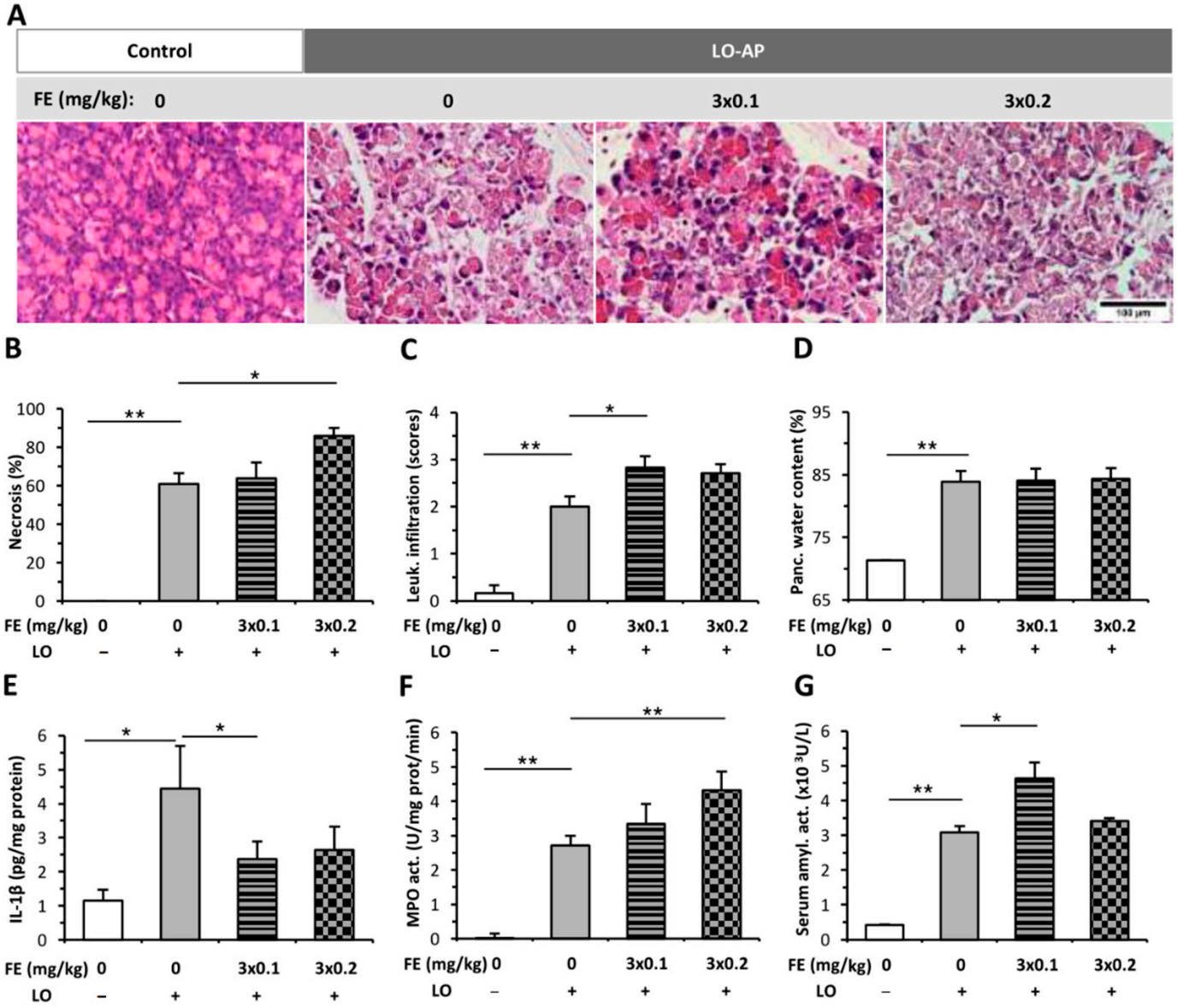

Figure 1. Fentanyl (FE) pre-treatment in L-ornithine (LO)-induced necrotizing acute pancreatitis (AP). Rats were treated with 3 × 0.1 or 3 × 0.2 mg/kg FE intraperitoneally (i.p.), whereas i.p. injection with 3 g/kg LO-HCl (LO +) was used to induce AP. Control animals received physiological saline instead of LO (LO −) or FE (0 mg/kg). Animals were sacrificed at 24 h after LO or physiological saline injection. (**A**) Representative histopathological images of pancreatic tissues of the treatment groups. Bar charts show the extent of pancreatic (**B**) necrosis, (**C**) leukocyte infiltration, (**D**) water content, (**E**) interleukin-1β (IL-1β) concentration, (**F**) myeloperoxidase (MPO) activity, and (**G**) serum amylase activity measurements. Values represent means with standard error, n = 9–11. Two-way ANOVA was performed followed by the Holm–Sidak post hoc test. * $p < 0.05$; ** $p < 0.001$.

2.2. The Effect of Fentanyl Post-Treatment on AP

In contrast to FE pre-treatment (Figure 1), both doses of FE post-treatment decreased the extent of histopathological changes (pancreatic tissue necrosis and leukocyte infiltration) caused by LO-induced AP (Figure 3A–C). On the other hand, FE administration did not alter pancreatic water content in the AP groups (Figure 3D). LO-induced AP increased pancreatic MPO and serum amylase activities, which were decreased by both FE doses

tested (Figure 3F,G). Pancreatic IL-1β levels only decreased significantly in case of the LO + 3 × 0.2 mg/kg FE group (Figure 3E).

Intra-ductal (i.d.) infusion of sodium taurocholate (NaTc) induced necrotizing AP in the head but not in the tail of the pancreas (not shown), which is in accord with the finding of others [22]. Therefore, only the pancreatic heads were used for analysis. NaTc also elevated the extent of pancreatic necrosis, leukocyte infiltration, and edema (Figure 4A–D). Both necrosis and immune cell infiltration were decreased by the higher dose of FE (0.2 mg/kg, Figure 4B,C), while the score of edema did not change in the AP groups after FE treatment (Figure 4D). Serum amylase activity also decreased in the NaTc + 3 × 0.2 mg/kg FE group versus the AP group without FE treatment (Figure 4E).

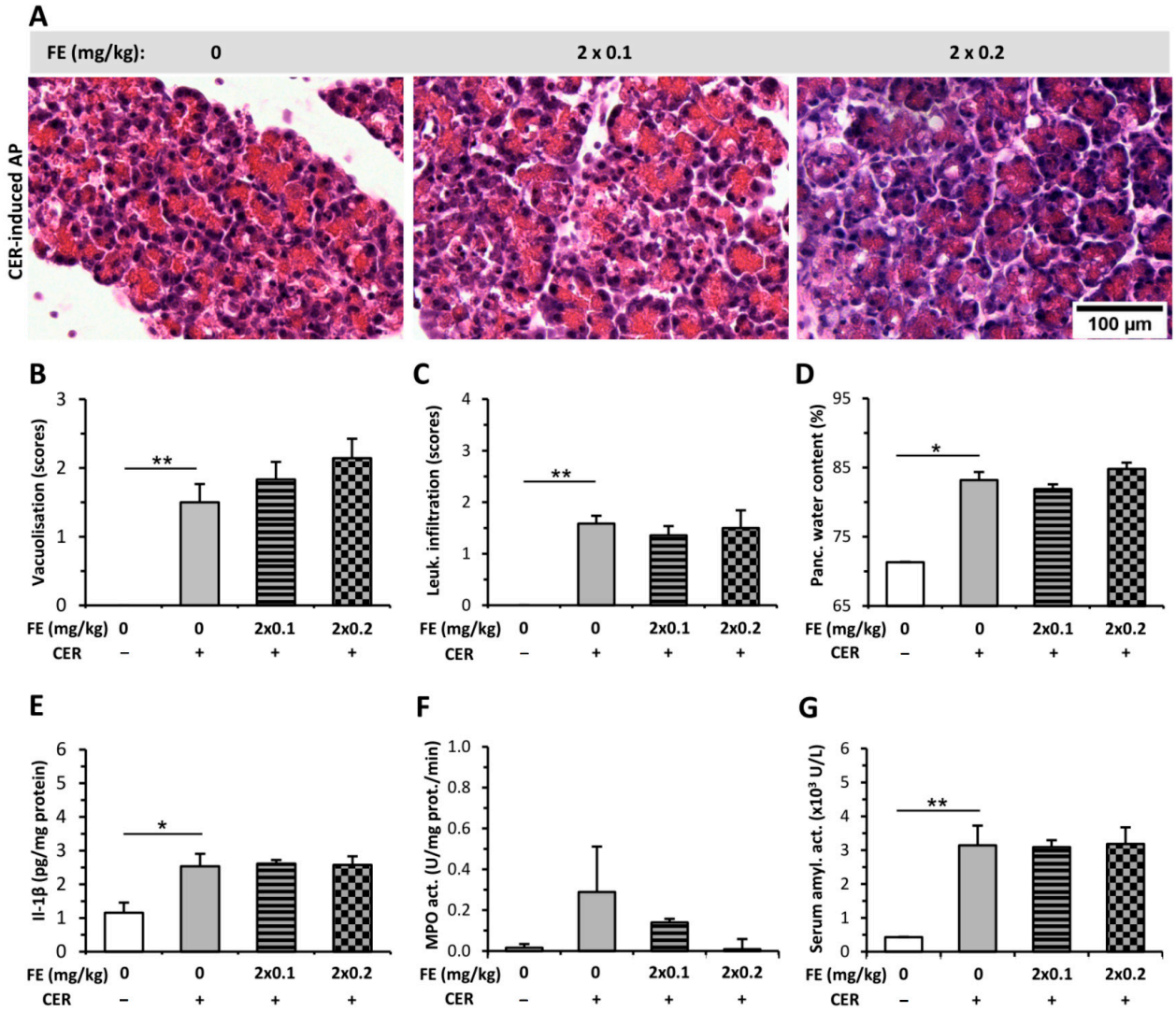

Figure 2. Fentanyl (FE) treatment started before the induction of mild acute pancreatitis (AP) with cerulein (CER) does not affect disease severity. Rats were treated with 2 × 0.1 or 2 × 0.2 mg/kg FE i.p., whereas i.p. injection with 4 × 20 µg/kg CER (CER +) was used to induce AP. Control animals received physiological saline instead of CER (CER −) or FE (0 mg/kg). Animals were sacrificed at 12 h after the first CER or physiological saline injection. (**A**) Representative histopathological images of pancreatic tissues of the treatment groups. Bar charts show the extent of pancreatic (**B**) vacuolization, (**C**) leukocyte infiltration, (**D**) water content, (**E**) interleukin-1β (IL-1β) concentration, (**F**) myeloperoxidase (MPO) activity, and (**G**) serum amylase activity measurements. Values represent means with standard error, n = 5–7. Two-way ANOVA was performed followed by the Holm–Sidak post hoc test. * $p < 0.05$; ** $p < 0.001$.

I.p. injections of CER increased the extent of pancreatic vacuolization, leukocyte infiltration, and tissue water content causing mild edematous AP (Figure 5A–D). FE treatment did not affect either histological parameters (tissue necrosis, leukocyte infiltration) or pancreatic water content (Figure 5A–D). The elevated amylase and MPO activities during AP were unaffected by FE post-treatment (Figure 5E,F). Interestingly, the smaller dose of FE (0.1 mg/kg) further increased the elevated serum IL-1β during AP, while the higher dose of FE had no effect (Figure 5G).

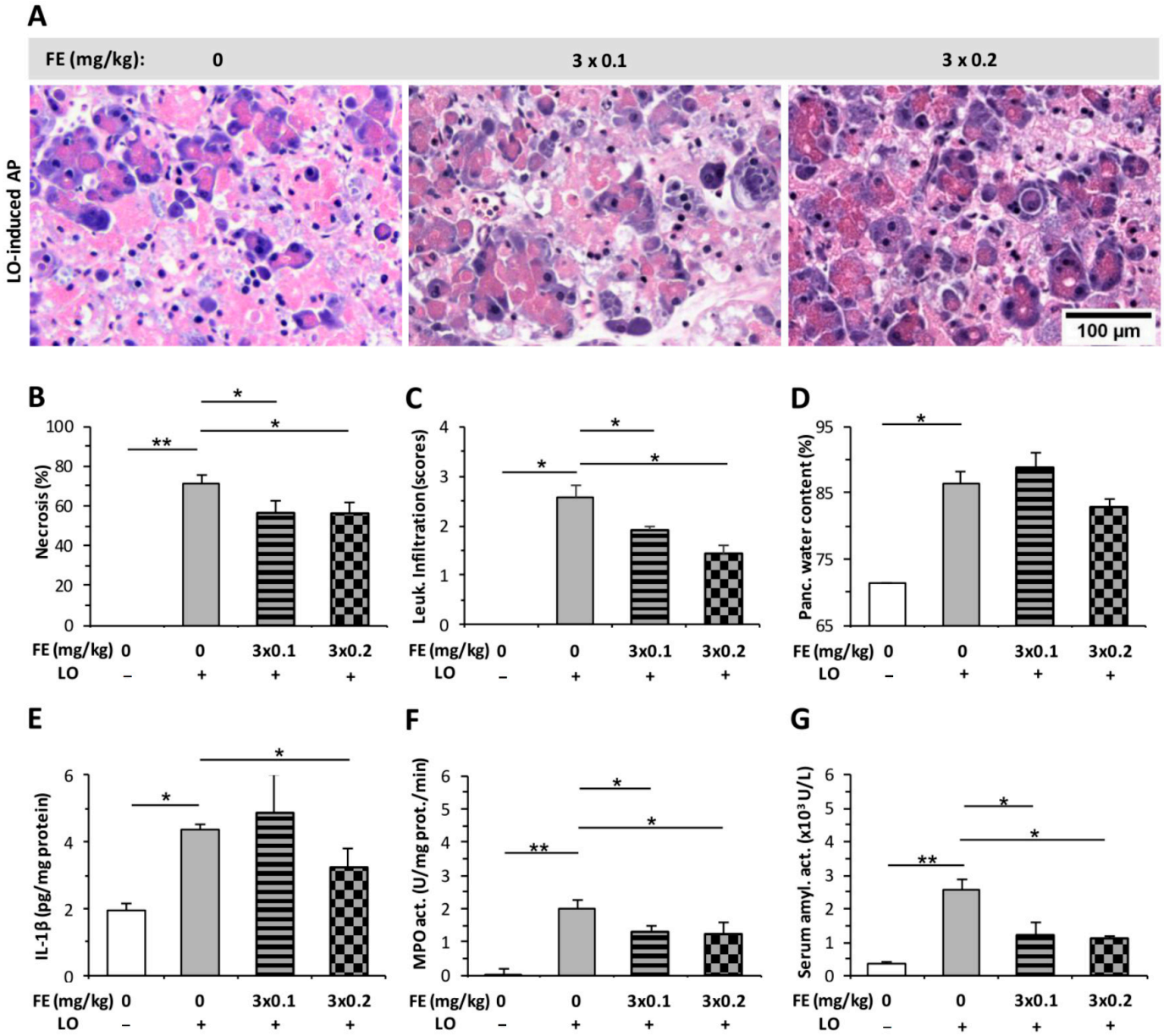

Figure 3. Fentanyl (FE) treatment started after the induction of L-ornithine (LO) acute pancreatitis (AP) reduces disease severity. (**A**) Representative histopathological images of pancreatic tissues of the treatment groups. Bar charts show the extent of pancreatic (**B**) necrosis, (**C**) leukocyte infiltration, (**D**) water content, (**E**) interleukin-1β (IL-1β) concentration, (**F**) myeloperoxidase (MPO) activity, and (**G**) serum amylase activity measurements. Values represent mean with standard error, n = 10–18. Two-way ANOVA was performed followed by the Holm–Sidak post hoc test. * $p < 0.05$; ** $p < 0.001$.

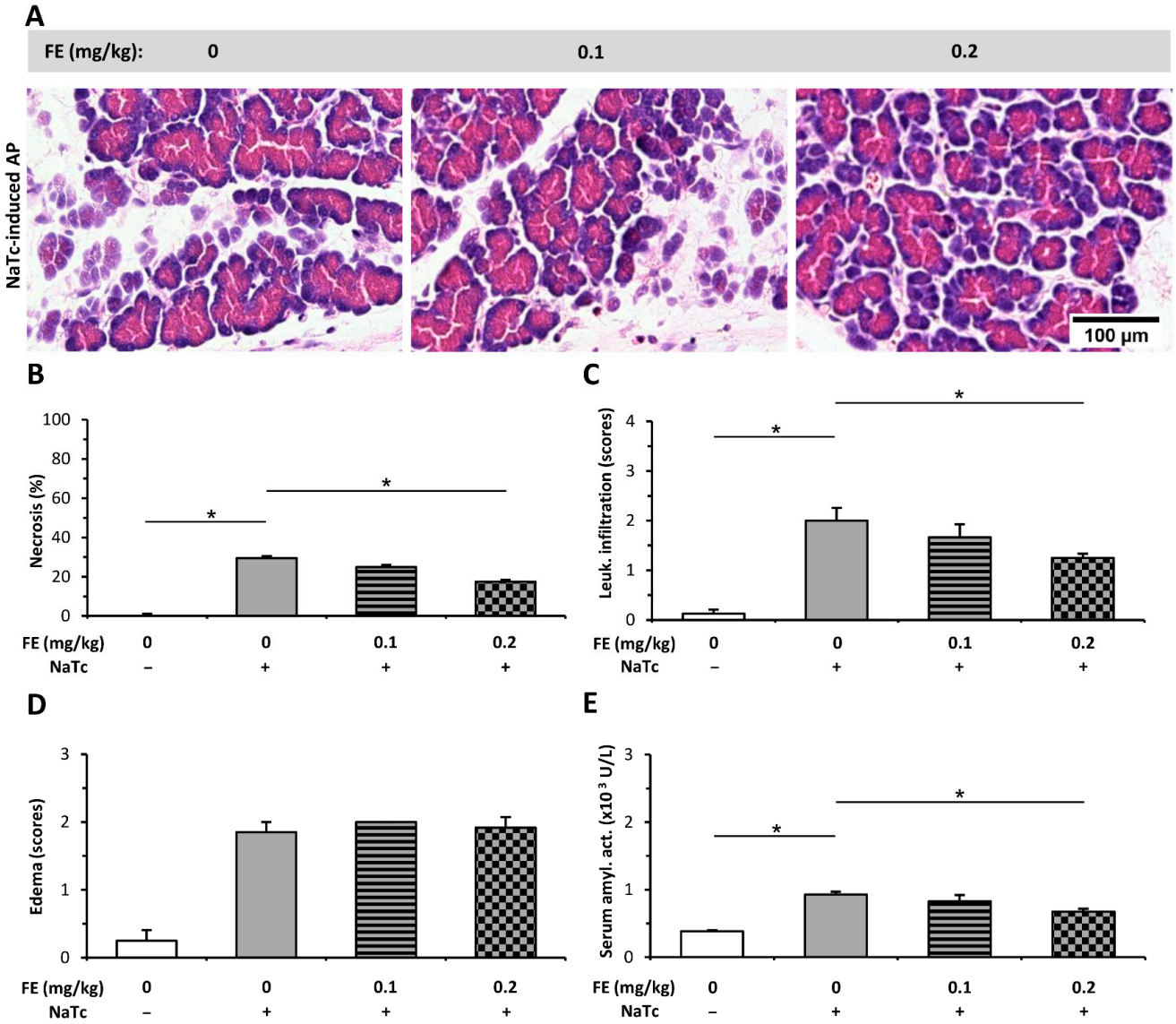

Figure 4. Fentanyl (FE) treatment started after the induction of necrotizing acute pancreatitis (AP) with sodium taurocholate (NaTc) reduces disease severity. Rats were treated with 0.1 or 0.2 mg/kg FE i.p., whereas the intra-ductal injection of 40 mg/kg NaTc (NaTc +) was used to induce AP. Control animals received physiological saline instead of NaTc (NaTc −) or FE (0 mg/kg). Animals were sacrificed at 16–24 h after the NaTc or physiological saline injection. (**A**) Representative histopathological images of pancreatic tissues of the treatment groups. Bar charts show the extent of pancreatic (**B**) necrosis, (**C**) leukocyte infiltration, (**D**) edema, and (**E**) serum amylase activity measurements. Values represent mean with standard error, n = 9–12. Two-way ANOVA was performed followed by the Holm–Sidak post hoc test. * $p < 0.05$.

2.3. Morphine Administration Does Not Affect the Severity of AP

The effect of MO on the severity of AP was investigated by using different doses of the drug: 8 × 5, 9 × 10, and 4 × 5 mg/kg. MO at the tested doses did not induce any structural changes in the pancreatic tissues of rats, and no inflammatory cell infiltration could be observed in histological sections (Figure S1B). Treatment with LO induced AP and resulted in marked pancreatic damage (tissue necrosis, leukocyte infiltration, and increased pancreatic water content Figure 6A–D). MO did not significantly alter the value of these parameters during AP. Furthermore, MO did not influence pancreatic MPO or serum amylase activity in the AP groups, either (Figure 6E,F).

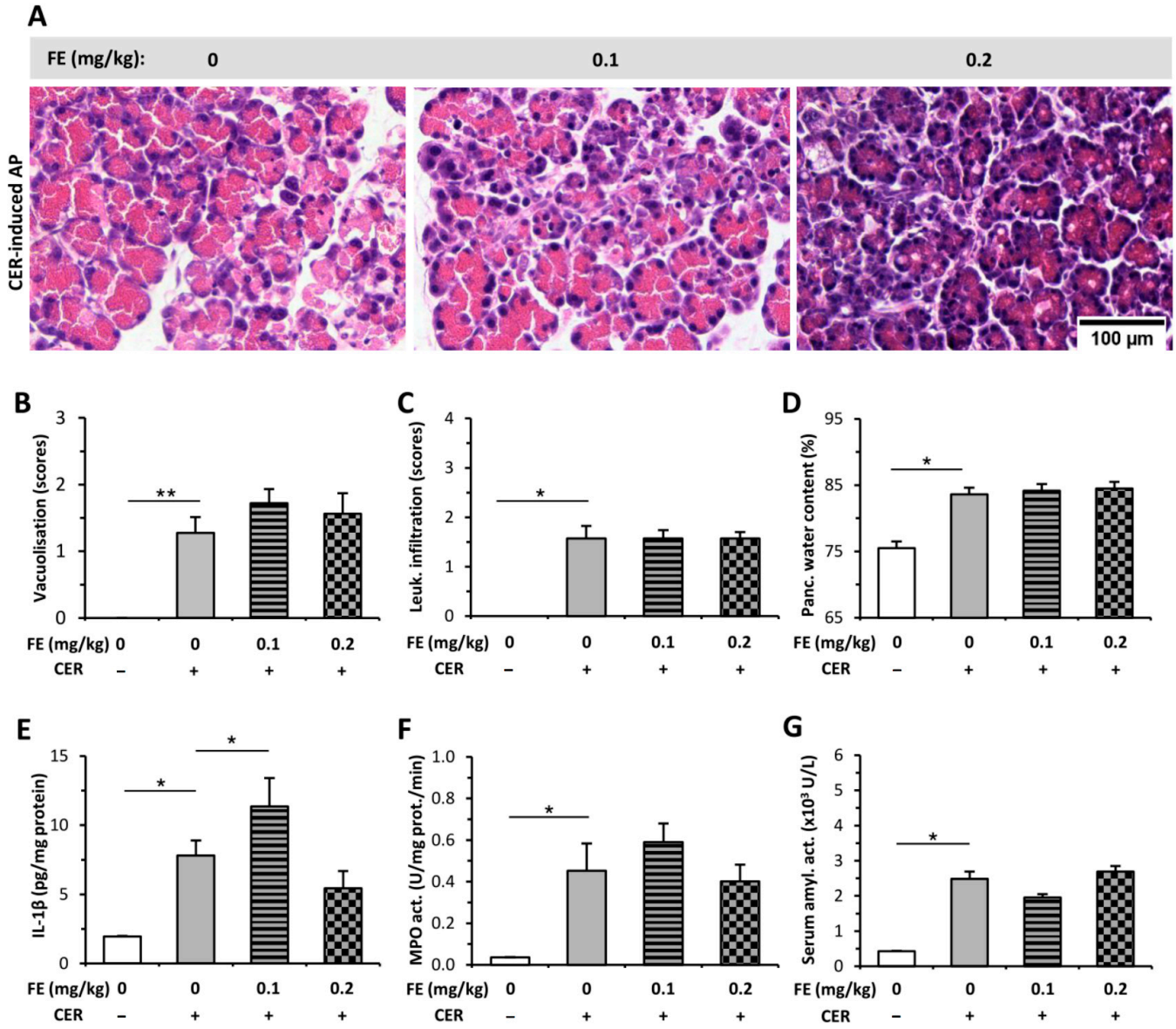

Figure 5. Fentanyl (FE) treatment started after the induction of acute pancreatitis (AP) with cerulein (CER) does not affect disease severity. (**A**) Representative histopathological images of pancreatic tissues of the treatment groups. Bar charts show the extent of pancreatic (**B**) vacuolization, (**C**) leukocyte infiltration, (**D**) water content, (**E**) interleukin-1β (IL-1β) concentration, (**F**) myeloperoxidase (MPO) activity, and (**G**) serum amylase activity measurements. Values represent mean with standard error, $n = 6$. Two-way ANOVA was performed followed by the Holm–Sidak post hoc test. * $p < 0.05$; ** $p < 0.001$.

The effect of 4 × 5 mg/kg MO was tested in a CER-induced AP model. Due to the shorter duration of AP in case of CER (12 h) compared to the LO model (24 h), the number of MO injections was reduced from eight (applied in LO-induced AP, Figure 6) to four. In the CER-induced edematous AP, MO significantly reduced vacuolization (Figure 7A,B), but it had no effect on leukocyte infiltration or pancreatic water content (Figure 7C,D). Serum amylase activity was significantly elevated after AP induction, and MO had no further effect on it (Figure 7F). However, AP did not induce any significant increase in pancreatic MPO activity (Figure 7E). MO had no additional effect on MPO activity during AP (Figure 7E).

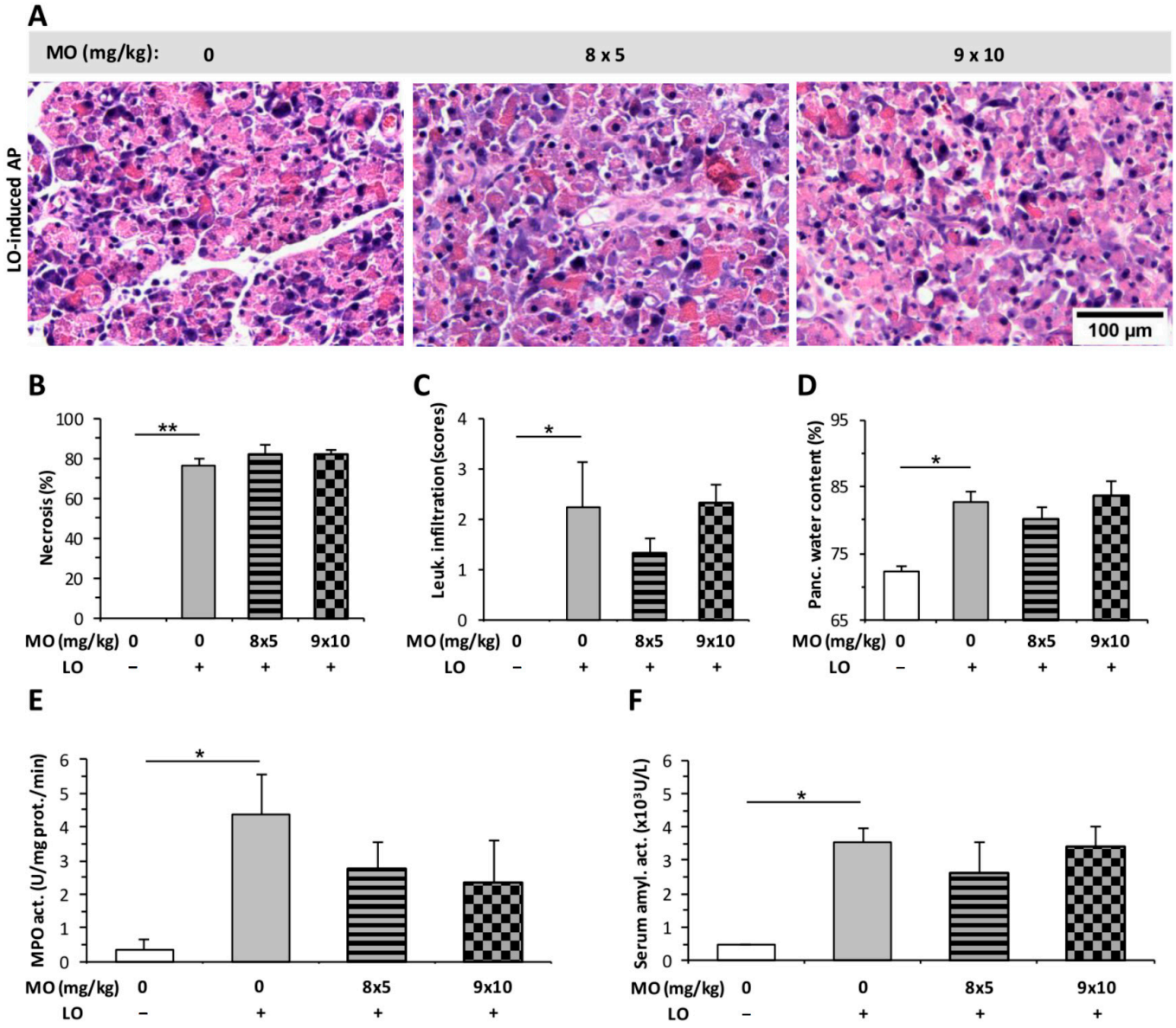

Figure 6. Morphine (MO) treatment does not affect the severity of L-ornithine (LO)-induced acute pancreatitis (AP). Rats were treated with 8 × 5 or 9 × 10 mg/kg MO i.p., whereas 3 g/kg LO-HCl (LO +) was used i.p. to induce AP. Control animals received physiological saline instead of LO (LO −) or MO (0 mg/kg). Animals were sacrificed at 24 h after LO or physiological saline injection. (**A**) Representative histopathological images of pancreatic tissues of the treatment groups. Bar charts show the extent of pancreatic (**B**) necrosis, (**C**) leukocyte infiltration, (**D**) water content, (**E**) myeloperoxidase (MPO) activity, and (**F**) serum amylase activity measurements. Values represent mean with standard error, $n = 6$. Two-way ANOVA was performed followed by the Holm–Sidak post hoc test. * $p < 0.05$; ** $p < 0.001$.

2.4. Buprenorphine Has No Effect on the Severity of LO-Induced AP

The effect of BQ was tested by i.p. and i.t. administrations. BQ alone did not induce any changes in pancreatic tissues (Figure S1C). The tested i.p. doses (2 × 0.1; 2 × 0.5; 2 × 1 mg/kg) of BQ did not affect the LO-induced pancreatic necrosis, leukocyte infiltration, or serum amylase activity (Figure 8A–C,E). However, 2 × 1 mg/kg BQ slightly enhanced the pancreatic water content in AP (Figure 8D).

Intrathecal (i.t.) administration of BQ was also tested on rats during AP (Figure 9). The dose of 3 × 3 µg/kg BQ had no effect on any parameters of AP, while the 3 × 6 µg/kg dose significantly decreased the extent of leukocyte infiltration in AP (Figure 9C).

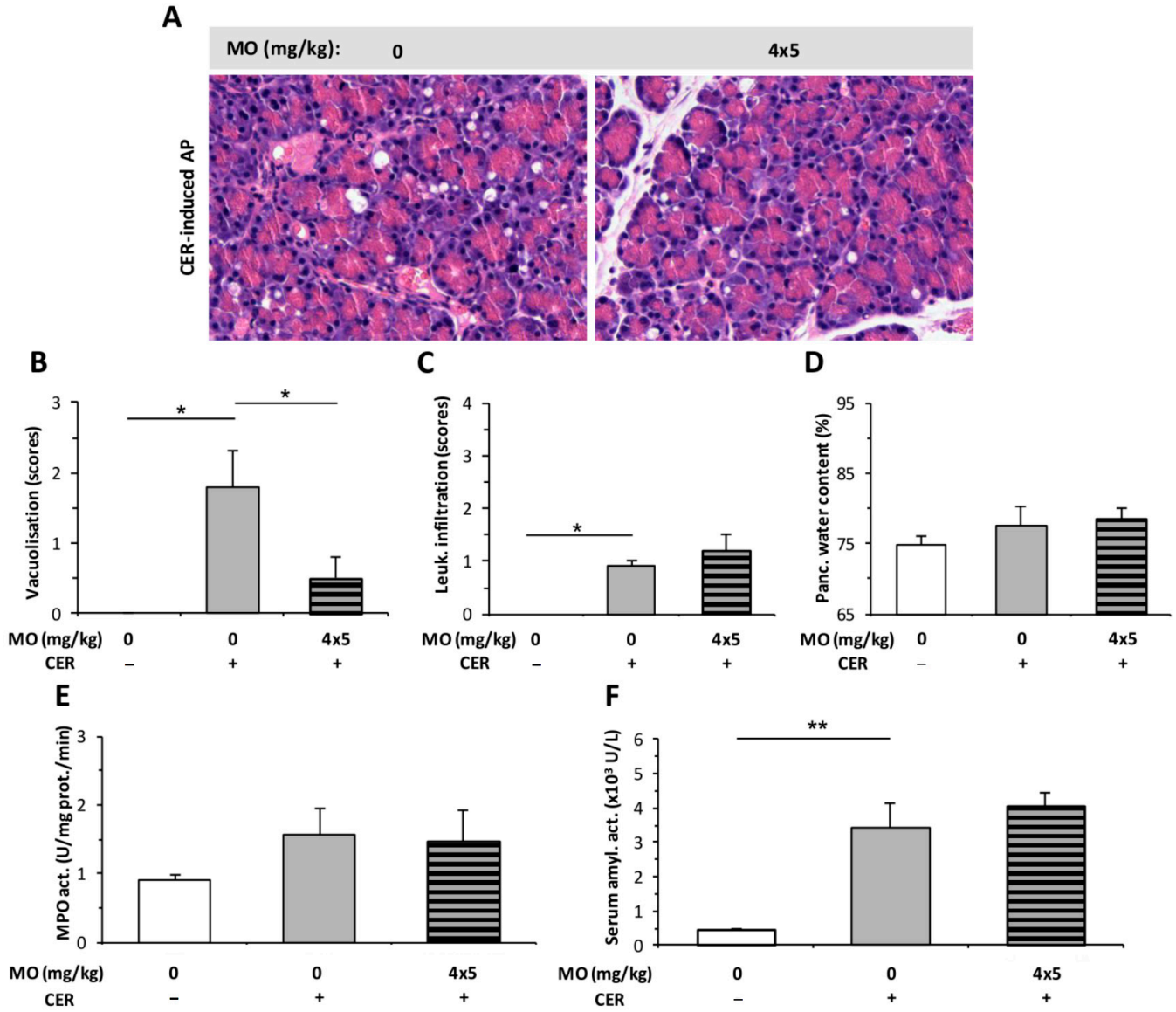

Figure 7. Morphine (MO) treatment does not affect the severity of cerulein (CER)-induced acute pancreatitis (AP). Rats were treated with 4 × 5 mg/kg MO i.p., whereas 4 × 20 µg/kg CER (CER +) was used i.p. to induce AP. Control animals received physiological saline instead of CER (CER −) or MO (0 mg/kg). Animals were sacrificed at 12 h after the first CER or physiological saline injection. (**A**) Representative histopathological images of pancreatic tissues of the treatment groups. Bar charts show the extent of pancreatic (**B**) vacuolization, (**C**) leukocyte infiltration, (**D**) water content, (**E**) myeloperoxidase (MPO) activity, and (**F**) serum amylase activity measurements. Values represent mean with standard error, $n = 6$. Two-way ANOVA was performed followed by the Holm–Sidak post hoc test. * $p < 0.05$; ** $p < 0.001$. Scale bar.

2.5. Pancreatic mu Opioid Receptor Expression Is Decreased in LO-Induced AP

The mRNA and protein expression of mu opioid receptor (MOR) were investigated in the pancreas and brain (Figure 10). In the brain, MOR was detected in control animals, and AP did not influence the amount of MOR after 24 h (Figure 10A,C). In case of the pancreas, control animals also expressed MOR, but the induction of AP significantly reduced the presence of the receptor (Figure 10B,D).

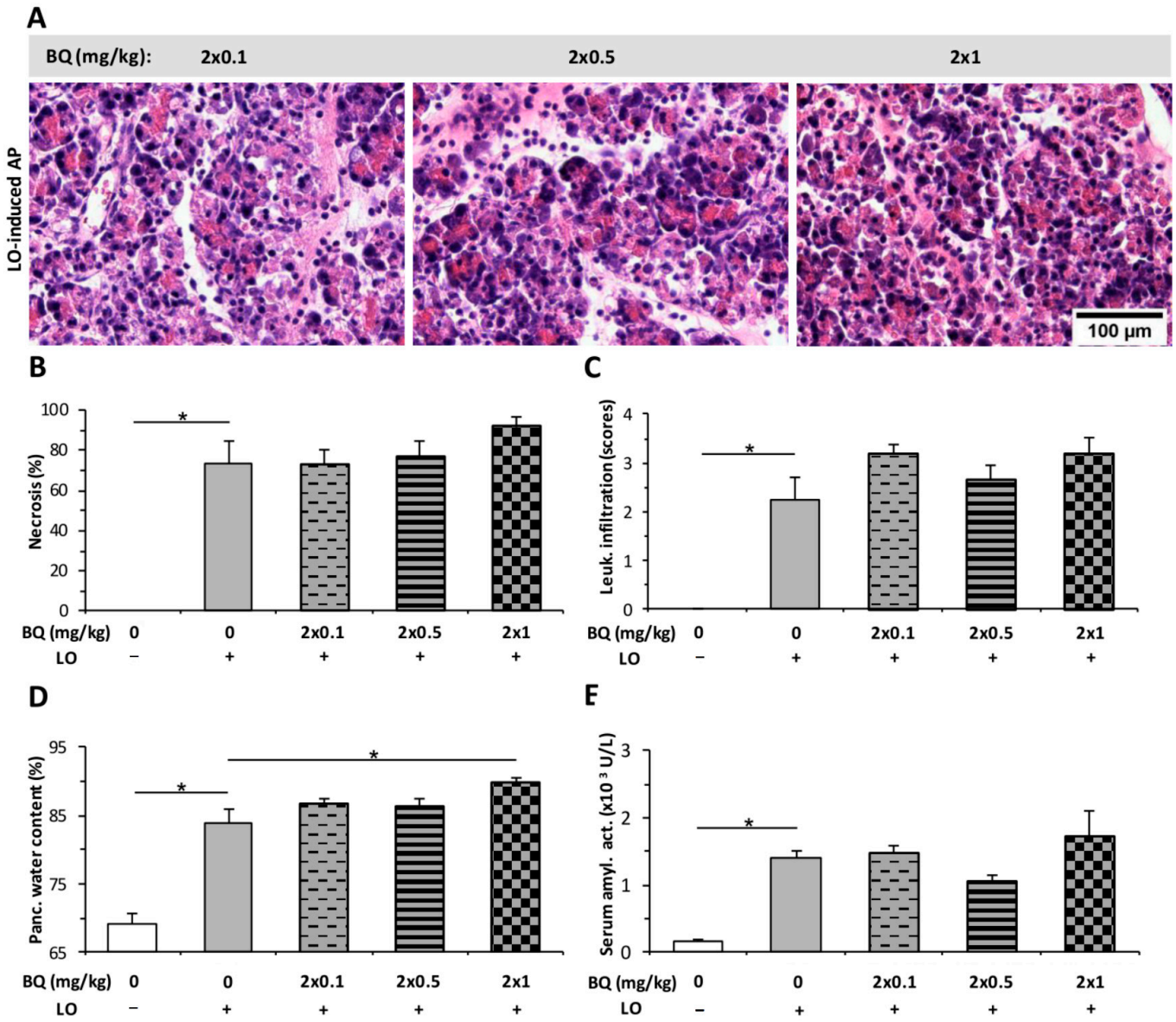

Figure 8. Intraperitoneal (i.p.) buprenorphine (BQ) treatment does not affect the severity of L-ornithine (LO)-induced acute pancreatitis (AP). Rats were treated with 2 × 0.1, 2 × 0.5, or 2 × 1 mg/kg BQ i.p., whereas i.p. injection with 3 g/kg LO (LO +) was used to induce AP. Control animals received physiological saline instead of LO (LO −) or BQ (0 mg/kg). Animals were sacrificed at 24 h after the first CER or physiological saline injection. (**A**) Representative histopathological images of pancreatic tissues of the treatment groups. Bar charts show the extent of pancreatic (**B**) necrosis, (**C**) leukocyte infiltration, (**D**) water content, and (**E**) serum amylase activity measurements. Values represent mean with standard error, $n = 6$. Two-way ANOVA was performed followed by the Holm–Sidak post hoc test. * $p < 0.05$.

2.6. Pancreatic and Brain mu Opioid Receptor Functions Are Reduced in AP

The functional activity of opioid receptors in pancreatic and brain-derived cell membrane homogenates were studied by receptor mediated in vitro G-protein stimulation (Figure 11). The G-protein activating effect of three well-known MOR agonists (FE, MO, and the highly selective synthetic opioid peptide Tyr-D-Ala-Gly-$_{(NMe)}$Phe-Gly-ol—DAMGO) was measured at a concentration above the saturation level of the receptor (10 µM). The involvement of opioid receptors in G-protein activation was demonstrated by the inhibition with the well-known opioid receptor specific antagonist naloxone at equimolar concentration. In our experiments, brain and pancreatic preparations were investigated in animals with or

without AP. All three tested agonists efficiently activated Gi/o proteins in guanosine-5′-[^{35}S] thiophosphate ([^{35}S]GTPγS) binding experiments. The level of pancreatic activation was lower than the corresponding values found in the brain samples (statistics were not performed in that comparison). In the pancreas, the rank order of efficacy of the activating agonist ligands was fentanyl > morphine ≅ DAMGO. The activation of G proteins was virtually eliminated in samples from AP compared to the control group (Figure 11).

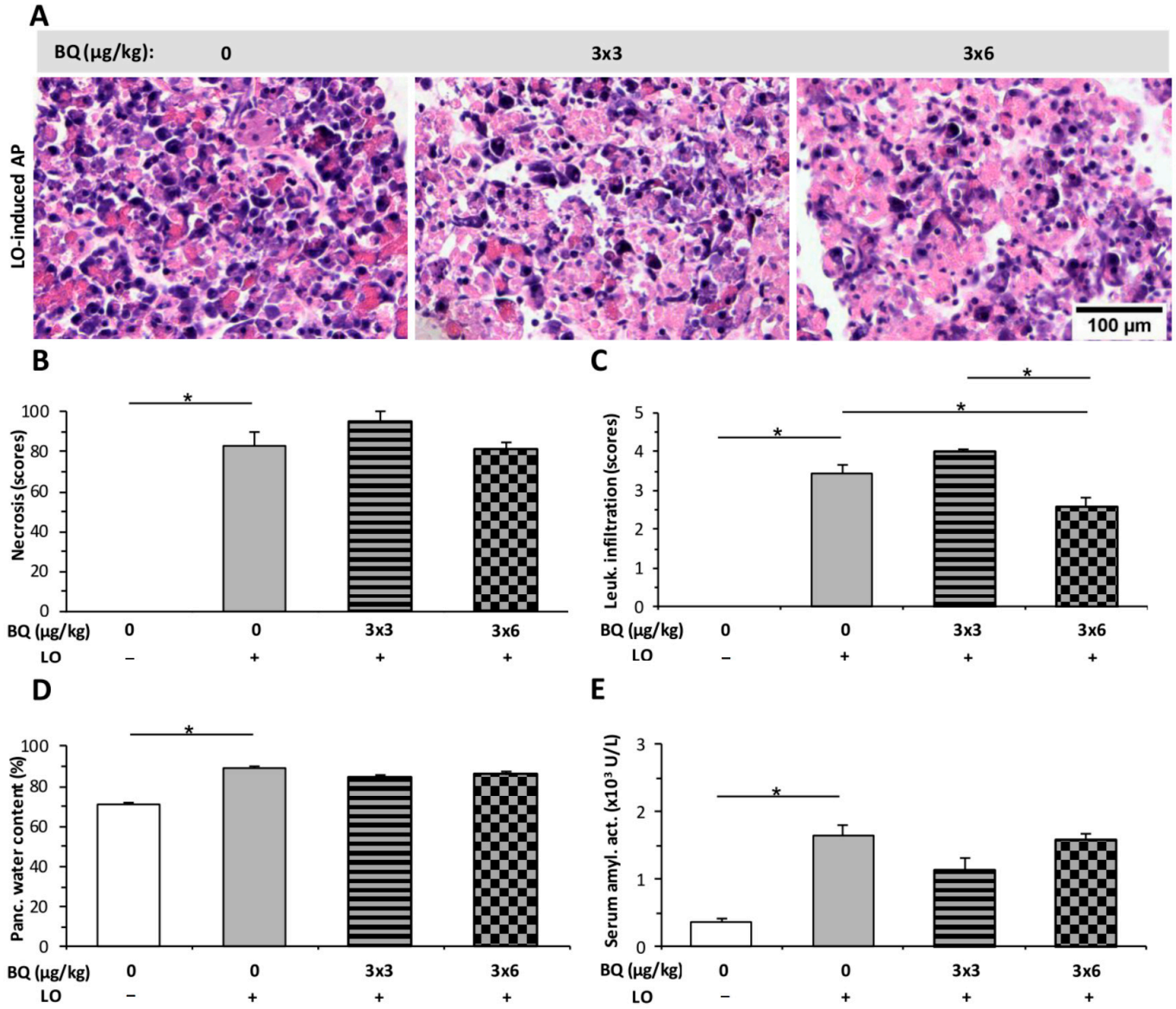

Figure 9. Intrathecal (i.t.) buprenorphine (BQ) treatment does not affect the severity of L-ornithine (LO)-induced acute pancreatitis (AP). Rats were treated with 3 × 3 or 3 × 6 mg/kg BQ i.t., whereas i.p. injection with 3 g/kg LO (LO +) was used to induce AP. Control animals received physiological saline instead of LO (LO −) or BQ (0 mg/kg). Animals were sacrificed at 24 h after the first CER or physiological saline injection. (**A**) Representative histopathological images of pancreatic tissues of the treatment groups. Bar charts show the extent of pancreatic (**B**) necrosis, (**C**) leukocyte infiltration, (**D**) water content, and (**E**) serum amylase activity measurements. Values represent mean with standard error, $n = 6$. ANOVA was performed followed by the Holm–Sidak post hoc test. * $p < 0.05$.

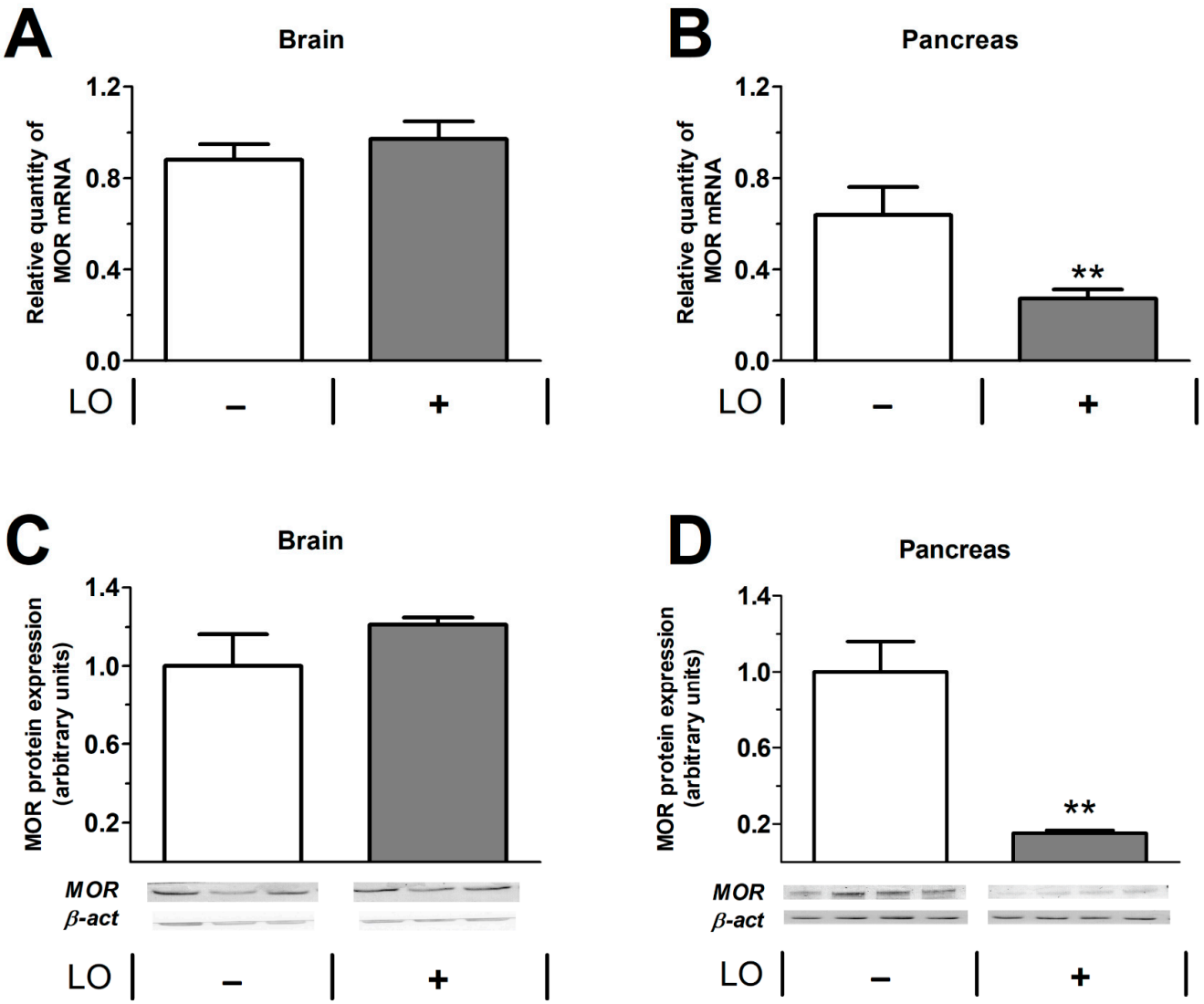

Figure 10. Expression of mu opioid receptor (MOR) in the brain and pancreas in control and LO-induced AP. Rats were treated with vehicle or 3 g/kg LO-HCl and were sacrificed at 24 h. MOR mRNA (**A**,**B**) and protein (**C**,**D**) expression levels were determined in the brain (**A**,**C**) and pancreas (**B**,**D**). In (**C**,**D**), the bar charts show the quantitative analysis of Western blot images. Values represent mean with standard error, n = 13–17 (RT-PCR), n = 3–4 (Western blot analysis). Student's t test was performed, ** $p < 0.01$. Abbreviations: LO, L-ornithine-induced acute pancreatitis; β-act, β-actin; MOR, mu opioid receptor.

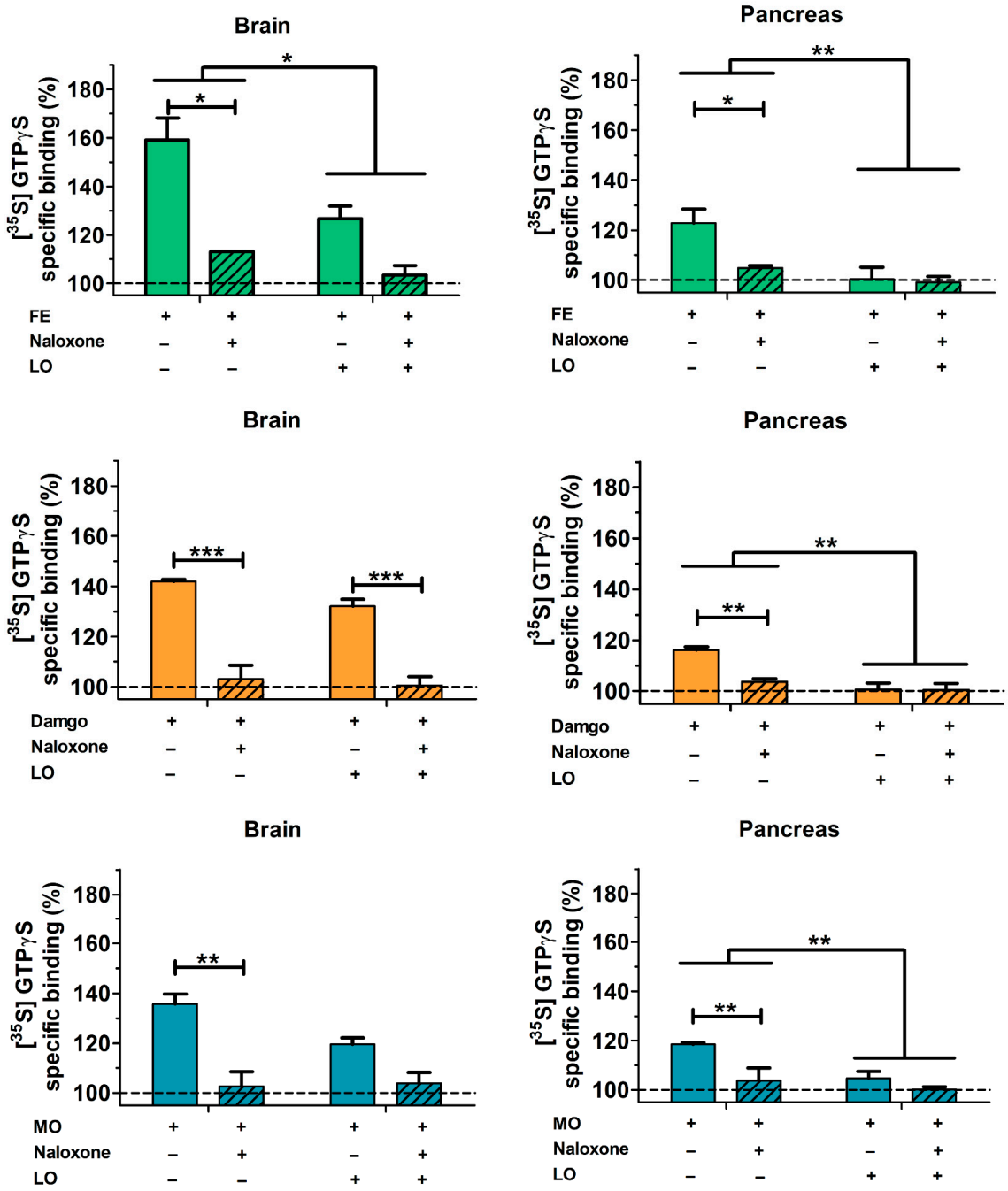

Figure 11. Stimulation of G-protein activation in rat brain and pancreas membrane homogenates. Tissue samples were derived from control and AP animals. Treatments of pancreatic homogenates were as follows: 10 μM FE; 10 μM DAMGO; 10 μM MO. Striped bars represent the combined treatment with mu receptor ligands (FE, MO, DAMGO) and equimolar naloxone. Values represent mean with standard error, $n = 6$. Two-way ANOVA was performed followed by Bonferroni post hoc test. * $p < 0.05$, ** $p < 0.01$; *** $p < 0.001$.

3. Discussion

Opioids are commonly used for pain control in AP patients. It has been speculated that these analgesics (such as morphine) may affect AP progression. Therefore, we comprehensively investigated the effects of FE on the severity of experimental AP, and this research was further supplemented with the examination of the effects of MO and BQ. It is important to note that measurements were performed when the experimental AP reached its maximal severity.

I.p. FE pre-treatment significantly increased the severity of necrotizing AP induced by LO, but it had no effect on edematous AP evoked by CER. Interestingly, the clinically more relevant post-treatment with FE either decreased or had no effect on the various parameters of AP severity in different models. Wang and Chen [23] also tested the effect of FE on NaTc-induced AP. They administered FE i.v. 23–23.5 h after AP induction and sacrificed the animals 24 h after the induction of the disease. Surprisingly, FE exerted anti-inflammatory effects on the pancreas and AP-induced myocardial damage within that really short time (30–60 min). In clinical settings, Stevens et al. [24] showed that FE did not have any side effects compared to the placebo control group (intramuscular Demerol containing pethidine). Some studies draw attention to the importance of the administration site of FE, especially into the epidural site. The use of FE in epidural anesthesia partially restored the decrease in microcirculatory flow caused by AP and prevented the development of tissue necrosis and systemic complications [25,26].

MO pre- or post-treatment did not affect the severity of the disease in case of LO-induced necrotizing AP. Furthermore, the simultaneous administration of MO and CER had no remarkable effect on disease progression either, except for vacuolization, which was decreased by MO. In a recent study, Barlass et al. [21] also investigated MO in two necrotizing mouse AP models. They concluded that MO application delayed AP resolution and reduced intestinal motility, which increased the risk for bacterial translocation. MO also delayed macrophage migration and caused a persistence of inflammation. Their findings related to macrophages are in accordance with earlier studies showing mononuclear cell suppression and chemokine receptor transdeactivation after MO treatment [27,28]. Our study focused on the early-mid events of AP and showed no adverse effects of MO, while Barlass et al. [21] investigated the later effects of MO (at 48, 72, or 120 h). However, our results do not rule out the possibility of later side effects that were shown by Barlass et al. [21]. Marked differences in the results can be explained by species differences, the latter study used mice, while in the present study, rats were investigated. Moreover, one randomized clinical trial [29] and two related reviews [17,30] did not find any significant difference in the effects of MO vs. the non-opioid metamizole. It should be noted that a relatively low number of patients (eight per group) were included in this randomized clinical trial. Based on these observations, we conclude that MO does not affect the severity of the AP at the early-mid stage of the disease, but later side effects may appear according to literature data.

The partial opioid receptor agonist BQ did not cause any adverse effects during AP in i.p. pre-treatment; only tissue water content was increased by the highest dose. I.t injection of the smaller dose of BQ did not affect any other aspects of disease severity measured in our experiments. However, the higher dose significantly decreased immune cell infiltration. Based on this, i.t. administration could be more beneficial during experimental AP. Furthermore, we demonstrated first the effects of BQ on AP at the spinal level. Literature data showed that in an NaTc-induced AP rat model, i.v. BQ administration did not influence disease severity [31]. In a CER-AP model, subcutaneous 0.5 mg/kg BQ reduced the zymogen content and protein synthesis of acinar cells [32]. These results strengthen the beneficial effect of BQ during AP.

Opioids exert their effects primarily through mu, kappa, or delta opioid receptors, which are expressed mainly by neuronal or immune cells. The effects can differ depending on their affinity or specificity to certain receptors. Publications showed that MO has immunosuppressant properties through full mu receptor agonism. MO treatment resulted in the inhibition of cytokine production, NK cell activity, cellular responses to mitogens, antibody production, cell growth, and decreased phagocytic activity [33,34]. FE is 80 times more potent than MO and is a highly selective full MOR agonist ligand [35]. Therefore, it can also suppress the immune system [19]. MO and FE can also cause a sphincter of Oddi spasm, which could further aggravate AP severity [36]. In contrast to MO and FE, BQ is a partial agonist of the mu receptor, while it is an antagonist of kappa and delta opioid receptors [19]. Therefore, BQ has a different pharmacological profile than the other

opioids, and it does not inhibit NK cells, T cells, phagocytosis of macrophages, or cytokine production [19], and it has no morphine-like effect on the sphincter of Oddi [37]. These effects of opioids on cellular processes or on the sphincter of Oddi may explain the changes observed during AP in our experiments. Only FE pre-treatment resulted in increased AP severity. The early immunosuppression by FE may cause this adverse effect, while FE post-treatment was beneficial for AP outcome. However, the later consequences were not investigated by this work. For all clinically applied opioids, including FE, MO, or BQ, these effects should be considered and investigated in future studies. Moreover, the timing of opioid administration can be critical, especially in case of FE.

We demonstrated MOR mRNA and protein expression in the control rat pancreas and brain. It is well known that the brain expresses large amounts of opioid receptors [38,39]; in case of the pancreas, other research groups have also shown MOR expression in rats [40], sheep [41], and humans [42]. Pancreatic islet cells express MOR [43], which influences glucose homeostasis and insulin secretion. There is no direct evidence on opioid receptor expression in exocrine pancreatic cells. However, it has been demonstrated that enkephalin and MO inhibit pancreatic bicarbonate and protein secretion during endogenous or exogenous stimulation (secretin or cholecystokinin-octapeptide) in dogs [44], which may indicate the presence of MOR in both acinar and ductal cells. Other opioid receptors (nociception/orphanin FQ and delta opioid receptors) also play a role in regulating exocrine pancreatic secretion [45]. Furthermore, pancreatic cholinergic neurons have opiate receptors as well [46].

The efficiency of G-protein stimulation by mu opioid agonists was markedly higher in the rat brain than in pancreatic preparations. Transmembrane signaling mediated by opioid agonists was almost completely eliminated in the pancreatic cell membrane preparations of AP animals at 24 h. This can be explained by the dramatic decrease in pancreatic MOR mRNA and protein expression. In case of brain tissue, no reduction in MOR protein and mRNA levels could be observed. At 24 h, pancreatic tissue necrosis is extensive, which can contribute to the reduction of different receptors such as MOR, while there is no tissue necrosis in the brain; therefore, MOR expression remained unaltered. To the best of our knowledge, we demonstrated for the first time that AP reduced the function of opioid receptors not only in the pancreas but also in the brain. Notably, other groups have shown that mu opioid receptor expression is upregulated in hind paw or intestinal inflammatory animal models [47,48]. However, tissue acidification induced by injury or inflammation impaired MOR signaling [49]. Since the extent of AP severity is influenced by FE acting via opioid receptors (predominantly on MOR), we wanted to check their expression in the pancreas and brain and their functional activity in cell membrane fractions prepared from both tissues. The expression of MOR in the brain was unchanged in response to AP, whereas its functional activity was decreased during FE stimulation. This means that AP may affect MOR activity independently of changes in protein expression. The increase in serum pro-inflammatory cytokine (interleukin 1β) concentration has been shown to reduce central opioid neurotransmitter function [50]. Furthermore, there is a crosstalk between chemokines and opioid receptors, since certain chemokines (e.g., CCR2, CCR5, CCR7, CXCR4) can desensitize opioid receptors [34]. The most prominent symptom of AP is pain. During the disease, endogenous opioids (such as enkephalins, endorphins, and dynorphins) are released [51]. These substances may cause MOR desensitization [52,53], which could also contribute to the observed reduction in MOR activity. Moreover, high amounts of MOR are expressed in the spinal cord, which modulates pain sensation via the descending pain pathway system [54]. It is known that chronic pancreatitis causes chronic pain, which will result in epigenetic modulations of pain-related genes [55]. The latter is mediated by increased histone deacetylase 2 activity during chronic pancreatitis in the spinal cord. Consequently, there will be a reduction of MOR expression within some weeks. AP lasts for a shorter period, but due to the persistent pain, MOR expression can also be affected in the spinal cord. Further studies could investigate MOR not just in the pancreas and brain but also in the spinal cord. Overall, the mechanisms by which AP affects opioid

receptor activity is partly unknown, but we must infer a very likely interaction between the biochemical processes of opioid ligand binding and G-protein-mediated transmembrane signaling and organ inflammation.

In the clinical setting, there are no guidelines or recommendations suggesting which is the best opioid to use in AP. However, the application of effective and strong analgesics is necessary in the treatment of this disease. In light of the results discussed above, post-treatments (e.g., FE, MO) do not increase disease severity, but some of the opioids (e.g., MO) may affect the resolution of AP. Therefore, the latter may not be the best treatment option in this severe disease. Our results showed that FE post- and BQ pre-treatments have promising effects besides pain relief; therefore, the use of these opioids could also be beneficial for AP severity. Overall, this research contributes to a better understanding of the opioid effect in AP and can help design further clinical trials that will be necessary to select the most appropriate opiate to treat this potentially lethal disease.

Although pre-treatment with analgesics in AP is clinically less relevant, rectal administration of nonsteroidal anti-inflammatory drugs (NSAIDs, e.g., indomethacin or diclofenac) is indicated for endoscopic retrograde cholangiopancreatography (ERCP) [56]. These agents reduce the development of post-ERCP-related AP. In this case, the use of opiates could be also tested.

The present study has limitations as well. The long-term consequences of opiates on AP were not investigated as it was performed by Barlass et al. [21]. Furthermore, the above-mentioned and beneficial epidural administration route [25,26] was not investigated by our group.

In conclusion, we showed for the first time that AP reduced the transmembrane signaling of mu opioid receptors in both the pancreas and the brain. We demonstrated that FE post-treatment improved, while FE pre-treatment exacerbated disease severity in necrotizing AP. However, FE did not affect the outcome of edematous AP. MO administration had minimal effects in both pre- and post-treatments including cellular vacuolization, pancreatic water content, and leukocyte infiltration. I.t. administration of BQ showed slight benefit over i.p. injection. FE post-treatment proved to be beneficial in AP. Finally, our results suggest that type, dosing, administration route, and timing of opioid treatment can determine the effects on AP outcome. Clinical studies are needed to determine which opioid(s) is the best in AP.

4. Materials and Methods

4.1. Animals

Female Wistar rats weighing 200–250 g were used for experiments. The animals were kept at a constant room temperature of 24 °C with a 12 h light–dark cycle and were allowed free access to water and standard laboratory chow (Biofarm, Zagyvaszántó, Hungary).

4.2. Materials

All chemicals were purchased from Sigma-Aldrich (Budapest, Hungary) unless indicated otherwise.

4.3. In Vivo Experiments: Acute Pancreatitis Induction, Opiate Treatments, and Tissue Collection

Three different models of AP were applied (Figure 12). Necrotizing AP was induced by (a) single i.p. injection of 3 g/kg L-ornithine-HCl (LO, 30%, pH = 7.4); (b) intra-ductal administration of 1 mL/kg Na-taurocholate solution (NaTc; 40 mg/mL) as described previously [9,22]. Edematous AP was induced by hourly i.p. injections of 20 µg/kg cerulein (CER, 50 µg/mL) four times. Briefly, in case of NaTc-induced AP, abdominal surgery was performed on anesthetized rats (with 70 mg/kg ketamine and 14 mg/kg xylazine i.p.—purchased from CP-Pharma-Handelsgesellschaft MBH (Burgdorf, Germany)). Then, a cannula was placed into the pancreatic duct, and the biliary duct was transiently occluded via a microvessel clip. The NaTc solution was injected at a speed of 50 µL/min. At the end of the procedure, rats were placed on a heating pad for 40 min or until they woke up.

Thereafter, rats were placed back into their cages for 16–24 h. Control groups were given physiological saline (0.9% NaCl) solution instead of LO/CER/NaTc, respectively. Animals were sacrificed at 24 h in the LO-induced experimental pancreatitis model, between 16 and 24 h in case of the NaTc model, and at 12 h in case of the CER model. In case of NaTc-induced AP, rats were extensively monitored, and when body temperature decreased below 30 °C, they were humanely sacrificed by deep anesthesia induced by 85 mg/kg i.p. pentobarbital injection (Bimeda MTC, Cambridge, ON, Canada).

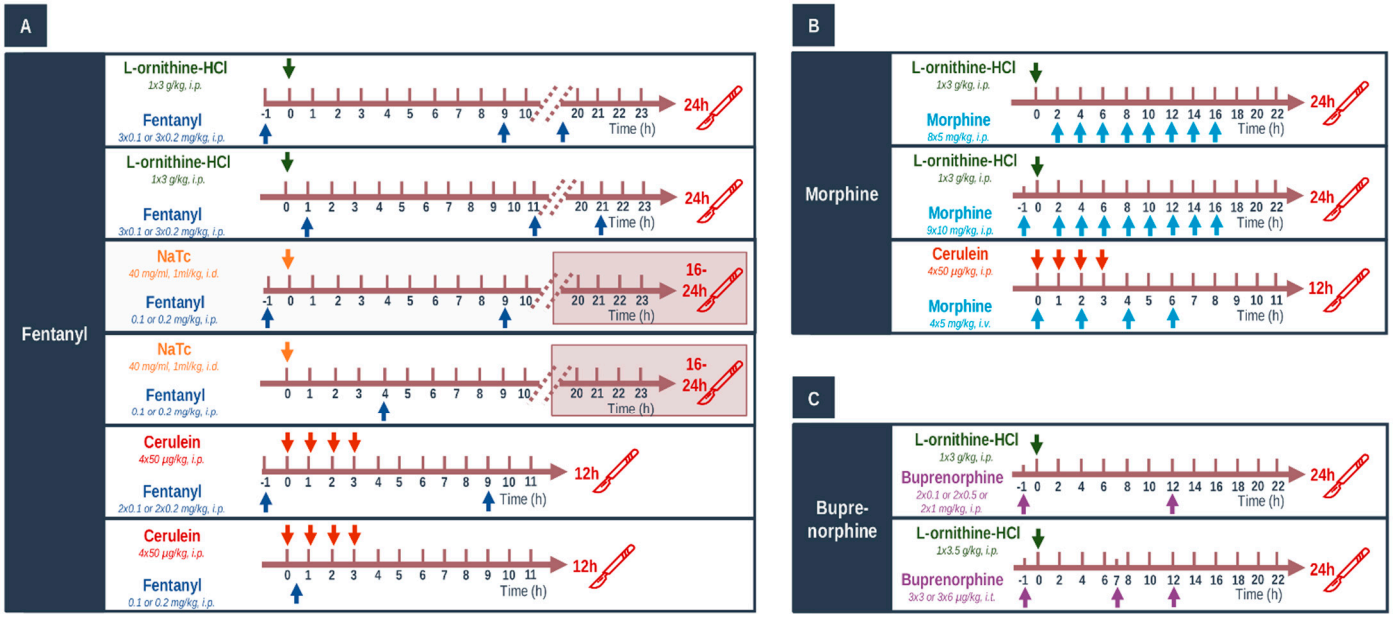

Figure 12. (**A**–**C**) Schematic view of experimental setup. Treatment arrangements for acute pancreatitis (AP) induction and opioid administration in Wistar rats. Arrows above or below the timeline show the injections. Control animals were injected with physiological saline. Abbreviations: i.p.—intraperitoneal; i.t.—intrathecal; i.v.—intravenous.

FE was administered i.p. at doses of 0.1 and 0.2 mg/kg based on the literature data [57]. Different timing arrangements were applied for FE in various AP models; repeated injections were performed when the analgesic effect of FE was decreased (this was determined in preliminary experiments or by literature data). In addition, FE was used as pre- or post-treatment. In the pre-treatment groups, the first FE injection was given 1 h prior to the induction of AP, and it was repeated every 11 h in LO- and every 10 h in NaTc- or CER-induced AP, respectively (Figure 12A). In preliminary experiments, FE pre-treatment was also tested in NaTc-induced AP, but the condition of animals was critical; therefore, humane termination was performed, and these investigations were stopped. In the post-treatment setup, animals received the first FE injection 1 h after AP induction in case of the LO model or 0.5 h after AP induction in case of the CER model. Since FE depresses respiration [58], it could not be administered within 3 h after surgery; therefore, FE was injected 4 h after the beginning of surgery in case of the NaTc model of AP (Figure 12A).

In the post-treatment setup, 5 mg/kg MO was administered i.p. 8 times every 2 h in case of the LO model (Figure 12B). The dose and timing of MO was chosen based on literature data; repeated injections were performed when the analgesic effect of MO was decreased [59]. During pre-treatment, 10 mg/kg MO was injected i.p. 9 times every 2 h (Figure 12B). When AP was induced by CER, 4 × 5 mg/kg dose of MO was used i.v. every 2 h, and analgesia started simultaneously with AP induction (Figure 12B). Animals were sacrificed 24 or 12 h after AP induction with LO or CER, respectively.

BQ has prolonged analgesic effects, and its recommended dosing intervals are between 8 and 12 h [60]. Instead of testing BQ in different AP models, it was administered via two

routes: i.p and intrathecally (i.t., Figure 12C). For i.t. administration, rats were anesthetized with a mixture of ketamine hydrochloride and xylazine (72 and 8 mg/kg i.p, respectively). An i.t. catheter (PE-10 tubing Intramedic, Clay Adams; Becton Dickinson; Parsippany, NJ, USA; I.D. 0.28 mm; O.D. 0.61 mm) was inserted via the cistern magna and passed 8.5 cm caudally into the subarachnoid space [61], which served to place the catheter tip between vertebrae Th12 and L2 vertebrae, corresponding to the spinal segments that innervate the hind paws [62]. After surgery, animals were injected by gentamycin (10 mg/kg, subcutaneously) to prevent infection and were housed individually. Rats exhibiting postoperative neurologic deficits, or those ones that did not show paralysis of one of the hindpaws after the administration of 100 µg lidocaine were excluded (about 10%) [62]. The drugs were applied at least after 4 days of recovery. I.p. injections of 0.1, 0.5, and 1 mg/kg BQ were given 1 h before and 12 h after the beginning of AP induction. I.t. injections of 3 and 6 µg/kg BQ were administered 1 h before AP induction and were repeated at 7 and 12 h after AP induction with LO. BQ was injected over 120 s in a volume of 10 µL, which was followed by a 10 µL flush of physiological saline. These BQ doses are in accordance with literature data [63,64].

At the end of experiments/treatments, deep anesthesia was induced by 85 mg/kg i.p. pentobarbital injection. Blood was collected through cardiac puncture; then, the pancreas was rapidly removed. Pancreata were cleaned from fat and lymph nodes on ice and then cut into pieces. Two parts of the pancreatic tissue were immediately frozen in liquid nitrogen and stored at −80 °C until biochemical assays or dry–wet weight measurements were performed. The third part of the pancreas was fixed in 8% neutral formaldehyde solution for histological analysis. In case of the NaTc model, pancreata were stored only for histological analysis due to the heterogeneity of AP induction. Blood samples were centrifuged at 2500 RCF for 15 min at 4 °C, and the sera were stored at −20 °C until use. Brains were also rapidly collected from rats, and the whole tissues were used for [^{35}S]GTPγS functional binding assay, whereas the cortex was used for PCR and Western blots. Brain samples were stored at −80 °C until further processing.

4.4. Laboratory Measurements

Serum amylase activity was measured on a Fluorostar Optima plate reader (BMG Labtech, Ortenberg, Germany) with a colorimetric kinetic method using a commercial kit purchased from Diagnosticum Zrt. (Budapest, Hungary). To evaluate the pancreatic water content, the wet weight (WW) of the pancreata was measured; then, the tissues were dried for 24 h at 100 °C, and the dry weight (DW) was also measured. The wet/dry weight ratio was calculated as follows: [(WW−DW)/WW] × 100. Pancreatic myeloperoxidase (MPO) activity is a hallmark of leukocytic infiltration and was measured according to Kuebler et al. [65]. MPO activities were normalized to total protein content as measured by the Lowry method [66]. To determine the extent of inflammatory response in the pancreata, we measured interleukin (IL)-1β levels by a commercial ELISA kit from R&D Systems (Minneapolis, MN, USA), as described by the manufacturer.

4.5. Histological Examination

Formalin-fixed pancreatic tissues were sectioned to 3 µm. These sections were prepared and stained with hematoxylin and eosin and were analyzed and scored by two independent experts blinded to the experimental protocol. Five different random areas were observed and scored per section per researcher. Edema was scored between 0 and 3 points (0: none; 1: patchy interlobular; 2: diffuse interlobular; 3: diffuse interlobular and intra-acinar), leukocytic infiltration between 0 and 4 points (0: none; 1: diffuse/mild; 2: diffuse/moderate; 3: diffuse/severe; 4: diffuse/very severe), vacuolization between 0 and 3 points (0: none; 1: mild; 2: moderate; 3: severe); the percentage of acinar cell damage was also evaluated.

4.6. Total RNA Preparation from Tissue

A small piece of pancreas or brain cortex was placed on ice in 1 mL of TRIzol reagent in a 13 mL centrifuge tube and was homogenized immediately with IKA Ultra Turrax (Type: TP18/10; Janke and Kunkel IKA, Staufen im Breisgau, Germany). Then, the tissue homogenate was instantly placed on liquid nitrogen and stored at −80 °C until use (for a maximum of 1 or 2 days). Total RNA purification was performed in three steps. In the first step, phase separation was performed by adding 200 µL of chloroform to the samples and shaking vigorously for 15 min, allowing to stand, and then centrifuging at 12,000 *g* for 15 min at 4 °C. From the resulting three phases, the top aqueous phase was aspirated into an empty Eppendorf tube, and 500 µL of isopropanol was added. Then, this was vortexed and allowed to stand for a few minutes, and after that, it was centrifuged at 12,000 *g* for 10 min at 4 °C. RNA precipitated in the Eppendorf tubes. The supernatant was removed, and 1 mL of 75% alcohol was added. It was vortexed and centrifuged at 7500 *g* for 5 min at 4 °C. After removal of the supernatant, the excess ethanol was evaporated briefly, and then, the RNA was redissolved in 70 µL of RNAse-free water. RNA was stored at −80 °C until further use.

RNA concentration was measured using a NanoDrop instrument from Thermo Fisher Scientific. We considered the optimal ranges for RNA to be A260/A280: 1.9–2.1 and A260/A230: 1.8–2.5. RNA integrity was examined after agarose gel electrophoresis.

4.7. Real-Time Quantitative Reverse Transcription-PCR (RT-PCR)

Reverse transcription and amplification of the PCR products were performed by using the TaqMan RNA-to-CT-Step One Kit (Thermo Fisher Scientific, Budapest, Hungary) and an ABI StepOne Real-Time cycler (Applied Biosystems, Thermo Fisher Scientific). Reverse-transcriptase PCR amplifications were performed as follows: at 48 °C for 15 min and at 95 °C for 10 min, followed by 40 cycles at 95 °C for 15 s and at 60 °C for 1 min. The generation of specific PCR products was confirmed by melting curve analysis. The following primers were used: assay ID Rn01430371_m1 for Oprm1 and Rn00667869_m1 for β-actin as endogenous control (Thermo Fisher Scientific). Each sample was run in triplicates. The fluorescence intensities of the probes were plotted against PCR cycle number. The amplification cycle displaying the first significant increase in the fluorescence signal was defined as the threshold cycle (Ct). Relative quantity of MOR mRNA expression was calculated by using the $2^{-\Delta\Delta Ct}$ method.

4.8. Western Blot Analysis

Pancreatic and brain tissues were homogenized using a Micro-Dismembrator (Sartorius AG, Göttingen, Germany) and centrifuged at 5000 g for 15 min at 4 °C in RIPA Lysis and Extraction Buffer (Thermo Fisher Scientific) with a protease and phosphatase inhibitor cocktail (10 mM Na-HEPES, 1 µM $MgCl_2$, 10 mM KCl, 1 mM DL-dithiothreitol, 5 mM iodoacetamide, 4 mM benzamidine-HCl, 1 mM phenylmethyl sulfonylfluoride). Total protein amounts from supernatant were determined with spectrophotometry (BioSpec-nano, Shimadzu, Kyoto, Japan).

Then, 25 µg of protein per well was subjected to electrophoresis on 4–12% NuPAGE Bis-Tris Gel in XCell SureLock Mini-Cell Units (Thermo Fisher Scientific). Proteins were transferred from gels to nitrocellulose membranes, using the iBlot Gel Transfer System (Thermo Fisher Scientific). Antibody binding was detected with the WesternBreeze Chromogenic Western blot immunodetection kit (Thermo Fisher Scientific). The blots were incubated on a shaker with OPRM1 (1:200, cat. no.: AOR-011, Alomone Labs, Jerusalem, Israel) and β-actin (cat. no.: bs-0061R, 1:200, Bioss Antibody, Woburn, MA, USA) polyclonal antibodies in the blocking buffer. Images were captured with the EDAS290 imaging system (Kodak Ltd., Rochester, NY, USA), and the optical density of each immunoreactive band was determined with Kodak 1D Images analysis software. Optical densities were calculated as arbitrary units after local area background subtraction. MOR expression was corrected for β-actin levels. Values were normalized to control groups.

4.9. Preparation of Brain and Pancreas Samples for Binding Assays

Frozen rat brain and pancreas samples from LO or physiological saline-treated animals were prepared for membrane preparation according to Szűcs et al. [67]. Briefly, tissue samples were homogenized in 30 volumes (*v*/*w*) of ice-cold 50 mM Tris-HCl pH 7.4 buffer (containing 4 mM benzamidine hydrochloride hydrate, 1 mM phenylmethyl sulfonylfluoride (Serva Electrophoresis GmbH, Heidelberg, Germany), 5 mM iodoacetamide, and 1 mM DL-dithiothreitol (Fluka Honeywell Research Chemicals, Charlotte, NC, USA)) with a Teflon-glass Braun homogenizer operating at 1500 rpm. The homogenate was centrifuged at 40,000 rcm for 20 min at 4 °C, after which the pellet was taken up in the original volume of Tris-HCl buffer. The homogenate was incubated at 37 °C for 30 min in a shaking water-bath. Then, centrifugation was repeated as described before. The final pellet was suspended in 5 volumes of TEM buffer (50 mM Tris-HCl, 1 mM EGTA, 5 mM $MgCl_2$, pH 7.4) and stored at −80 °C.

4.10. [^{35}S]GTPγS Functional Binding Assay

The functional [^{35}S]GTPγS binding experiments were performed as previously described [68]. Briefly, the membrane proteins (≈10 μg/mL) were incubated at 30 °C for 60 min with [^{35}S]GTPγS (20 MBq/0.05 cm^3; 0.05 nM; Perkin Elmer, Boston, MA, USA) and with 10 μM FE, DAMGO (Bachem Holding AG, Bubendorf, Switzerland) or MO in Tris-EGTA buffer (containing 30 μM GDP, 1 mM EGTA, 5 mM $MgCl_2$, 100 mM NaCl, and 50 mM Tris-HCl, pH 7.4) in a final volume of 1 mL/reaction tube. The non-selective opioid receptor antagonist naloxone (Endo Laboratories DuPont de Nemours, Wilmington, DE, USA) was used to detect receptor specificity. Non-specific binding was determined with 10 μM unlabeled GTPγS and subtracted from total binding. Basal activity (was defined as 100%) indicates constitutive G-protein activity level in the absence of any stimulating ligand. Bound and free [^{35}S]GTPγS were separated by vacuum (Brandel M24R Cell Harvester) filtration through Whatman GF/B glass fiber filters washed three times with 5 mL of ice-cold 50 mM Tris-HCl (pH 7.4) buffer. The results were performed in triplicates and repeated at least three times.

4.11. Statistical Analysis

The sufficient animal number per group was estimated by power analysis before each experiment, using the G*Power (3.1.9.2., Heinrich-Heine-Universität Düsseldorf, Germany) software [69] and setting the effect size to 0.8. Data are presented as means ± SEM. Experiments were evaluated by Student's *t*-test or by one- or two-way ANOVA followed by Holm–Sidak or Bonferroni post hoc tests (SPSS, IBM, Armonk, NY, USA). $p < 0.05$ was accepted as statistically significant.

Supplementary Materials: The following are available online at https://www.mdpi.com/article/10.3390/ijms23031192/s1.

Author Contributions: Conceptualization, Z.R.J.; Funding acquisition, Z.R.J.; Investigation, E.R.B., G.F., B.K., Z.B., E.S.K., E.M.O., B.T., G.H., E.S., S.B., E.D., P.P. and L.K.; Methodology, E.R.B., G.F., B.K., Z.B., E.S.K., B.T., E.M.O., G.H., E.S., S.B., E.D., P.P., J.M., V.V. and P.H.; Supervision, L.K. and Z.R.J.; Writing—original draft, E.R.B., L.K. and Z.R.J.; Writing—review and editing, P.P., J.M., V.V., P.H., L.K. and Z.R.J. All authors have read and agreed to the published version of the manuscript.

Funding: This work was supported by EFOP-3.6.2–16–2017–00006, GINOP-2.3.2-15-2016-00048, Bólyai János Research Grant (BO/00866/20/5), ÚNKP Grant (ÚNKP-20-5-SZTE-163), NKFIH PD129114 and NKFIH K119938. The funders did not influence the interpretation of results in any way.

Institutional Review Board Statement: The study was conducted according to the guidelines of the Declaration of Helsinki and the Hungarian Government Decree 40/2013 (II.14.) and approved by the Institutional Review Board of the University of Szeged and national ethics committees (X/3354/2017) for investigations involving animals.

Informed Consent Statement: Not applicable.

Data Availability Statement: The datasets generated during and/or analyzed during the current study are available from the corresponding author on reasonable request.

Conflicts of Interest: The authors declare no conflict of interest.

References

1. Peery, A.F.; Crockett, S.D.; Barritt, A.S.; Dellon, E.S.; Eluri, S.; Gangarosa, L.M.; Jensen, E.T.; Lund, J.L.; Pasricha, S.; Runge, T.; et al. Burden of Gastrointestinal, Liver, and Pancreatic Diseases in the United States. *Gastroenterology* **2015**, *149*, 1731–1741.e3. [CrossRef] [PubMed]
2. Forsmark, C.E.; Vege, S.S.; Wilcox, C.M. Acute Pancreatitis. *N. Engl. J. Med.* **2016**, *375*, 1972–1981. [CrossRef] [PubMed]
3. Roberts, S.E.; Akbari, A.; Thorne, K.; Atkinson, M.; Evans, P.A. The Incidence of Acute Pancreatitis: Impact of Social Deprivation, Alcohol Consumption, Seasonal and Demographic Factors. *Aliment. Pharmacol. Ther.* **2013**, *38*, 539–548. [CrossRef] [PubMed]
4. Roberts, S.E.; Morrison-Rees, S.; John, A.; Williams, J.G.; Brown, T.H.; Samuel, D.G. The Incidence and Aetiology of Acute Pancreatitis across Europe. *Pancreatology* **2017**, *17*, 155–165. [CrossRef] [PubMed]
5. Párniczky, A.; Kui, B.; Szentesi, A.; Balázs, A.; Szűcs, Á.; Mosztbacher, D.; Czimmer, J.; Sarlós, P.; Bajor, J.; Gódi, S.; et al. Prospective, Multicentre, Nationwide Clinical Data from 600 Cases of Acute Pancreatitis. *PLoS ONE* **2016**, *11*, e0165309. [CrossRef] [PubMed]
6. Banks, P.A.; Bollen, T.L.; Dervenis, C.; Gooszen, H.G.; Johnson, C.D.; Sarr, M.G.; Tsiotos, G.G.; Vege, S.S. Classification of Acute Pancreatitis—2012: Revision of the Atlanta Classification and Definitions by International Consensus. *Gut* **2013**, *62*, 102–111. [CrossRef]
7. Abu-El-Haija, M.; Gukovskaya, A.S.; Andersen, D.K.; Gardner, T.B.; Hegyi, P.; Pandol, S.J.; Papachristou, G.I.; Saluja, A.K.; Singh, V.K.; Uc, A.; et al. Accelerating the Drug Delivery Pipeline for Acute and Chronic Pancreatitis. *Pancreas* **2018**, *47*, 1185–1192. [CrossRef]
8. Barreto, S.G.; Habtezion, A.; Gukovskaya, A.; Lugea, A.; Jeon, C.; Yadav, D.; Hegyi, P.; Venglovecz, V.; Sutton, R.; Pandol, S.J. Critical Thresholds: Key to Unlocking the Door to the Prevention and Specific Treatments for Acute Pancreatitis. *Gut* **2021**, *70*, 194–203. [CrossRef]
9. Pallagi, P.; Balla, Z.; Singh, A.K.; Dósa, S.; Iványi, B.; Kukor, Z.; Tóth, A.; Riederer, B.; Liu, Y.; Engelhardt, R.; et al. The Role of Pancreatic Ductal Secretion in Protection Against Acute Pancreatitis in Mice. *Crit. Care Med.* **2014**, *42*, e177–e188. [CrossRef]
10. Pallagi, P.; Madácsy, T.; Varga, Á.; Maléth, J. Intracellular Ca^{2+} Signalling in the Pathogenesis of Acute Pancreatitis: Recent Advances and Translational Perspectives. *Int. J. Mol. Sci.* **2020**, *21*, 4005. [CrossRef]
11. Hritz, I.; Czakó, L.; Dubravcsik, Z.; Farkas, G.; Kelemen, D.; Lásztity, N.; Morvay, Z.; Oláh, A.; Pap, Á.; Párniczky, A.; et al. Acute Pancreatitis: Evidence Based Management Guidelines of the Hungarian Pancreatic Study Group 2014. *Orv. Hetil.* **2015**, *156*, 244–261. [CrossRef]
12. Crockett, S.D.; Wani, S.; Gardner, T.B.; Falck-Ytter, Y.; Barkun, A.N.; Crockett, S.; Falck-Ytter, Y.; Feuerstein, J.; Flamm, S.; Gellad, Z.; et al. American Gastroenterological Association Institute Guideline on Initial Management of Acute Pancreatitis. *Gastroenterology* **2018**, *154*, 1096–1101. [CrossRef]
13. Leppäniemi, A.; Tolonen, M.; Tarasconi, A.; Segovia-Lohse, H.; Gamberini, E.; Kirkpatrick, A.W.; Ball, C.G.; Parry, N.; Sartelli, M.; Wolbrink, D.; et al. 2019 WSES Guidelines for the Management of Severe Acute Pancreatitis. *World J. Emerg. Surg.* **2019**, *14*, 27. [CrossRef]
14. Mandalia, A.; Wamsteker, E.-J.; DiMagno, M.J. Recent Advances in Understanding and Managing Acute Pancreatitis. *F1000Research* **2019**, *7*, 959. [CrossRef]
15. Stigliano, S.; Sternby, H.; de Madaria, E.; Capurso, G.; Petrov, M.S. Early Management of Acute Pancreatitis: A Review of the Best Evidence. *Dig. Liver Dis.* **2017**, *49*, 585–594. [CrossRef] [PubMed]
16. Working Group IAP/APA Acute Pancreatitis Guidelines. IAP/APA Evidence-Based Guidelines for the Management of Acute Pancreatitis. *Pancreatology* **2013**, *13*, e1–e15. [CrossRef] [PubMed]
17. Ona, X.B.; Rigau Comas, D.; Urrútia, G. Opioids for Acute Pancreatitis Pain. *Cochrane Database Syst. Rev.* **2013**, *7*, CD009179. [CrossRef]
18. Erbil, Y.; Berber, E.; Seven, R.; Çaliş, A.; Eminoğlu, L.; Koçak, M.; Bilgiç, L. The Effect of Intestinal Transit Time on Bacterial Translocation. *Acta Chir. Belg.* **1998**, *5458*, 245–249. [CrossRef]
19. Franchi, S.; Moschetti, G.; Amodeo, G.; Sacerdote, P. Do All Opioid Drugs Share the Same Immunomodulatory Properties? A Review From Animal and Human Studies. *Front. Immunol.* **2019**, *10*, 2914. [CrossRef] [PubMed]
20. Thompson, D.R. Narcotic Analgesic Effects on the Sphincter of Oddi: A Review of the Data and Therapeutic Implications in Treating Pancreatitis. *Am. J. Gastroenterol.* **2001**, *96*, 1266–1272. [CrossRef]
21. Barlass, U.; Dutta, R.; Cheema, H.; George, J.; Sareen, A.; Dixit, A.; Yuan, Z.; Giri, B.; Meng, J.; Banerjee, S.; et al. Morphine Worsens the Severity and Prevents Pancreatic Regeneration in Mouse Models of Acute Pancreatitis. *Gut* **2018**, *67*, 719–727. [CrossRef] [PubMed]
22. Perides, G.; Van Acker, G.J.D.; Laukkarinen, J.M.; Steer, M.L. Experimental Acute Biliary Pancreatitis Induced by Retrograde Infusion of Bile Acids into the Mouse Pancreatic Duct. *Nat. Protoc.* **2010**, *5*, 335–341. [CrossRef]
23. Wang, Y.; Chen, M. Fentanyl Ameliorates Severe Acute Pancreatitis-Induced Myocardial Injury in Rats by Regulating NF-KB Signaling Pathway. *Med. Sci. Monit.* **2017**, *23*, 3276–3283. [CrossRef] [PubMed]

24. Stevens, M.; Esler, R.; Asher, G. Transdermal Fentanyl for the Management of Acute Pancreatitis Pain. *Appl. Nurs. Res.* **2002**, *15*, 102–110. [CrossRef] [PubMed]
25. Demirag, A.; Pastor, C.M.; Morel, P.; Jean-Christophe, C.; Sielenkämper, A.W.; Güvener, N.; Mai, G.; Berney, T.; Frossard, J.L.; Bühler, L.H. Epidural Anaesthesia Restores Pancreatic Microcirculation and Decreases the Severity of Acute Pancreatitis. *World J. Gastroenterol.* **2006**, *12*, 915–920. [CrossRef]
26. Sadowski, S.M.; Andres, A.; Morel, P.; Schiffer, E.; Frossard, J.L.; Platon, A.; Poletti, P.A.; Bühler, L. Epidural Anesthesia Improves Pancreatic Perfusion and Decreases the Severity of Acute Pancreatitis. *World J. Gastroenterol.* **2015**, *21*, 12448–12456. [CrossRef] [PubMed]
27. Grimm, M.C.; Ben-Baruch, A.; Taub, D.D.; Howard, O.M.Z.; Resau, J.H.; Wang, J.M.; Ali, H.; Richardson, R.; Snyderman, R.; Oppenheim, J.J. Opiates Transdeactivate Chemokine Receptors: δ and μ Opiate Receptor–Mediated Heterologous Desensitization. *J. Exp. Med.* **1998**, *188*, 317–325. [CrossRef]
28. Peterson, P.K.; Gekker, G.; Brummitt, C.; Pentel, P.; Bullock, M.; Simpson, M.; Hitt, J.; Sharp, B. Suppression of Human Peripheral Blood Mononuclear Cell Function by Methadone and Morphine. *J. Infect. Dis.* **1989**, *159*, 480–487. [CrossRef]
29. Peiró, A.M.; Martínez, J.; Martínez, E.; De Madaria, E.; Llorens, P.; Horga, J.F.; Pérez-Mateo, M. Efficacy and Tolerance of Metamizole versus Morphine for Acute Pancreatitis Pain. *Pancreatology* **2008**, *8*, 25–29. [CrossRef]
30. Meng, W.; Yuan, J.; Zhang, C.; Bai, Z.; Zhou, W.; Yan, J.; Li, X. Parenteral Analgesics for Pain Relief in Acute Pancreatitis: A Systematic Review. *Pancreatology* **2013**, *13*, 201–206. [CrossRef] [PubMed]
31. Wereszczyńska-Siemiatkowska, U.; Nebendahl, K.; Pohl, U.; Otto, J.; Groene, H.J.; Wilms, H.; Lankisch, P.G. Influence of Buprenorphine on Acute Experimental Pancreatitis. *Res. Exp. Med.* **1987**, *187*, 211–216. [CrossRef] [PubMed]
32. Ogden, J.M.; Modlin, I.M.; Gorelick, F.S.; Marks, I.N. Effect of Buprenorphine on Pancreatic Enzyme Synthesis and Secretion in Normal Rats and Rats with Acute Edematous Pancreatitis. *Dig. Dis. Sci.* **1994**, *39*, 2407–2415. [CrossRef] [PubMed]
33. Eisenstein, T.K. The Role of Opioid Receptors in Immune System Function. *Front. Immunol.* **2019**, *10*, 2904. [CrossRef]
34. Rogers, T.J. Bidirectional Regulation of Opioid and Chemokine Function. *Front. Immunol.* **2020**, *11*, 94. [CrossRef]
35. Trescot, A.M.; Datta, S.; Lee, M.; Hans, H. Opioid Pharmacology. *Pain Physician* **2008**, *11*, 133–154. [CrossRef]
36. Afghani, E.; Lo, S.K.; Covington, P.S.; Cash, B.D.; Pandol, S.J. Sphincter of Oddi Function and Risk Factors for Dysfunction. *Front. Nutr.* **2017**, *4*, 1. [CrossRef] [PubMed]
37. Cuer, J.C.; Dapoigny, M.; Ajmi, S.; Larpent, J.L.; Lunaud, B.; Ferrier, C.; Bommelaer, G. Effects of Buprenorphine on Motor Activity of the Sphincter of Oddi in Man. *Eur. J. Clin. Pharmacol.* **1989**, *36*, 203–204. [CrossRef] [PubMed]
38. Przewlocki, R.; Przewlocka, B. Opioids in Chronic Pain. *Eur. J. Pharmacol.* **2001**, *429*, 79–91. [CrossRef]
39. Delfs, J.M.; Kong, H.; Mestek, A.; Chen, Y.; Yu, L.; Reisine, T.; Chesselet, M.-F. Expression of Mu Opioid Receptor MRNA in Rat Brain: An in Situ Hybridization Study at the Single Cell Level. *J. Comp. Neurol.* **1994**, *345*, 46–68. [CrossRef] [PubMed]
40. Khawaja, X.Z.; Green, I.C.; Thorpe, J.R.; Titheradge, M.A. The Occurrence and Receptor Specificity of Endogenous Opioid Peptides within the Pancreas and Liver of the Rat. Comparison with Brain. *Biochem. J.* **1990**, *267*, 233–240. [CrossRef]
41. Ng, S.L.; Ng, T.N. Materials with Opiate Receptor Binding Activity in Bovine Testis and Ovine Pancreas. *Biochem. Int.* **1987**, *14*, 1087–1096. [PubMed]
42. Peng, J.; Sarkar, S.; Chang, S.L. Opioid Receptor Expression in Human Brain and Peripheral Tissues Using Absolute Quantitative Real-Time RT-PCR. *Drug Alcohol Depend.* **2012**, *124*, 223–228. [CrossRef]
43. Wen, T.; Peng, B.; Pintar, J.E. The MOR-1 Opioid Receptor Regulates Glucose Homeostasis by Modulating Insulin Secretion. *Mol. Endocrinol.* **2009**, *23*, 671–678. [CrossRef] [PubMed]
44. Konturek, S.J.; Tasler, J.; Cieszkowski, M.; Jaworek, J.; Coy, D.H.; Schally, A.V. Inhibition of Pancreatic Secretion by Enkephalin and Morphine in Dogs. *Gastroenterology* **1978**, *74*, 851–855. [CrossRef]
45. Linari, G.; Agostini, S.; Broccardo, M.; Petrella, C.; Improta, G. Regulation of Pancreatic Secretion In Vitro by Nociceptin/Orphanin FQ and Opioid Receptors: A Comparative Study. *Pharmacol. Res.* **2006**, *54*, 356–360. [CrossRef] [PubMed]
46. Louie, D.S.; Chen, H.T.; Owyang, C. Inhibition of Exocrine Pancreatic Secretion by Opiates Is Mediated by Suppression of Cholinergic Transmission: Characterization of Receptor Subtypes. *J. Pharmacol. Exp. Ther.* **1988**, *246*, 132–136. [PubMed]
47. Pol, O.; Alameda, F.; Puig, M.M. Inflammation Enhances μ-Opioid Receptor Transcription and Expression in Mice Intestine. *Mol. Pharmacol.* **2001**, *60*, 894–899. [CrossRef] [PubMed]
48. Zhang, Q.; Schäfer, M.; Elde, R.; Stein, C. Effects of Neurotoxins and Hindpaw Inflammation on Opioid Receptor Immunoreactivities in Dorsal Root Ganglia. *Neuroscience* **1998**, *85*, 281–291. [CrossRef]
49. Meyer, J.; Del Vecchio, G.; Seitz, V.; Massaly, N.; Stein, C. Modulation of M-opioid Receptor Activation by Acidic pH Is Dependent on Ligand Structure and an Ionizable Amino Acid Residue. *Br. J. Pharmacol.* **2019**, *176*, 4510–4520. [CrossRef]
50. Prossin, A.R.; Zalcman, S.S.; Heitzeg, M.M.; Koch, A.E.; Campbell, P.L.; Phan, K.L.; Stohler, C.S.; Zubieta, J.K. Dynamic Interactions Between Plasma IL-1 Family Cytokines and Central Endogenous Opioid Neurotransmitter Function in Humans. *Neuropsychopharmacology* **2014**, *40*, 554–565. [CrossRef] [PubMed]
51. Satake, K.; Ha, S.S.; Hiura, A. Effects of Bradykinin Receptor Antagonist on the Release of Beta-Endorphin and Bradykinin and on Hemodynamic Changes in a Canine Model of Experimental Acute Pancreatitis. *Pancreas* **1996**, *12*, 92–97. [CrossRef] [PubMed]
52. Llorca-Torralba, M.; Pilar-Cuéllar, F.; Bravo, L.; Bruzos-Cidon, C.; Torrecilla, M.; Mico, J.A.; Ugedo, L.; Garro-Martínez, E.; Berrocoso, E. Opioid Activity in the Locus Coeruleus Is Modulated by Chronic Neuropathic Pain. *Mol. Neurobiol.* **2019**, *56*, 4135–4150. [CrossRef] [PubMed]

53. Clark, M.J.; Traynor, J.R. Endogenous Regulator of g Protein Signaling Proteins Reduce {mu}-Opioid Receptor Desensitization and down-Regulation and Adenylyl Cyclase Tolerance in C6 Cells. *J. Pharmacol. Exp. Ther.* **2005**, *312*, 809–815. [CrossRef]
54. Tao, Z.Y.; Wang, P.X.; Wei, S.Q.; Traub, R.J.; Li, J.F.; Cao, D.Y. The Role of Descending Pain Modulation in Chronic Primary Pain: Potential Application of Drugs Targeting Serotonergic System. *Neural Plast.* **2019**, *2019*, 1389296. [CrossRef]
55. Liao, Y.H.; Wang, J.; Wei, Y.Y.; Zhang, T.; Zhang, Y.; Zuo, Z.F.; Teng, X.Y.; Li, Y.Q. Histone Deacetylase 2 Is Involved in Mopioid Receptor Suppression in the Spinal Dorsal Horn in a Rat Model of Chronic Pancreatitis Pain. *Mol. Med. Rep.* **2018**, *17*, 2803–2810. [CrossRef]
56. Patai, Á.; Solymosi, N.; Mohácsi, L.; Patai, Á.V. Indomethacin and Diclofenac in the Prevention of Post-ERCP Pancreatitis: A Systematic Review and Meta-Analysis of Prospective Controlled Trials. *Gastrointest. Endosc.* **2017**, *85*, 1144–1156.e1. [CrossRef]
57. Almousa, A.A.; Ikeda, R.; Wada, M.; Kuroda, N.; Hanajiri, R.K.; Nakashima, K. HPLC-UV Method Development for Fentanyl Determination in Rat Plasma and Its Application to Elucidate Pharmacokinetic Behavior after i.p. Administration to Rats. *J. Chromatogr. B Anal. Technol. Biomed. Life Sci.* **2011**, *879*, 2941–2944. [CrossRef]
58. Hill, R.; Santhakumar, R.; Dewey, W.; Kelly, E.; Henderson, G. Fentanyl Depression of Respiration: Comparison with Heroin and Morphine. *Br. J. Pharmacol.* **2020**, *177*, 254–266. [CrossRef]
59. Bouw, M.R.; Gårdmark, M.; Hammarlund-Udenaes, M. Modelling of Morphine Transport across the Blood-Brain Barrier as a Cause of the Antinociceptive Effect Delay in Rats—A Microdialysis Study. *Pharm. Res.* **2000**, *17*, 1220–1227. [CrossRef] [PubMed]
60. Foley, P.L.; Kendall, L.V.; Turner, P.V. Clinical Management of Pain in Rodents. *Comp. Med.* **2019**, *69*, 468–489. [CrossRef] [PubMed]
61. Yaksh, T.L.; Rudy, T.A. Chronic Catheterization of the Spinal Subarachnoid Space. *Physiol. Behav.* **1976**, *17*, 1031–1036. [CrossRef]
62. Dobos, I.; Toth, K.; Kekesi, G.; Joo, G.; Csullog, E.; Klimscha, W.; Benedek, G.; Horvath, G. The Significance of Intrathecal Catheter Location in Rats. *Anesth. Analg.* **2003**, *96*, 487–492. [CrossRef]
63. Tejwani, G.A.; Rattan, A.K. The Role of Spinal Opioid Receptors in Antinociceptive Effects Produced by Intrathecal Administration of Hydromorphone and Buprenorphine in the Rat. *Anesth. Analg.* **2002**, *94*, 1542–1546. [CrossRef] [PubMed]
64. Guarnieri, M.; Brayton, C.; Detolla, L.; Forbes-Mcbean, N.; Sarabia-Estrada, R.; Zadnik, P. Safety and Efficacy of Buprenorphine for Analgesia in Laboratory Mice and Rats. *Lab Anim.* **2012**, *41*, 337–343. [CrossRef] [PubMed]
65. Kuebler, W.M.; Abels, C.; Schuerer, L.; Goetz, A.E. Measurement of Neutrophil Content in Brain and Lung Tissue by a Modified Myeloperoxidase Assay. *Int. J. Microcirc. Clin. Exp.* **1996**, *16*, 89–97. [CrossRef] [PubMed]
66. Lowry, O.H.; Rosebrough, N.J.; Farr, A.L.; Randall, R.J. Protein Measurement with the Folin Phenol Reagent. *J. Biol. Chem.* **1951**, *193*, 265–275. [CrossRef]
67. Szűcs, E.; Büki, A.; Kékesi, G.; Horváth, G.; Benyhe, S. Mu-Opioid (MOP) Receptor Mediated G-Protein Signaling Is Impaired in Specific Brain Regions in a Rat Model of Schizophrenia. *Neurosci. Lett.* **2016**, *619*, 29–33. [CrossRef]
68. Traynor, J.R.; Nahorski, S.R. Modulation by Mu-Opioid Agonists of Guanosine-5′-O-(3-[35S]Thio)Triphosphate Binding to Membranes from Human Neuroblastoma SH-SY5Y Cells. *Mol. Pharmacol.* **1995**, *47*, 848–854.
69. Faul, F.; Erdfelder, E.; Lang, A.G.; Buchner, A. G*Power 3: A Flexible Statistical Power Analysis Program for the Social, Behavioral, and Biomedical Sciences. *Behav. Res. Methods* **2007**, *39*, 175–191. [CrossRef]